GEORGIA INSTITUTE OF TECHNOLOGY
OFFICE OF CONTRACT ADMINISTRATION
SPONSORED PROJECT INITIATION

Date: 12/3/79

Project Title: A Cooperative Program of Applied Energy Research and Technology Development

Project No: A-2494

Project Director: Dr. R.A. Cassanova

Sponsor: Atlanta University; Atlanta, Georgia 30314

Agreement Period: From 10/1/79 Until 6/30/80

Type Agreement: Unnumbered Agreement under DOE Grant No. DE-FG05-79ET60058

Amount: $137,895

Reports Required: Quarterly Progress Reports; Final Technical Report

Sponsor Contact Person (s):

Technical Matters

Dr. Frank E. Cummings
Department of Chemistry
Atlanta University
Atlanta, Ga. 30314

(404) 525-6204

Contractual Matters
(thru OCA)

Mr. Robert McKinnon
223 Chestnut Street
Atlanta University
Atlanta, Ga. 30314

(404) 681-0251

Defense Priority Rating: None

Assigned to: ERL/ODL (School/Laboratory) XXXXXX

COPIES TO:

Project Director
Division Chief (EES)
School/Laboratory Director
Dean/Director–EES
Accounting Office
Procurement Office
Security Coordinator (OCA)
Reports Coordinator (OCA) ✓

Library, Technical Reports Section
EES Information Office
EES Reports & Procedures
Project File (OCA)
Project Code (GTRI)
Other

GA 3 (3/76)

2-4
SR494 161

GEORGIA INSTITUTE OF TECHNOLOGY
OFFICE OF CONTRACT ADMINISTRATION

SPONSORED PROJECT TERMINATION

Date: 8/3/81

Project Title: A Cooperative Program of Applied Energy Research and Technology Development

Project No: A2494

Project Director: Dr. R.A. Cassanova ~~Cassanova~~

Sponsor: Atlanta University; Atlanta, GA 30314

Effective Termination Date: 12/31/80

Clearance of Accounting Charges: 12/31/80

Grant/Contract Closeout Actions Remaining:

- x Final Invoice ~~and Closing Documents~~
- _ Final Fiscal Report
- x Final Report of Inventions
- x Govt. Property Inventory & Related Certificate
- _ Classified Material Certificate
- _ Other _____

Assigned to: EMSL/ODL (~~School~~/Laboratory)

COPIES TO:

Administrative Coordinator
Research Property Management
Accounting Office
Procurement Office
Research Security Services
~~Reports~~ Coordinator (OCA)

Legal Services (OCA)
Library, Technical Reports
EES Research Public Relations (2)
Project File (OCA)
Other: _____

A-2494

GEORGIA INSTITUTE OF TECHNOLOGY

Engineering Experiment Station

Atlanta, Georgia

Quarterly Report No. 1

October 1, 1979 - December 31, 1979

Project A-2494-003

COAL DESULFURIZATION

by

J. A. Knight, L. W. Elston and D. R. Hurst

January 9, 1980

COAL DESULFURIZATION

SUMMARY

A computer search of related technical literature has been conducted and has been partially reviewed, and the review will be continued during the next work period. A pulverized coal sample will be obtained from the Georgia Power Company for the initial experiments. Based on the literature review, other coal samples will be selected for this study. An experimental design of the pyrolysis apparatus has been made, and a glass model will be constructed for cold flow studies prior to construction of the pyrolysis apparatus. Initial experiments will be conducted with the sample of coal from the Georgia Power Company and an analysis will be performed for sulfur content in the coal and char samples. Char yields will be determined by analysis of the coal and char for an inorganic element such as calcium.

OBJECTIVE

The objective of this program is to investigate desulfurization of coal by pyrolysis in an inert atmosphere. If the sulfur content of coal can be reduced to an acceptable level in an effective method prior to combustion, this could reduce the need for the removal of sulfur dioxide from flue gases, particularly for users, such as power plants, of large quantities of coal. The parameters that are being considered are temperature, residence time and particle size. The initial experiments will be conducted so that the coal particles are suspended in a stream of the hot inert gas.

LITERATURE

A computer search of related technical literature has been conducted to supplement our own technical literature file on coal desulfurization. A review of literature has been underway during this quarter and it will be continued in the next work period. Two of the more comprehensive references are by Anthony and Howard (1) and Wen and Tone (2). Our review of the literature will be focused on the desulfurization of coals of different ranks when heated, particularly in an inert atmosphere, and the type of experimental reactor or method used for the pyrolysis, such as fluidized bed, entrained flow or free fall.

---

1. D. B. Anthony and J. B. Howard, "Coal Devolatilization and Hydrogasification", AIChE Journal, 22 625 (1976).

2. C. Y. Wen and S. Tone, "Coal Conversion Reaction Engineering", ACS Symposium Series 74, 57 (1978).

EXPERIMENTAL APPROACH

The coal sample for our initial experiments will be obtained from the Georgia Power Company. The coal sample will be taken from the pulverized coal stream that is fed directly to the border. The coal is pulverized prior to combustion so that 70 percent will pass a 200 mesh screen. For our experiments, the coal will be sized to obtain narrower cuts. Other ranks of coal will be selected for future experiments based on our review of the literature.

The initial experiments will be conducted by suspension of the coal particles in a stream of nitrogen gas in a heated zone of a vertical tube. Prior to conducting the pyrolysis experiments, a glass model of the apparatus will be constructed so that cold flow studies of the suspension of the coal particles can be conducted.

The analysis to be performed for our initial experiments will be for total sulfur in the coal and char samples. It is proposed that char yields will be determined by analysis for an element that would not be present in the pyrolysis tube but would be common to the char and coal. Calcium is being considered, and analysis would be performed by atomic absorption spectrophotometry. Another element may prove more satisfactory.

PLANS FOR NEXT PERIOD

During the next work period, January 1 to March 31, 1980, the review of the literature will be continued. A pulverized coal sample will be obtained from the Georgia Power Company for the initial experiments. From the literature review, coals of other ranks will be selected for future experiments. The reactor design for the pyrolysis experiments will be completed and a glass model will be constructed for cold flow studies of the coal particles in nitrogen gas. Necessary changes, if any, will be made in the reactor design,

and the apparatus will be constructed. Initial experiments will be conducted with the coal sample obtained from the Georgia Power Company. Analysis will be centered on the sulfur content of the coal and char samples and the char yield.

A-2494

GEORGIA INSTITUTE OF TECHNOLOGY

Engineering Experiment Station

Atlanta, Georgia

Quarterly Report No. 2

January 1, 1980 - March 31, 1980

Project A-2494-001

CATALYTIC CONVERSION OF BIOMASS TO USEFUL FUELS

by

J. A. Knight, D. R. Hurst and L. W. Elston

March 31, 1980

CATALYTIC CONVERSION OF BIOMASS TO USEFUL FUELS

SUMMARY

Three pyrolysis experiments were carried out in a six inch tube furnace with sawdust alone, sawdust with potassium carbonate, and sawdust with charcoal. All products were collected and analyzed, and material and energy balances determined. In the potassium carbonate experiments, the heavy organics had a heating value of 16,350 BTU/lb on a dry basis which is considerably higher than the heating value of most pyrolytic oils. However, the yield of the heavy organics was only about one-half that for the baseline experiment with sawdust. In the experiment with charcoal added to the sawdust, the non-condensible gas showed an increase about about five percent over the gas yield of the baseline run. Evaluation of the data will be continued in the next quarter.

EXPERIMENTAL PROCEDURES

GENERAL PROCEDURES

Three samples of analyzed pine sawdust were pyrolyzed in the six inch laboratory tube furnace. The evolved liquids and gases and the chars were collected and analyzed. The first run (baseline) was made with pine sawdust alone. The second and third runs were made with mixtures of pine sawdust and potassium carbonate and of pine sawdust and char, respectively.

Baseline Pyrolysis (94-1-1)

A 2,000 g charge of pine sawdust containing 6.55 percent moisture was loaded into the pyrolysis tube using spacers to retain the charge in the uniformly heated center section of a three-zone Lindberg furnace. The tube was closed and attached to a condensate collection train consisting of water cooled condensers, ice cooled traps, glass wool demisters, a calcium sulfate dryer, a cold trap system of dry ice and acetone

traps and condensers chilled by alcohol circulating through a coil immersed in a bath of dry ice and ethylene glycol, and a final magnesium perchlorate drying section. The condensate collection train was followed by a noncondensible gas collection system consisting of a dry test gas meter and a series of 100 liter gas collection bags.

The closed system was thoroughly purged with Nitrogen, and the furnace was turned on. The temperature rise was recorded by means of chromel alumel thermocouples in each of the three furnace zones and throughout the pyrolysis tube and a multi-channel strip chart recorder.

The furnace was heated as rapidly as possible to 650°C. The temperature of the center furnace zone rose continuously at an average rate of 6°C to 7°C per minute to the desired maximum temperature. The faster end zones were heated in stepwise 100°C increments as the center zone temperature reached the temperature of the end zone.

The evolved gas samples were collected in 90 liter increments. When the gas evolution rate fell to less than five liters per hour, final gas syringe samples were drawn by puncturing the connecting tubing and analyzed to determine the composition of the gas in the system at the end of the run. A stainless steel ball valve in the downstream end of the pyrolysis tube was then closed, and the furnace was cooled overnight.

The cooled char, the liquid condensates, and the noncondensible gases were retained for chemical analysis.

Pyrolysis with Potassium Carbonate Catalyst (94-1-2)

An aqueous solution prepared from 375 g freshly opened anhydrous potassium carbonate and 500 ml deionized water was thoroughly mixed with 2,500 g of pine sawdust taken from the analyzed lot used in the baseline pyrolysis. The mixture was air dried for ten days with frequent stirring, and the percent moisture in the air dried mixture was determined. A 2,350 g pyrolysis charge was placed in the pyrolysis tube. This charge was calculated to contain a weight of dry sawdust exclusive of moisture and catalyst, equal to that used in the baseline pyrolysis. The pyrolysis procedures were identical to those described for the baseline run.

Pyrolysis with Charcoal Catalyst (94-1-3)

The pyrolysis charge was prepared by mixing 280 g of finely ground char from the baseline run with 2,000 g of pine sawdust taken from the lot used in the baseline pyrolysis. The amount of dry sawdust, exclusive of catalyst and moisture, was equal to that used in the baseline pyrolysis. After four hours of mixing in a tightly closed jar mill the finely divided char had evenly coated the sawdust particles, and no fine dust remained. The mixed contents of the jar mill were quantitatively transferred to the pyrolysis tube. The pyrolysis procedures were identical to those described for the baseline run

Analytical Methods

The yields of char and condensates were determined by weighing the products in tared containers. Heavy organic and aqueous phases were separated by decantation. Gas yields were calculated from the volumes indicated by the dry test meter and the compositions determined by gas chromatography. None of the data were normalized.

Feed Analysis

The percent moisture in the feed was determined by drying 100 g samples of unground material to constant weight at 105°C in a forced air oven. The dried sample was finely ground in a Model 4 Wiley Mill and stored in a tightly closed container. The percent ash was determined by igniting 1.0000 g samples to constant weight at 650°C in a muffle furnace. The percent acid insoluble ash was determined by the method used for sand and insoluble silicates by the Association of Florida Phosphate Chemists. Heating values were determined by oxygen bomb calorimetry following the plain calorimeter procedure described in Parr Manual No. 1.47.*

Char Analysis

The proximate analysis of the chars were performed following ASTM Method F-1762-64. Heating values were determined by oxygen bomb calorimetry.

---

*Parr Instrument Company, Moline Ill. 61265

Condensate Analysis

The percent moisture in the separated heavy organic and aqueous phases was determined by azeotropic distillation and tolune (Dean and Stark Method). The difference between the apparent percent moisture in the aqueous phase and 100 percent was assumed to be dissolved or dispersed heavy organic material whose heating value was similar to that determined by oxygen bomb calorimetry for the heavy organic phase from the same pyrolysis, adjusted to a water free basis. The heating value of the dry ice trap condensate (light oil) was estimated to be 18,000 BTU/lb.

RESULTS AND DISCUSSION

Detailed results of the laboratory analyses and the recorded temperature rise and gas evolution rate data are being tabulated for inclusion in later reports.

MASS BALANCES

The mass balances derived from these experiments are summarized in TABLE I.

The experiments were planned so that the amount of pine sawdust, exclusive of moisture and catalyst, and the procedure for pyrolyzing the charge would remain unchanged for all of the experiments. The input moistures and catalysts and the products resulting from the moisture and catalysts are shown in TABLE 1, but they are not included in the percent yields, which are based entirely on the dry pine sawdust. The total percent yields for the first and third runs, 100 ± 1.3 percent are a reasonable indication of the precision of the pyrolysis and analytical procedures. The char from these two runs was free flowing, dead black, and granular. The char from the second run (with potassium carbonate) was a very friable porous cake with blue-green streaks on a slightly lighter colored char. As the recovered char contained nearly 25 percent by weight of anhydrous potassium oxide dispersed on a high sutface area support it is believed that the high total percent recovery is due to rapid reaction of the potassium oxide with atmospheric carbon dioxide.

TABLE 1. MASS BALANCES

	94-1-1 Baseline		94-1-2 K_2CO_3 Catalyst		94-1-3 Char Catalyst	
	g	Percent yield	g	Percent yield	g	Percent yield
INPUTS						
Dry Sawdust	1,869	100	1,869	100	1,869	100
Input Water	131	0	190.3	0		0
K_2CO_3	-	-	290.7	0	-	
Char	-	-	-	-	280	0
Total	2,000	100	2,350	100	2,280	100
OUTPUTS						
Pyrolysis Char	513.6	27.5	600.5	32.1	502.7	26.9
K_2O	-	-	198.1	0	-	-
Catalyst Char	-	-			280	0
Heavy Organics	246.4	13.2	125.6	6.7	223.7	12.0
Light Oil	22.4	1.2	23.8	1.3	27.2	1.5
Pyrolysis Water	525.3	28.1	565	30.2	508.2	27.2
Input Water	131	0	190.3	0	131	0
Pyrolysis Gas	538.9	28.8	668.3	35.8	616.1	33.7
Catalyst CO_2	-	-	92.5	0	-	-
Total		98.8		106.1*		101.3

*Apparently considerable atmospheric CO_2 was taken up by the K_2O in the char during processing.

On first examination, it appears that the potassium carbonate catalyst increases the noncondensible gas yield at the expense of the heavy organics yield. The heavy organic condensate from this pyrolysis experiment contained 63.2 percent and had a heating value of 16,350 Btu/lb on a dry basis, which is considerably higher than the heating values of most pyrolytic oils. Based on this one experiment, it appears that the potassium carbonate altered the oil characteristics to produce one with a greater heating value. In the experiment with charcoal added to the sawdust, the only noticeable difference is the increase in the noncondensible gas yield from 28.8 percent for the base line run to 33.7 percent. Closer study of the experimental logs and critical examination of the analyses are underway.

ENERGY BALANCES

The distribution of the recovered energy values among the recovered pyrolysis products is shown in TABLE 2.

TABLE 2. ENERGY BALANCES*

	94-1-1		94-1-2		94-1-3	
	HHV Btu/lb Dry Feed	Energy Percent	HHV Btu/lb Dry Feed	Energy Percent	HHV Btu/lb Dry Feed	Energy Percent
INPUTS						
Dry sawdust	8,574	100	8,574	100	8,574	
OUTPUTS						
Char	3,921	45.7	4,006	46.7	3,884	45.3
Heavy Organic	1,900	22.2	1,100	12.8	1,557	18.2
Light Oil	216	2.5	234	2.7	270	3.1
Gases	1,617	18.9	2,187	25.5	1,998	23.3
Latent heat of H_2O Vaporization	341	4.0	372	4.3	332	3.9
Total	7,995	93.3	7,899	92.0	8,041	93.8

*Basis: 1 lb. dry pine sawdust

The difference between the sum of the recovered energy components and 100 percent is believed to be contained in volatile low molecular weight organic compounds soluble in water. These compounds would be included in the aqueous distillate phases resulting from the moisture determinations. Samples of these aqueous distillates have been stored in tightly closed vials for future analysis by gas chromatography.

The higher heating values reported for the yield components have been corrected to a moisture and catalyst free basis. The latent heat of water vaporization was calculated from the sum of the pyrolysis yield and input waters.

PLANS FOR APRIL 1 - JUNE 30 PERIOD

During the next quarter, the evaluation of the data from the three completed experiments will be continued. Also, the literature review will be continued. Based on the evaluation of the completed experiments, additional experimental work will be planned.

LIBRARY DOES NOT HAVE

Quarterly Report No. 3 - April 1, 1980 - June 30, 1980

A-2494

GEORGIA INSTITUTE OF TECHNOLOGY

Engineering Experiment Station

Atlanta, Georgia

Quarterly Report No. 4

July 1, 1980 - September 30, 1980

Project A-2494-003

COAL DESULFURIZATION

by

J. A. Knight, D. R. Hurst and L. W. Elston

October 14, 1980

COAL DESULFURIZATION

SUMMARY

A sample of Illinois coal was pretreated by controlled oxidation at 232°C. Slightly more than 20 percent of the original sample weight was removed as volatiles during the pretreatment. Four free fall experiments conducted with the oxidized Illinois coal showed that for each of the comparable temperatures the fraction of oxidized coal reaching the receiver was greater than the corresponding untreated coal fractions at equal temperatures. The fraction of the sulfur in the volatiles was proportionally greater than the weight fraction of the sample volatilized. The experimental data have been compared, and a preliminary draft of the final technical report is being completed. Comparison of the mass, energy, and sulfur distributions in the recovered solids and the volatiles phases indicates that free fall heating of pulverized coal can be a useful method of sulfur removal.

EXPERIMENTAL WORK AND RESULTS

A sample of 50 X 100 mesh Illinois high volatiles bituminous coal was preoxidized for 30 minutes at 232°C in a 1.5 liter per minute stream of air. The weight of the recovered preoxidized coal was 121.3g (79.2 percent of the charge weight). Results of the analyses of untreated and pretreated Illinois coal samples compared are in Table 1.

TABLE 1. ANALYSIS OF ILLINOIS COAL

Coal Sample	Nonoxidized	Oxidized
Moisture, wt %	7.0	1.5
Volatiles, wt %	34.0	29.2
Sulfur, wt %	4.43	5.58
Ash, wt %	13.0	13.2
Calcium, wt %	1.77	2.18
Heating Value, kJ/kg	29,761	27,815
(Btu/lb)	(12,803)	(11,966)

Four free fall experiments were performed with pretreated Illinois coal following the experimental procedures described for untreated Illinois coal in Report No. 3. The results of these experiments are shown in Tables 2, 3, and 4.

TABLE 2. FREE FALL REACTOR EXPERIMENTAL DATA USING PRETREATED ILLINOIS COAL

Exp. No.	Reactor Temperature °C	Coal Feedrate g/min	Run Time Minutes	% Yields Receiver wt %	Reactor wt %	Volatiles* wt %
12	500	.14	60	93.3	0.0	6.7
13	550	.14	60	54.7	0.0	45.3
14	600	.14	60	49.2	1.5	49.3
15	650	.14	60	62.7	0.0	37.3

*Calculated by difference

The anomalous high receiver yeild at 650°C (Experiment No. 15) can only be attributed to an undetected surge in the coal feeder rate.

TABLE 3. DISTRIBUTION OF SULFUR IN PRODUCTS FROM OXIDIZED ILLINOIS COAL

Exp. No.	% SULFUR DISTRIBUTION Receiver	Reactor	Volatiles*
12	68.5	0.0	31.5
13	44.1	0.0	55.9
14	31.7	1.0	67.3
15	41.6	0.0	58.4

*Calculated by difference

TABLE 4. DISTRIBUTION OF HEATING VALUES IN PRODUCTS FROM OXIDIZED ILLINOIS COAL

Exp. No.	Receiver KJ/kg (Btu/lb)	%	Reactor KJ/kg (Btu/lb)	%	Volatiles* KJ/kg (Btu/lb)	%
12	29,307 (12,608)	98.3	- - - -	-	27,739 (11,933)	1.7
13	25,442 (10,945	49.3	- - - -	-	26,276 (11,304)	50.7
14	26,174 (11,260)	46.3	26,174 (11,260)	1.4	18,289 (7,868)	52.3
15	29,986 (12,900)	67.6	- - - -	-	18,819 (8,096)	32.4

*Calculated by difference

Detailed descriptions of the experimental methods, calculations and results along with discussion and suggestions for future work will be given in the final technical report.

A-2494

TASK 2.2.3

MATERIALS AND DESIGNS FOR SOLAR CHEMICAL REACTORS

Henderson C. Ward
Steve H. Bomar, Jr.

Georgia Institute of Technology
Engineering Experiment Station
Atlanta, Georgia 30332

First Quarterly Report

January 1980

Task 2.3.3 Materials and Designs for Solar Chemical Reactors

This task is being conducted by the Engineering Experiment Station of the Georgia Institute of Technology and is a companion effort to a task entitled "Solar Fuels and Chemicals" being conducted by Atlanta University. This task's purpose is to develop designs for chemical reactors using concentrated solar radiation as the input energy source. The chemical reaction mechanisms might make use of either photon energy or thermal energy; at this early stage the investigation is focused very broadly on solar reactor hardware concepts.

The Atlanta University task is directed toward identification of chemical reaction systems which would be attractive for solar energy storage or fuel production. Ultimately, it is expected that the Georgia Tech reactor designs will be matched to the reactions selected by Atlanta University for further development. In the meantime, however, Georgia Tech is proceeding with general studies on optical and thermal analysis of reasonable reactor configurations. In order to do this effectively, one must make some broad assumptions on which types of chemical reactions appear to have commercial promise for use in the future.

Since concentrated radiant energy has unique properties, in comparison to conventional chemical process energy generated by burning fuels, it seems desirable to try to exploit these properties for the greatest benefit. One example of exploiting the special properties of concentrated solar radiation would be the direct use of photons to drive a chemical storage reaction, although no candidates with commercial potential have been identified up to now. A less exotic example is the use of solar radiation to heat particulate reactants directly, through a transparent reactor wall or window. Several examples

of this idea appear promising.

Identification of Solar Chemical Storage Reaction Types

A limited study has been initiated on general methods of energy storage and conversion utilizing solar energy. These methods include:

(1) Liquid solution concentration and dilution
(2) Reversible chemical reactions
(3) Irreversible chemical reactions
(4) Vaporization and condensation

The effort to date has been focused on reviewing those methods which have already been proposed, and identifying and comparing their relative advantages and disadvantages as a basis on which to extend the study to more promising systems and methods. Attention is being directed toward establishing those factors and variables pertinent to each method and system which influence their potential application. Of particular interest is the determination of the mode and method of heat transfer in the reactor and the resultant effect on reactor design.

Two categories of reaction are of wide enough interest that they have defined the early reactor configuration studies:

(1) Reactions in which gases are heated in the presence of solid particles
(2) Reactions in which liquids are heated or vaporized

These cover an extremely wide range of storage possibilities fitting within the four chemical storage methods listed above. For example, the first category of reactor design might be used for thermal decomposition of biomass, for production of syngas using carbon and steam, for heating reactant gases in the presence of powdered catalysts, or for dehydration of a compound such as calcium hydroxide. The second category of reactor design might be used for decomposition of sulfur trioxide in the reversible sulfur trioxide-sulfur dioxide system, for concentrating aqueous solutions, or for vaporizing a liquid.

Solar Chemical Reactor Concepts

Only a very few solar chemical reactor concepts have been proposed and studied. They are, of course, governed by the geometry of the available input beam of solar radiation:

(1) CNRS in France operates a batch-type rotary furnace which is used for fusing of refractory oxides. The aperture faces in a horizontal direction. The unit holds several tons of reactant powder and rotates at speeds up to 120 revolutions per minute; the rotation creates a horizontal cavity where the powder fuses to form a hollow egg.

(2) CNRS has operated a small, solar fired fluidized bed for decomposition of calcium carbonate. The unit was operated in a vertical-axis solar furnace with the fluidized bed contained in a cylindrical fused quartz tube. The vertical-axis geometry provided symmetric heating around the wall of the tubular reactor vessel.

(3) Lawrence-Livermore Laboratories has operated a "box reactor" with a horizontally-facing quartz window. The test program decomposed powdered coal and was conducted at the U. S. Army White Sands Solar Furnace in New Mexico.

(4) Princeton University operated a vertical tube reactor for pyrolysis of biomass. The powdered reactant was dropped through the tube. The tests were conducted with a horizontal beam at the CNRS Solar Furnace.

(5) Several organizations have built and operated solar steam boilers, using both once-through and free convection flow schemes. Martin Marietta and Georgia Tech operated a free convection 1 MW boiler at the CNRS Solar Furnace, Georgia Tech operated a 400 kW

once-through boiler at the Advanced Components Test Facility in Atlanta, and McDonnell-Douglas operated a once-through 5 MW boiler at the Central Receiver Test Facility in Albuquerque. Francia has operated several different boilers similar to the Georgia Tech unit, in Italy.

Optical Analysis of a Fluidized Bed Reactor

As a starting point for quantitative design of solar chemical reactors, an optical analysis was conducted on the radiant energy entering a vertical tube containing a fluidized bed. A transparent fused quartz tube wall was assumed, and the first issue to be inspected was the fraction of arriving energy which should be transmitted by the tube wall into the bed. The mirror field angles associated with the Advanced Components Test Facility were assumed, with flux symmetric about the concentrator axis, as would be observed in a tracking dish. For an alternate case, an absorbing wall such as silicon carbide was taken in place of the transparent quartz wall.

The basic configuration of the fluidized bed reactor was a cylinder placed on the optical axis of the concentrator. The reflection coefficient for light rays arriving at a glass surface is a function of the angle of incidence measured from the normal to the surface. Since the outer edge of the concentrator represents most of the concentrator area, most of the energy striking the tubular reactor will have angles of incidence less than 60° and reflection coefficients less than 10 per cent. Rays which arrive from the inner portions of the concentrator, however, will have higher angles of incidence and higher reflection coefficients. The fraction of the energy passing through the wall into the bed is obtained by summing

the components arriving from various angles with appropriate concentrator areas and reflectivities.

The optical analysis computer program with which Georgia Tech models solar receivers accounts for the finite diameter of the sun and appropriate heliostat aiming errors. This program was modified to model the cylindrical receiving surface of the fluidized bed reactor. For the particular cases run, the flux was assumed to come from an 11-meter faceted paraboloidal concentrator, masked to provide 67 kW of thermal power at the focal plane; facets at the center were removed.

The results of this analysis for absorbing and transmitting vessel walls were:

(1) Peak fluxes on the walls are dependent on wall diameter.

(2) The flux patterns are sharply peaked along the length of the vessel wall.

(3) The peak flux passing through a transparent wall is about 10 per cent lower than that passing through an absorbing wall, because of reflection losses in the transparent wall.

(4) The integrated flux passing through a transparent wall is about 13 per cent lower than that passing through an absorbing wall.

These preliminary conclusions represent only one fluidized bed vessle geometry and do not account for other losses such as convection, thermal emission from hot surfaces, etc. They do show, however, that reflective losses are less serious than expected and that a fluidized bed with transparent walls is tentatively feasible.

Future Work

During the next quarter, both the reaction investigations and the analytical studies will be continued. More detailed modelling of fluidized bed heat transfer will be conducted and terminal concentrators will be inspected. The effects of cavity enclosures around reactor vessels will be modelled.

A-2494

Task 2.3.3

MATERIALS AND DESIGNS FOR SOLAR CHEMICAL REACTORS

Henderson C. Ward

Steve H. Bomar, Jr.

Georgia Institute of Technology
Engineering Experiment Station

Second Quarterly Report

April 1980

Task 2.3.3 Materials and Designs for Solar Chemical Reactors

The purpose of this task, being conducted by the Engineering Experiment Station of the Georgia Institute of Technology, is to develop designs for chemical reactors using concentrated solar radiation as the energy input source. This task is a companion effort to the Atlanta University task "Solar Fuels and Chemicals" which is directed toward identifying chemical reaction systems for solar energy storage or fuel production.

Systems Selection for Solar Reactor Designs

Based on preliminary results from the Atlanta University task, the following two heat-transfer categories have been chosen for reactor design studies:

(1) heat transfer to reacting gases in the presence of solid particles

(2) heat transfer to subcooled and boiling liquids.

In category one, the system chosen to represent fuel or chemical feedstock production is the reaction between steam and carbon particles in the presence of a catalyst to produce synthesis gas. A second system in this category, representing energy storage and conversion by means of a reversible chemical reaction and employing solid particles as a heat-transfer mechanism, will be selected from candidate systems to be recommended in the near future by the Atlanta University.

In category two, the system chosen for study to represent energy storage and conversion is the vaporization and condensation of suitable Freon compounds.

Synthesis Gas Production

Synthesis gas is produced by heating steam and carbon in the presence of a catalyst. The reactions involved, with carbon in the form of graphite, are:

1. $C_{(s)} + H_2O(g) \rightleftarrows CO_2(g) + H_2(g)$ - 56,488 Btu/lb atom C

2. $C_{(s)} + 2\ H_2O(g) \rightleftarrows CO_2(g) + 2\ H_2(g)$ - 38,799 Btu/lb atom C

3. $C_{(s)} + CO_2(g) \rightleftarrows 2CO(g)$ - 74,197 Btu/lb atom C

4. $CO(g) + H_2O(g) \rightleftarrows CO_2(g) + H_2(g)$ + 17,709 Btu/lb mole CO

Only two of the above four reactions are independent and the chosen two and temperature pressure, concentration, reaction rates, carbon particle size, heat transfer rates, catalyst type and size, and residence time are the controlling variables.

Calculations made to date have focused on determining the concentrations of the various species present at equilibrium, the percentage of steam reacted, and the initial steam-carbon ratio required to provide excess carbon at various operating pressures and temperatures. Selected results of these calculations are given in Table I. These calculations indicate operation at the highest temperature and the lowest pressure is the most favorable and further that the pressure effect is small. Therefore, the reactor will be designed for operation at substantially 1 atm and at the highest temperature obtainable that is compatible with the selected materials of construction.

TABLE I

SELECTED RESULTS OF EQUILIBRIUM CALCULATIONS FOR STEAM-CARBON REACTION

Pressure (atm abs)	Temperature (K)	Required Initial Steam-Carbon Ratio (molar)	Equilibrium Gas Composition (%) H_2O	H_2	CO	CO_2	Steam Reacted (%)
0.5	1000	$\leq$ 1.16708	3.337	50.518	41.772	4.373	93.80
0.5	1500	$\leq$ 1.00055	0.0208	49.994	49.980	0.0077	99.96
1	1000	$\leq$ 1.29056	5.881	50.463	36.851	6.806	89.56
1	1100	$\leq$ 1.07836	2.008	49.878	46.352	1.763	96.13
1	1300	$\leq$ 1.00679	0.2194	49.950	49.712	0.1187	99.56
1	1500	$\leq$ 1.00114	0.0416	49.987	49.956	0.0154	99.92
5	1000	$\leq$ 1.84413	17.007	47.833	22.488	12.672	73.77
5	1500	$\leq$ 1.005686	0.2069	49.935	49.782	0.0764	99.59

These calculations are currently being extended to include rate effects, catalyst type and size, carbon particle size, and required heat-transfer rates.

Solar Chemical Reactor Design

Optical modeling studies were conducted on the solar furnace configurations which would focus concentrated solar radiation onto upward facing, horizontal focal planes. These system configurations were: a true vertical-axis solar furnace having a symmetric paraboloid dish concentrator and a system having a horizontal optical axis with an asymmetric concentrator which turns the radiation onto a horizontal receiving plane.

The modeling was carried out using a ray-tracing computer program written at Georgia Tech. The program traces a large number of solar rays and sums the number of rays arriving at various positions on the focal plane. Each ray is traced from a point on the solar disk to a point on the paraboloid surface to a position on the receiving surface. The solar disk is represented by 13 points placed at four radii and at randomly selected angular positions; the power emitted by each point is weighted by the area it represents on the solar disk. The reflecting points on the parabola have a slope error whose direction varies randomly and whose magnitude varies to give a specified standard deviation (for example, if the specified standard deviation is 2 milliradians, the slope error magnitudes will have different values but collectively will have a standard deviation of 2). The receiving surface can be planar or conical, but in the present study was always taken as a horizontal plane through the origin of the coordinate system (focus).

The number of ray positions sampled on the paraboloid surface ranges from a few hundred to several thousand, depending on the precision desired in

the output data (each ray position is hit by 13 sun rays). In the present study, calculations using 10,800 and 21,600 ray positions were performed; the 21,600 ray cases gave somewhat smoother plots, but otherwise were identical to the 10,800 ray cases. For the present application, the ray-tracing program was incremented in steps of radius and angle about the x-axis of the coordinate system, with the condition that the flux contribution from a reflecting point was not summed if that point was outside the boundaries of the paraboloid mirror. (The assumption of perfect heliostat alignment is implied by the fact that rays are traced from the solar disk to the paraboloid surface to the receiving plane, without an intermediate reflection at a heliostat.)

Flux patterns at the focal plane are shown for four cases in Figures 1 through 4. It is recognized that the assumptions used in the analyses limit the ability of these plots to show the true incident fluxes which might be obtained in real solar furnaces. They are, however, valid for comparing the various design alternatives.

Figures 1 and 2 are plots for what we presently believe to be an optimum asymmetric paraboloid reflector; they differ only in the number of ray positions sampled on the concentrator. As mentioned earlier, the 21,600 ray case is somewhat smoother than the 10,800 ray case, but otherwise they are essentially the same.

Figures 3 and 4 are for two symmetric paraboloid concentrators in true vertical-axis facilities. Comparison of Figures 2, 3 and 4 gives support to the proposition that good performance could be obtained from a solar furnace having a horizontal optical axis and an asymmetric paraboloid concentrator.

Future Work

During the next quarter, both the reaction investigations and the analytical studies will be continued. More detailed modeling of fluidized bed heat transfer will be conducted and terminal concentrators will be inspected. The effects of cavity enclosures around reactor vessels will be modeled.

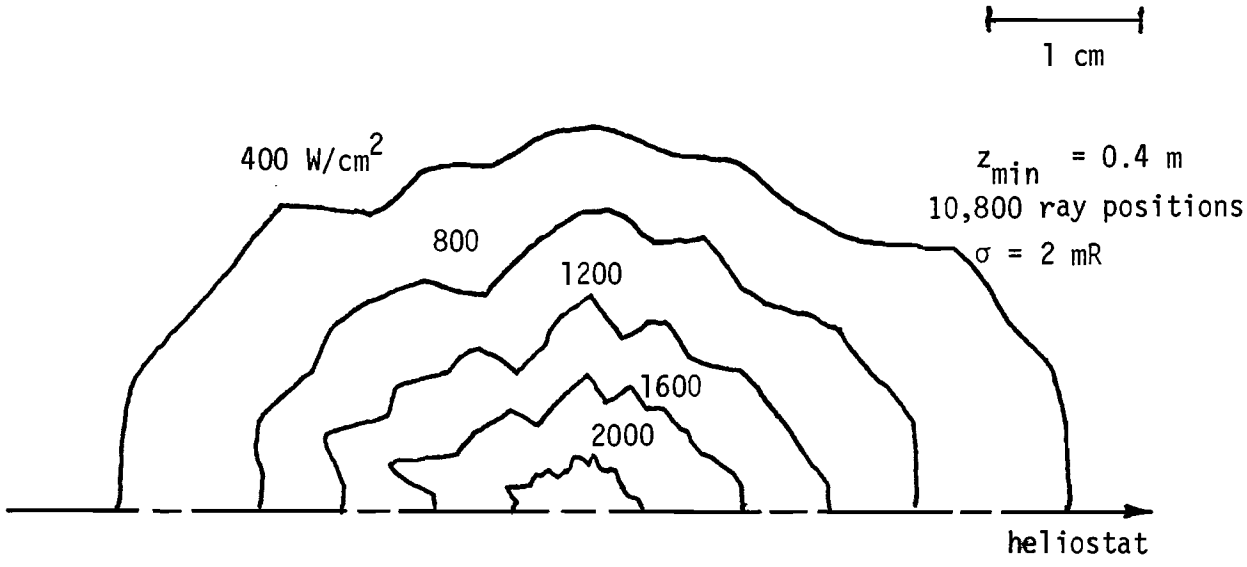

Figure 1. Flux Plot for Asymmetric Paraboloid Concentrator.

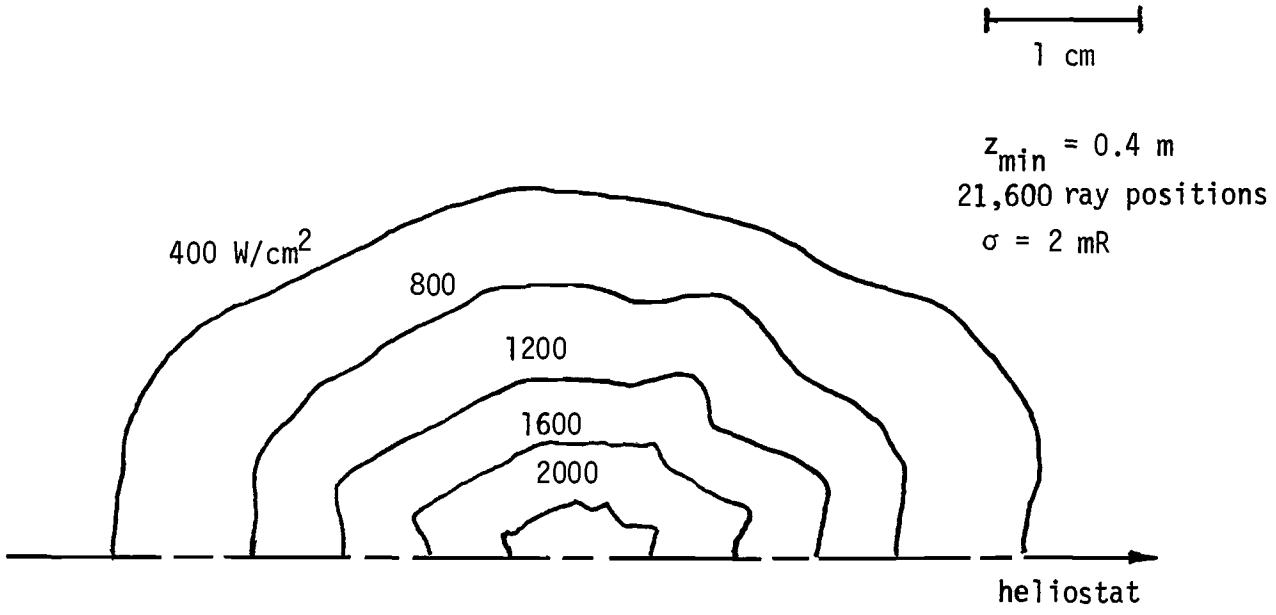

Figure 2. Flux Plot for Asymmetric Paraboloid Concentrator.

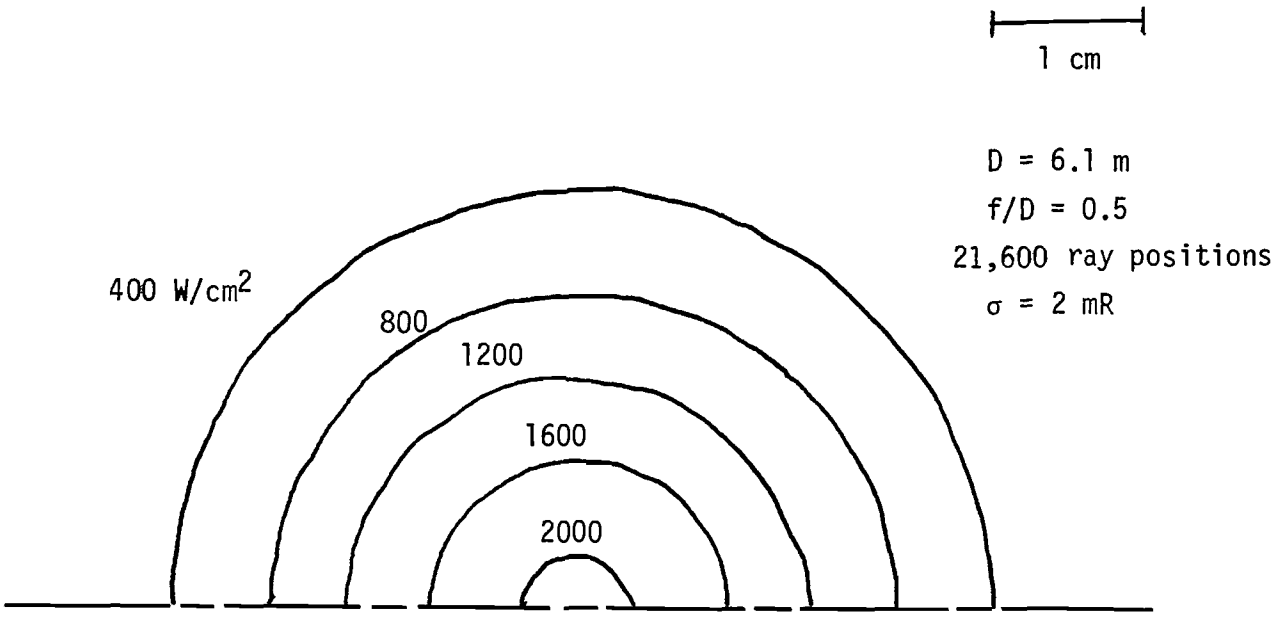

Figure 3. Flux Plot for Symmetric Paraboloid Concentrator.

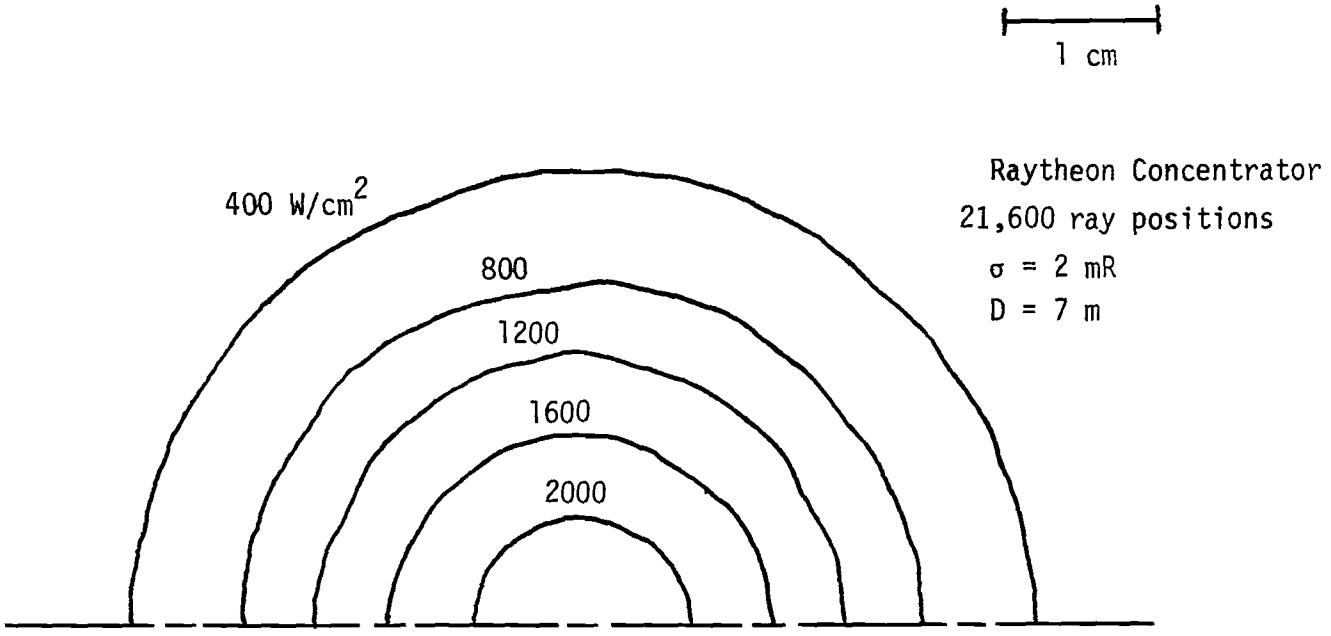

Figure 4. Flux Plot for Symmetric Paraboloid Concentrator.

A-2494

TASK 2.3.3

MATERIALS AND DESIGNS FOR SOLAR CHEMICAL REACTORS

Henderson C. Ward
Steve H. Bomar, Jr.
Dalip K. Sondhi

Georgia Institute of Technology
Engineering Experiment Station
Atlanta, Georgia 30332

Third Quarterly Report

July 1980

Task 2.3.3 Materials and Designs for Solar Chemical Reactors

The purpose of this task, being conducted by the Engineering Experiment Station of the Georgia Institute of Technology, is to develop designs for chemical reactors using concentrated solar radiation as the energy input source. This task is a companion effort to the Atlanta University task "Solar Fuels and Chemicals" which is directed toward identifying chemical reaction systems for solar energy storage or fuel production.

The major effort during the past quarter has been focused on the carbon-steam reaction for the production of synthesis gas. The objectives of this effort were:

1. to extend the studies and calculations made during the previous reporting period to include rate effects, catalyst types, carbon particle size, and required heat-transfer rates,

2. to design conceptually several solar chemical reactors for this reaction,

3. to design conceptually a synergistically co-sited complex based on syngas produced via solar coal gasification.

The results of these efforts are summarized below.

Synthesis Gas

Gas mixtures containing CO, H_2, and N_2 in various ratios are used as feedstocks to produce a number of different chemical commodities. These mixtures, with the ratios of the components suitably adjusted, are called

synthesis gases. Table 1 shows the volume ratios of the components required to produce various synthesis gases.

TABLE 1

VOLUME RATIOS IN SYNTHESIS GAS

Commodity or Process	H_2	CO	N_2
Ammonia	3	0	1
Methanol	2	1	0
Fisher-Tropsch (synthol)	2	1	0
Oxo (higher alcohols)	1	1	0
SNG	3	1	0

By reacting steam with carbon under suitable conditions, a basic gas mixture, called blue water gas, is produced which can be used to make each of the above as well as other synthesis gases. In Table 2, which is an extension of the table presented in the previous Quarterly Report, selected results are given of calculations made to determine the concentrations of the various species present at equilibrium and the initial carbon-steam ratio required to provide excess carbon at various operating pressures and temperatures. Also shown in this table are the reactions involved (with carbon in the form of graphite), the percentages of the steam reacted, and the heat requirements per lb atom of carbon reacted at the various pressures and temperatures. Note that the heat input requirement, neglecting heat losses, is approximately 4850 Btu/lb carbon reacted.

TABLE 2

SELECTED RESULTS OF EQUILIBRIUM CALCULATIONS FOR CARBON-STEAM REACTION*

Pressure (atm abs)	Temperature (°C)	Temperature (K)	Temperature (°F)	Required Initial Steam-Carbon Ratio (molar)	Equilibrium Gas Composition (%) H_2O	H_2	CO	CO_2	Steam Reacted (%)	Heat Required (Btu/lb atom C reacted)
0.5	727	1000	1340	$\leq$ 1.16708	3.337	50.518	41.772	4.373	93.80	57,081
0.5	1227	1500	2240	$\leq$ 1.00055	0.0208	49.994	49.980	0.0077	99.96	57,837
1	727	1000	1340	$\leq$ 1.29056	5.881	50.463	36.851	6.806	89.56	56,164
1	827	1100	1520	$\leq$ 1.07836	2.008	49.878	46.352	1.763	96.13	57,946
1	1027	1300	1880	$\leq$ 1.00679	0.2194	49.950	49.712	0.1187	99.56	58,261
1	1227	1500	2240	$\leq$ 1.00114	0.0416	49.987	49.956	0.0154	99.92	57,838
5	727	1000	1340	$\leq$ 1.84413	17.007	47.833	22.488	12.672	73.77	53,101
5	1227	1500	2240	$\leq$ 1.005686	0.2069	49.935	49.782	0.0764	99.59	57,822

*Reactions

	ΔH_{25^oC}
1. $C_{(s)} + H_2O(g) \rightleftarrows CO(g) + H_2(g)$	56,488 Btu/lb atom carbon
2. $C_{(s)} + 2H_2O(g) \rightleftarrows CO_2(g) + 2H_2(g)$	38,799 Btu/lb atom carbon
3. $C_{(s)} + CO_2(g) \rightleftarrows 2CO(g)$	74,197 Btu/lb atom carbon
4. $CO(g) + H_2O(g) \rightleftarrows CO_2(g) + H_2(g)$	-17,709 Btu/lb mole CO.

Although the carbon-steam reaction has been known and investigated for many years with a large amount of literature available on the reactions involved, it is still not completely characterized or understood. Excellent summaries of the present knowledge and conjectures of the mechanisms involved are given by Smoot and Pratt[1], Wen and Tone[2] and Wen and Lee[3] with particular interest placed on coal. Kinetic data and calculation methods are given by Von Fredersdroff[4].

In summary, here briefly is what is known and conjected about these reactions.

- equilibrium is seldom attained
- the percentage conversion of steam is greatly influenced by carbon type and size, time of contact, and temperature
- temperatures must exceed 1475^{o} F with appreciable reaction occurring around 1800^{o}-1900^{o} F
- CO and H_2 are the principal reaction products
- H_2 has a strong retarding effect on the reactions
- graphitized carbons tend to be the least reactive form of carbon, coconut shell charcoals the most reactive, and coal/chars exhibit immediate reactivity
- reactivities of coal/chars depend on parent coals and pretreatment conditions

- the reaction is chemically controlled for smaller carbon/char particles (approximately <500 μ) and at temperatures up to about 1000^{o}-1200^{o} C with the reaction occurring uniformly throughout the interior of the pore surfaces of the solid particles
- the reactions are catalyzed by ash in the coke or coal
- all reactions take place on the carbon surface
- reaction 4 (Table 2) occurs in space to a negligible extent
- diffusional effects become important above 2100^{o} F.

Wen and Tone[2] point out that char-gas reactions are catalyzed by metal salts, particularly alkali, alkali earth and transitional metals and that some of the metal salts are present in coal ash. They list catalysts for various purposes as given in Table 3.

TABLE 3

CATALYST (STRONG → WEAK)

For production of CH_4	Li_2CO_3, Pb_3O_4, Fe_3O_4, MgO
For production of H_2	K_2CO_3, Li_2CO_3, Pb_3O_4, CuO
For production of CO	K_2CO_3, Li_2CO_3, Fe_3O_4, Cr_2O_3
For gasification of C	K_2CO_3, Li_2CO_3, Pb_3O_4, Cr_2O_3

These authors also discussed recent experiments in coal gasification by Exxon and Battelle using catalysts. In the Exxon experiments, it was found that Illinois coal treated with Na_2CO_3 and/or K_2CO_3 (up to 15% K in C) had

significantly less agglomerating tendency than when untreated and further that the gasification rate was proportioned to the catalyst concentration. Battelle found that impregnation of CaO into coal before gasification prevented agglomeration and greatly influenced the reactivity and hydrocarbon yields even with large coal particles.

Conceptual Designs of Solar Chemical Reactors for Production of Syngas

A conceptual design of a fluidized bed solar chemical reactor, suitable for the production of syngas, was described in the First Quarterly Report in January 1980. Conceptual designs, generated during the past quarter, for three other types of solar chemical reactors for this purpose are described below.

Vortex-Flow Solar Chemical Reactor

CONFIGURATION: Reactor is a vertical, cylindrical cavity in which solid reactant particles are suspended in a vortex of gases.

Radiation enters through a flat window at the bottom of the reactor.

The vortex flow of the gas stream is kept in motion by an externally mounted fan.

Gas products are withdrawn through a tube in the center of the reactor; unconsumed particles fall back into the vortex.

ADVANTAGES:
1. The particles can readily interact with solar radiation.
2. Product withdrawal rates and reactant inlet rates can be independently controlled.

3. Residence time in reaction zone can be made relatively long.

4. Design is unique.

5. No secondary reflector is needed since the radiation enters from the bottom.

DISADVANTAGES: 1. An external fan operating at the reactor temperature is needed, with shaft seals, etc.

2. The reactor and fan assembly must be kept at a fairly uniform temperature to avoid cooling the steam.

3. The reactor might be difficult to construct.

SKETCH: Vortex-Flow Solar Chemical Reactor

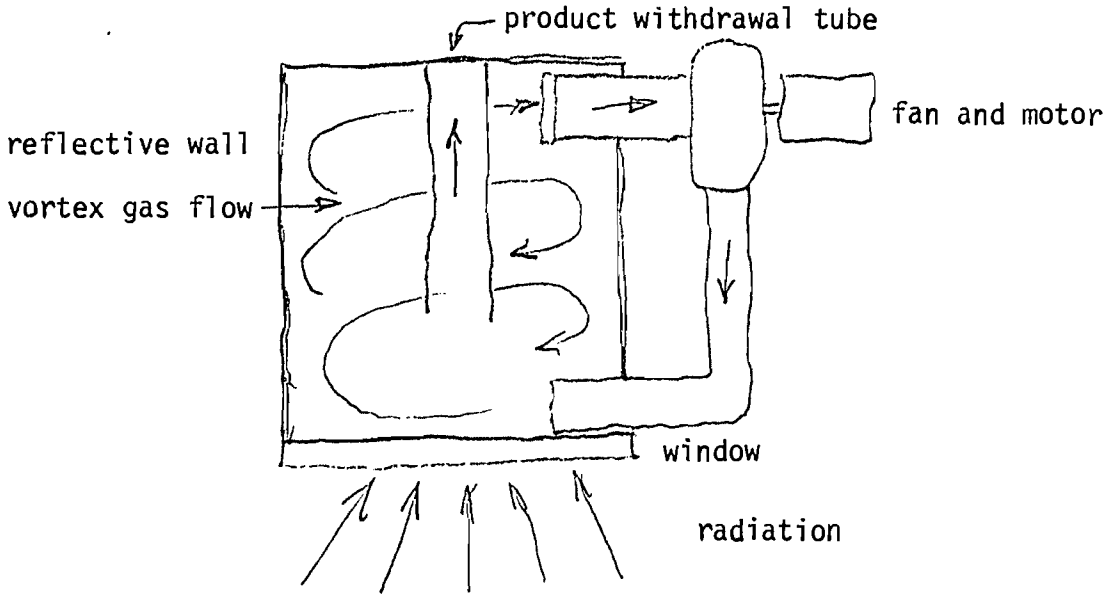

Plug-Flow Solar Chemical Reactor

CONFIGURATION: Vertical, cylindrical carbon bed, fed by screw feeder from below.

Solar radiation arrives on upper surface of carbon bed through upward-facing, horizontal window.

Water preheated in shielding and injected directly on bed surface.

ADVANTAGES: 1. Carbon will not come into contact with window; no danger of abrasion or deposits on window surface.

2. The carbon and water injection rates can be varied independently in response to radiant power input levels.

3. Reactant resistance times can be long (several seconds) in order to approach chemical equilibrium.

DISADVANTAGES: 1. A secondary reflector is required to turn the solar beam downward in any high-power test facility currently available.

2. The concept is not very "sexy" but may be very practical.

3. Scheme is similar to that used by Bob Taylor at CNRS.

SKETCH:

Plug-Flow Solar
Chemical Reactor

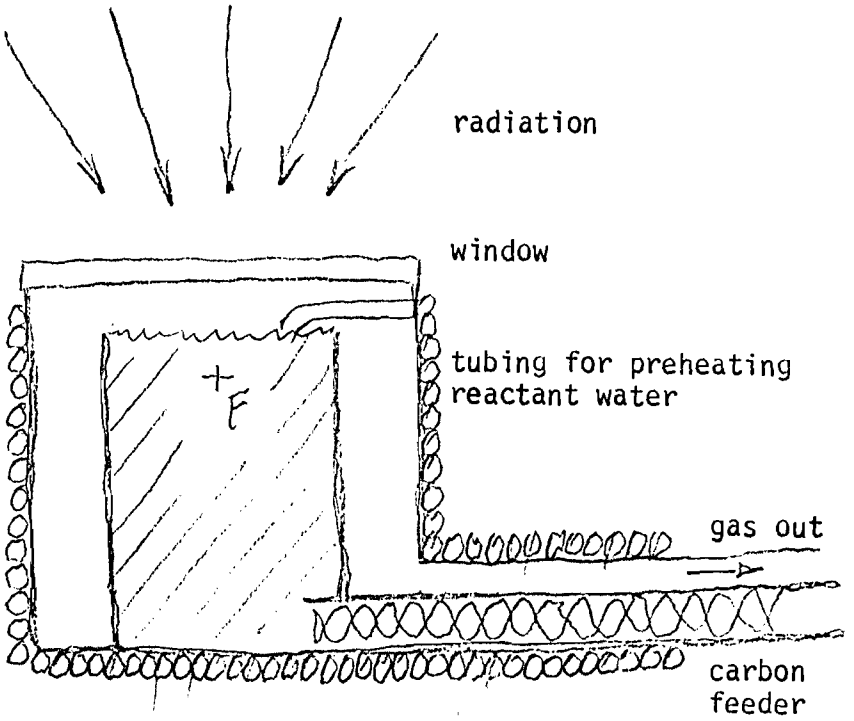

Entrained-Flow Solar Chemical Reactor

CONFIGURATION: Solar radiation arrives through a flat window at the top of the reactor.

Solid carbon particles are entrained in a cylindrical, vertical reactor volume in a flowing gas stream.

Gas stream is kept in motion by a fan within the reactor.

ADVANTAGES:

1. The particles can be readily heated by direct interaction with radiation.
2. Carbon and water injection rates can be controlled as required to respond to radiant power input levels.

DISADVANTAGES:

1. Non-caking carbon powders must be used.
2. The entire reactor must be kept at a fairly uniform temperature to avoid the cooling of steam.
3. An internal fan and high-temperature shaft seal are required.
4. Control of particle residence time in reaction zone may be difficult.

5. A secondary reflector is required to turn the solar beam downward in any high-power solar facility available now.

6. Scheme is similar to that used by Mike Antal at Princeton.

SKETCH: Entrained-Flow Solar Chemical Reactor

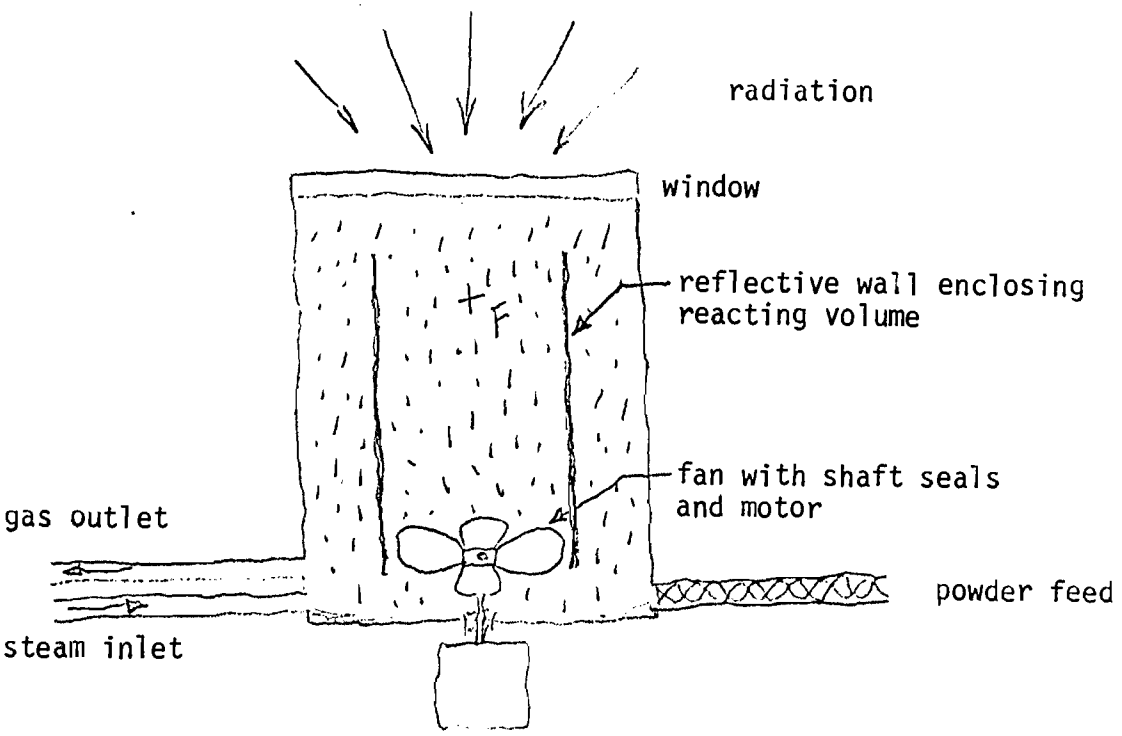

Co-Sited Solar-Chemicals Facility

It has been shown that chemicals produced through co-sited operations offer the potential for significant savings in capital investment[5,6]. The savings are achieved due to the economics of scale which result from the synergistically co-sited operations. Figure 1 is an example of a co-sited chemicals facility built around syngas. An economic analysis of a modifed version of this complex is currently being performed.

A syngas co-sited complex could further benefit from the integration of a solar coal gasification system. The solar complex would involve the production of syngas via a solar coal gasifier which would be capable of furnishing the feedstock and energy requirements of the entire complex. The potential benefits of such a complex are:

(1) Savings in capital investment.

(2) Partial substitution by solar energy of total fuel required.

(3) Ability to use conventional or developing technologies for producing ammonia, methanol, SNG, gasoline, formaldehyde, etc.

It is believed that such a complex could be designed for optimal production rates of syngas and the chosen end-products. Central to the viability of the optimized complex would be the availability of a reliable solar coal gasification system which could generate enough syngas to meet all feedstock and energy requirements. A syngas storage system or a hybrid system to

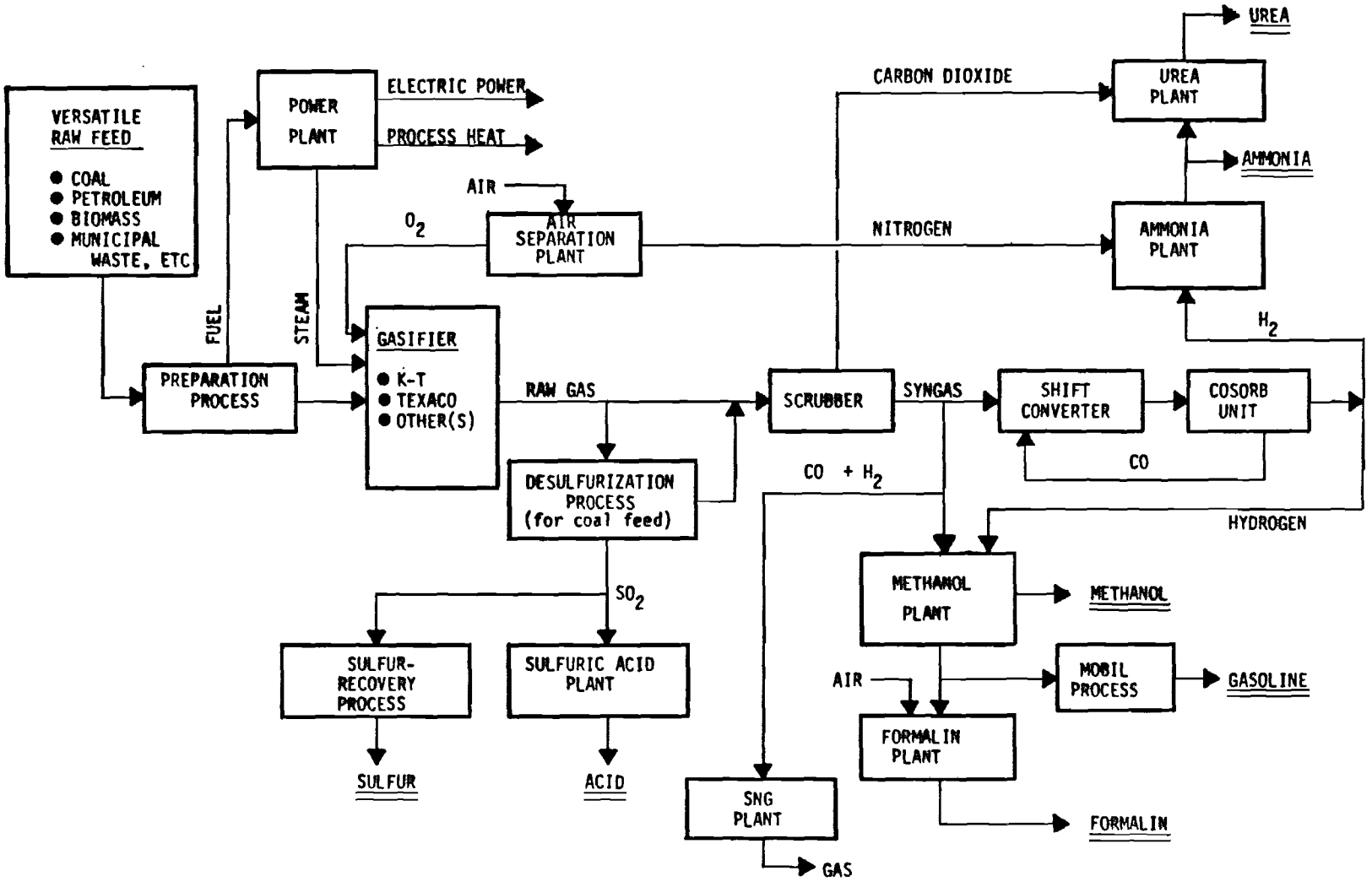

Figure 1. Hypothetical Example of a Synergistically Co-Sited Complex Based on Synthesis-Gas Feedstock from either Coal, Petroleum, Biomass or Municipal Waste

ensure continuous operation of the complex would be necessary. Preliminary technical and economic evaluations of solar coal gasification have recently been published[7,8].

Future Work

During the next quarter, all work in progress will be completed and a final project report prepared and submitted.

References

1. Smoot, L. D. and D. T. Pratt, "Pulverized-Coal Combustion and Gasification," Plenum Press, New York, 1979.

2. Wen, C. Y. and S. Tone, "Coal Conversion Reaction Engineering," Chemical Reaction Engineering Reviews - Houston, American Chemical Society Symposium Series 72, 57-109 (1978).

3. Wen, C. Y. and E. S. Lee, "Coal Conversion Technology," Addison-Wesley, Reading, Mass., 1979.

4. Von Fredersdroff, C. G., "Reactions of Carbon with Carbon Dioxide and with Steam," Chicago Institute of Gas Technology Research Bulletin 19, 1955.

5. Spurlock, J. M., H. C. Ward, J. M. Sommerfeld, and D. K. Sondhi, "Study to Investigate Potential Benefits from Synergistic Co-siting of Industrial Activities," Final Report prepared by EES, Ga. Tech for the Applachian Regional Commission, Washington (Sept. 1976).

6. Spurlock, J. M., H. C. Ward, J. M. Sommerfeld, and D. K. Sondhi, "Synergistic Co-siting of Industrial Activities," paper presented at the DESIGN 79 Conference of the Midland's Branch of I.Ch.E. held at the Univ. of Aston, Birmingham, England (Sept. 12-14, 1979).

7. Gregg, David "Solar Coal Gasification," Proceedings of Solar Fuels Workshop held by Solar Thermal Test Facilities Users Association at Albuquerque, New Mexico (November 28-29, 1979).

8. Mathur, V. K. "Economics and Technology of Solar Gasification," Proceedings of Solar Fuels Workshop held by Solar Thermal Test Facilities Users Association at Albuquerque, New Mexico (November 28-29, 1979).

FINAL REPORT

Project A–2494

A COOPERATIVE PROGRAM OF APPLIED ENERGY RESEARCH AND TECHNOLOGY DEVELOPMENT

I. Catalytic Conversion of Biomass to Useful Fuels

II. Materials and Designs for Solar Chemical Reactor

III. Coal Desulfurization

By

R.A. Cassanova
J.A. Knight
S.H. Bomar
D.R. Hurst
L.W. Elston
H.C. Ward

Subcontract From Atlanta University
U.S. Department of Energy
Grant No. DE–FG05–79ET60058

June 1981

GEORGIA INSTITUTE OF TECHNOLOGY
A Unit of the University System of Georgia
Engineering Experiment Station
Atlanta, Georgia 30332

1981

GEORGIA INSTITUTE OF TECHNOLOGY

Engineering Experiment Station

Atlanta, Georgia

Final Technical Report

October 1, 1979 - December 31, 1980

Project A-2494-001

CATALYTIC CONVERSION OF BIOMASS TO USEFUL FUELS

by

J. A. Knight, D. R. Hurst, and L. W. Elston

December 31, 1980

SUMMARY

The Georgia Institute of Technology and the Atlanta University have participated in a cooperative project directed to applied research in alternative energy technologies. Exploratory studies of biomass, solar thermal processes and coal were conducted and included:

(1) production of medium Btu gas from woody biomass

(2) gasification kinetics

(3) solar fuels and chemicals for energy storage

(4) high temperature solar reactor materials and configurations

(5) entrained systems for pyrolysis of coal.

Atlanta University acted as the prime contractor to the U.S. Department of Energy and subcontracted to the Georgia Institute of Technology Engineering Experiment Station through the Georgia Tech Research Institute for research on:

(1) Catalytic conversion of biomass to useful fuels

(2) Materials and designs for solar chemical reactors

(3) Coal desulfurization

This final subcontractor report covers these three tasks conducted by Georgia Tech.

CONTENTS

LIST OF FIGURES

LIST OF TABLES

SECTION I

INTRODUCTION

The pyrolysis of lignocellulosic waste materials typically yields char, an oil condensate, an aqueous condensate, and noncondensible gases. The char and condensed oil are storable and transportable products. The noncondensible gas yield, depending on the process method chosen, has a low to medium higher heating value (5,500 -16,700 kJ/kg) and must be consumed on site for process energy or as a synthesis gas feedstock. The aqueous yield typically contains two to fifteen percent dissolved or entrained organic material.

The purpose of this study was to examine the effect in the Georgia Tech 15.2 cm tube furnace apparatus (Appendix A) of catalysts mixed with the feed material on the resulting yield distributions and on the properties of the recovered products. These catalysts should be inexpensive, recoverable, and inoffensive to the environment. The results sought in these experiments were a high yield of noncondensible gas with a high heating value and a ratio approaching two moles of hydrogen per mole of carbon monoxide for potential synthesis applications. It was also desired to reduce the miscibility of the organic and aqueous condensates to enhance the recovery of condensible organics and to minimize the required cleanup of the aqueous condensate.

This study includes only catalysts reported to be effective in increasing the overall gas yields. Future proposals are planned for the study of transition metal catalysts and combined catalyst systems.

SECTION 2

REPRESENTATIVE PYROLYSIS LITERATURE

The literature describing pyrolytic conversion of lignocellulosic materials and wastes to more useful fuels is voluminous and largely repetitive. Therefore, only a few representative publications directly related to this study are cited.

Feldman (1) used both alkaline salts and wood ash to increase the gasification yields from the catalyzed pyrolysis of several types of wood.

J. L. Cox et al. (2) gasified entrained organic waste under pressurized conditions using nickel catalysts and alkaline earth salts. Although the feedstocks did not include lignocellulosic wastes, the data on raw paper indicate that the method might be useful for biomass gasification.

Appell and Pantages (3) describe the use of alkaline earth salts and zeolites as catalysts to decompose a carbohydrate model glucose and a sawdust feedstock. The results indicate that potassium carbonate is a potent gasification catalyst.

Sealock, et al. (4) report the preparation of synthetic natural gas by treatment of biomass with steam in the presence of an alkali metal carbonate gasification catalyst and a nickel methanation catalyst.

Mudge et al. (5) describe the gasification of biomass in the presence of alkali-metal carbonates and borax at 550 and 650°C. In all cases the barks produced higher yields of gas than their respective woods.

Feber and Antal (6) report that the presence of alkali metal carbonates led to a two to three-fold increase in the rate of char gasification with steam at 650°C and up to ten-fold increases in the rate of gasification with carbon dioxide.

Appell et al. (7) reported the decomposition of several cellulosic wastes at relatively low temperatures (250 - 425°C) and high pressures (1,500 - 4,000 psig) to produce high oil yields. Cobalt molybdate on alumina used with an alkali metal carbonate produced oil with a lower oxygen content and lower viscosity than did alkali metal carbonate alone.

Kaufman and Weiss (8) present an extensive survey of the literature on the liquefaction of cellulosic materials. The uses of catalysts, an oil carrier to reduce the necessary pressures and the role of water in the reactions are discussed.

SECTION 3

RECOMMENDATIONS

The experimental results of this study and the findings reported in the literature indicate that potentially valuable research with catalysts on the pyrolysis and gasification of biomass could be conducted in the following areas:

Examination of transition metal catalysts such as cobalt, molybdenum chromium and iron compounds in conjunction with alkali metal carbonate catalysts for beneficial effects on the total yield and composition of the noncondensible gas products,

Recirculation of noncondensible gases through the heated reaction mass to determine if the yield and calorific value of the evolved gas is increased,

Determination of the effect of recirculating the condensed water phase through the reaction mass at temperatures above 700^{o}C on the yields of gases and low molecular weight organic compounds, and

Exploring the effectiveness of reactions at moderate pressures in reducing the oxygen content of the condensible organics and the miscibility of the aqueous and organic phases.

SECTION 4

EXPERIMENTAL PROCEDURES

GENERAL PROCEDURES

Four samples, each containing 1,869 g (bone dry basis) pine sawdust were pyrolized in the 15.2 cm tube furnace apparatus. The first charge consisted only of air dried pine sawdust. The second charge consisted of an air dried mixture of pine sawdust and potassium carbonate. The third charge consisted of well mixed air dried pine sawdust and finely divided pine sawdust char. The fourth charge was a well blended mixture of air dried pine sawdust and ash from the combustion of pine char. The liquid products collected in the condensation trains, the noncondensible gases collected in 96 liter plastic bags, and the chars recovered from the cooled furnace tubes were analyzed in the laboratory. The furnace heating programs were similar for all of the runs, although the heating rates and gas evolution rates within the charges differed.

The charge weights, yields, and results of laboratory analysis were used to calculate mass and energy balances for the four experiments.

The construction and operation of the tube furnace apparatus and the condensation train are described in Appendix A and Appendix B, respectively.

PYROLYSIS PROCEDURES

To evaluate the effects of potassium carbonate, char, and ash additives on the rate of pyrolysis and the composition of pyrolysis products the quantities of "bone dry" sawdust feed and the furnace heating programs were the same for all four runs.

Charge Preparation

The charge for the first (baseline) pyrolysis consisted of 2 kg air dried pine sawdust.

The charge material for the second pyrolysis was prepared by wetting 2,500 g air dried pine sawdust with a solution prepared by dissolving 375 g anhydrous potassium carbonate in 500 ml deionized water. The mixture was air dried to constant weight with frequent stirring. The percent moisture in the air dried mixture was determined, and the weight of a pyrolysis charge containing 1,869 g "bone dry" sawdust was calculated

The charge for the third pyrolysis was prepared by mixing 180 g finely ground wood char from the first run with 2 kg air dried pine sawdust for two hours in a jar mill. The finely divided char appeared to coat the sawdust particles evenly, and there were no free char fines.

The charge for the fourth run consisted of 2,000 g air dried pine sawdust and 500 g wood ash as a catalyst.

The wood ash was prepared by igniting pine char prepared in the Georgia Tech Blue IV Waste Converter. The ash was spread in shallow layers on stainless steel trays, stirred occasionally for 72 hours, and passed through a series of screens on a Ro-tap sieve shaker. The fraction of the ash passing a 60 mesh screen was a uniform tan powder free from unburned material and clinkers. Subsequent analysis of the ash showed no moisture and 25.0 percent (by weight) carbon dioxide.

The weighed pine sawdust and ash were mixed for two hours in a jar mill to produce a uniformly coated granular material free from unbound ash. The charge was transferred quantitatively from the mixing jar to the furnace tube.

Heating Program

The center zone of the furnace was heated continuously at its maximum rate, 6.4 $\pm$ 0.5°C per minute, to 650°C and held at that temperature until there was no further evidence of reaction within the tube. The temperatures of the end zones of the furnace were allowed to rise to their minimum set point, 200°C, and then increased stepwise in 100°C increments and a final 50°C increment as the more slowly rising temperature of the center furnace zone reached the set temperature at the end zones. This procedure insured that the ends of the tube wall were sufficiently warm to prevent condensation of vapors formed in the cooler center zone, while the high mass of the tube, 48 kg, prevented the development of sharp temperature differences along the tube wall.

ANALYTICAL METHODS

The percent moisture and percent ash in the feeds and chars and the percent volatiles in the chars were determined by ASTM Method D1762-64. The acid insoluble ash in the feed and chars was determined by the method used for sand and insoluble silicates by the Association of Florida Phosphate Chemists. Heating values were determined by oxygen bomb calorimetry following the plain calorimeter method described in Parr Manual No. 130*. The bulk density of the chars was determined by weighing a measured volume of the unground material.

The heavy organic phases and the lighter aqueous phases were separated by decantation and weighed. The moisture content of each heavy organic phase and aqueous phase was determined by azeotropic distillation with toluene (Dean and Stark Method). The heating values of the heavy organic phases were determined by oxygen bomb calorimetry. The densities of these phases were determined by weighing well stirred samples of known volume.

The yields of light oil in the dry ice traps were determined by weighing the condensates in tared, tightly stoppered polyethylene bottles. Heating values were determined by oxygen bomb calorimetry.

The concentrations of the major gases in each of the collected samples for each of the runs were determined separately by gas chromatography. Evolved gas yields were calculated by adding the volumes of each gas in each of the collected samples. The gas remaining in the system at the end of each run was sampled by means of gas syringes inserted through the tubing wall near the gas meter. The total volume of the final gas sample was taken to be the sum of the volume of the collection train and the volume of gas in the pyrolysis tube corrected to 101.33 kiloPascals at 25°C.

* Parr Instrument Company, Moline, Illinois

SECTION 5

RESULTS AND DISCUSSION

Analytical Results

The analytical results for the feeds, chars, and condensates resulting from all four pyrolysis runs are shown in composite tables for easy comparison. The more voluminous gas analysis data require separate tables for each run, but a condensed summary table is presented for easy comparison.

Proximate Analysis of Feeds and Chars

Results of the proximate analyses of the feeds and chars are shown in Table 1.

The feed analysis for the first run (94-1-1) and the percent moisture in the second run (94-1-2) and all of the char data were determined experimentally. As the pine sawdust for the remaining three runs was identical to that used in the first run, the feed data for the second run were calculated from the first run feed data, the determined percent moisture in the mixture, and the known weight of potassium carbonate in the charge. The feed data for the third run (94-1-3) were calculated from the weights of the first run sawdust and char in the mixture and the experimentally determined properties of the components. The feed data for the fourth run (94-1-4) were calculated from the weights of the pine sawdust and dry ash, and the known values for the first run pine sawdust. It is immediately apparent that the presence of the catalyst strongly effects the heating value of the sawdust-catalyst mixture and the resulting char.

The percent moisture in the char for Run 94-1-2 could not be determined, as the sample gained weight in the drying oven. This observation is attributed to reaction between the potassium oxide catalyst residue and atmospheric carbon dioxide.

The presence of the char catalyst residue in Run 94-1-3 has little effect on the ash content or the heating value of the resulting char products. Residues from potassium carbonate (Run 94-1-2) and ash (Run 94-1-4) lead to sharp increases in ash and decreases in the heating value of the recovered char. The low concentrations of insoluble ash in these chars, however, suggests that much of the alkaline caalyst residue could be leached from the char and recycled and that the leached and dried char would constitute a clean burning solid fuel with less than five percent ash and heating values approaching 24,400 kJ/kg (10,500 Btu/lb) for the ash catalyzed char and 32,500 kJ/kg (14,000 Btu/lb) for the char prepared with potassium carbonate.

Condensates

Results of the laboratory analysis of the recovered condensates are shown in Table 2.

The presence of potassium carbonate catalyst (Run 94-1-2) led to a sharp increase in the percent water dissolved in the organic condensate phase and an almost complete absence of organics in the aqueous phase. A parallel but much smaller effect was observed with the ash catalyst (Run 94-1-4). The char catalyst (Run 94-1-3) slightly reduced the solubilities of the oil in water and water in oil. None of the catalysts greatly effected the yield of light oil.

Corrected Condensate Analysis

The detergent properties of many of the condensed organic compounds sharply increases the mutual solubilities of the organic and aqueous phases. Several years of pilot plant operating experience have indicated that good condenser design and careful selection of condenser temperatures can significantly reduce the moisture content of the recovered oil and the fraction of oil entrained in the gases and uncondensed water. These observations have been used in calculating values for oil-free water and water-free oil. The values shown in Table 3 represent an ideal case, which can be approached but probably never reached.

Inspection of these data indicates that the potassium carbonate catalyzed run (94-1-2) produced only about half as much total oil as did the baseline run (94-1-1) and that very little of the oil from potassium carbonate catalyzed pyrolysis was water soluble. The water free basis heating value of the K_2CO_3 catalyzed oil was 13.7 percent higher than that of the baseline oil. The char catalyzed heavy oil yield was 9 percent less than that of the baseline oil, and its water free basis heating value was nearly 10 percent less. Its water solubility was also diminished. The ash catalyzed heavy oil yield was only 60 percent of the baseline yield, but its "water free" higher heating value approached the 41,800 kJ/kg (18,000 Btu/lb) commonly associated with heavy (No. 6) petroleum fuels. Its water solubility was low.

Both the potassium carbonate and the char catalysts led to a decrease in water production. None of the catalysts greatly effected the yield of light oil.

Evolved Gases

The gases evolved during the four pyrolysis runs were collected in plastic bags and analyzed by gas chromatogaphy. Results of these analyses are shown in Tables 4, 5, 6 and 7. Each of the bags represents an integrated sample. Equipment for instantaneous (grab) sampling was used during the ash catalyzed run. The composition of these grab samples is shown in Table 8.

The data for these small samples have been corrected for the air in the connecting tubes, i.e., the percent oxygen and percent nitrogen, and the concentration of each of the remaining gases were adjusted to an air-free basis. The data shown in Tables 4-8 are not normalized.

Properties of Gases Evolved from Pyrolysis

The data in Tables 4-7 were used to calculate the total volumes of each of the gases evolved during the pyrolysis runs. The air introduced by sampling errors was subtracted, and the volume percentages were adjusted by the procedure applied to the grab samples. The volume of purge nitrogen present at the start of each run was then subtracted. The calculated volume of carbon dioxide evolved from the decomposition of the potassium carbonate catalyst was subtracted from the total carbon dioxide yield for Run 94-1-2. The percent carbon dioxide in the ash catalyst was determined using separate samples of the ash, and the calculated volume of carbon dioxide was subtracted from the total carbon dioxide yield for Run 94-1-4. The calculated evolved gas yields from the four pyrolysis runs are shown in Tables 9, 10, 11 and 12.

For ready comparison, the gas yield data are collected in Table 13.

The first four columns show the volumes of each gas evolved per kilogram of dry feed. Moles of each gas per kg of dry feed can be estimated by multiplying the gas

volumes by 0.0446. The last four columns show the relative effects of the catalysts on the evolved gas volume expressed as percent of the gas volume evolved in the absence of a catalyst. The alkaline catalysts, potassium carbonate and ash, led to large increases in the hydrogen yield and consequent decreases in the gas density, but only small effects on the volume basis higher heating values.

The pyrolysis yield data from the four runs are collected in Table 18 to permit ready comparison of the catalyst effects. The water yield data represent only water from the decomposition of dry sawdust, i.e. the input waters have been subtracted from the total water outputs shown in the heat and mass balance tables. Purge gas and gases evolved from catalyst decomposition are not included in the noncondensible gas yields.

Mass and Energy Balances

The input feed and catalyst weights and the yield data calculated from laboratory analyses of the inputs and products were used to prepare mass and energy balances for each of the four tube furnace experiments. These balances are shown in Tables 14, 15, 16, and 17.

Effects of Catalytic Agents on Product Yields and Heating Values

The data show that the wood char had the least effect of the catalysts studied on the product yields from sawdust. The oil yield decreased about nine percent of the oil yield the baseline experiment whereas the gas yield increased about 13 percent. The heating value of the gaseous product from the experiment with wood char as a catalyst is the same within experimental error as the gas from the baseline experiment. The heating value of the heavy oil from the wood char experiment decreased about 10 percent as compared with the heavy oil from the baseline experiment.

The potassium carbonate and wood ash had similar effects on the pyrolytic product yields. The yields of char were reduced about 23 percent with potassium carbonate and about 30 percent wood wood ash. With the heavy oil, the yield decreased 48 percent with potassium carbonate and only six percent with wood ash. The light oil yields for all four experiments were in the range of 1.2 to 1.5 percent. The total water yields increased to 35.6 and 41.1 percent for potassium carbonate and wood ash respectively as compared to a yield of 28.1 percent for the baseline sawdust experiment.

It is of interest that although the oil yields for both the potassium carbonate and wood ash experiments decreased, the heating values of the oil were 38,040 kJ/kg (16,365 Btu/lb) and 41,757 kJ/kg (17,964/Btu/lb) respectively. The heating value for the heavy oil from the sawdust alone was 33,4359 kJ/kg (14,394 Btu/lb). The heating value for the heavy oil from wood char catalytic experiment decreased about 10 percent of the heating value of the oil from the sawdust alone. The heating values for the gaseous products showed increases of about 9 percent and 14 percent for the potassium carbonate and wood ash experiments respectively. The gaseous product from the sawdust alone had a heating value of 13,054 kJ/kg (5,616 Btu/ lb) whereas the heating value of the gaseous phase from the wood char experiment had a value of 13,214 kJ/kb (5,686 Btu/lb). In summary, potassium carbonate and wood ash had the most pronounced effects on the products yields from sawdust. The heavy oils from the experiments with potassium carbonate and wood ash had significantly higher heating values than the oil from sawdust alone. The results indicate that alkali and alkaline oxides have potential as catalysts for the pyrolysis/gasification of biomass.

TABLE 1. ANALYSIS OF FEEDS AND CHARS

Run Number	94-1-1		94-1-2		94-1-3		94-1-4	
Catalyst	None		K_2CO_3		Char		Ash	
Heating Rate (°C/minute)	6.5		6.3		7.0			
Determination	Feed	Char	Feed	Char	Feed	Char	Feed	Char
Percent Moisture*								
Sample 1	6.5	0.4	8.1	N/A	5.7	0.2	5.2	N /A
Sample 2		0.5				0.3		
Average		0.5				0.3		
Percent Volatiles								
Sample 1	N/A	6.1	N/A	9.7	N/A	5.3	N/A	21.5
Sample 2		6.1		9.7		5.7		21.0
Average		6.1		9.7		5.5		21.3
Percent Ash								
Sample 1	0.6	5.6	12.3	37.6	—	4.2	—	35.7
Sample 2	0.6	5.4	12.8	37.2	—	4.2	—	35.9
Average	0.6	5.5	12.6	37.4	1.3	4.2	25.6	35.8
Percent Acid Insol. Ash								
Sample 1	0.1	2.3	0.1	2.3	N/A	2.5	N/A	4.6
Sample 2	0.2	2.0	0.1	2.7		2.3		4.9
Average	0.2	2.2	0.1	2.5	—	2.4		4.8
Higher Heating Value, kJ/kg								
Sample 1	20,014	33,027	17,093	21,858	—	33,737		17,146
Sample 2	19,704	33,027	17,091	21,825	—	33,868	17,183	
Average	19,861	33,027	17,092	21,842	21,586	33,711	15,889	17,164
(Btu/lb)	(8,532)	(14,188)	(7,343)	(9,383)	(9,273)	(14,842)	(6,826)	(7,384)

*Percent moisture on "as run" basis, others on bone dry basis.

TABLE 2. LABORATORY ANALYSIS OF CONDENSATES

Run Number	94-1-1	94-1-2	94-1-3	94-1-4
Catalyst	None	K_2CO_3	Char	Ash
Heating Rate (^oC/minute)	6.5	6.3	7.0	6.1
Organic Phase*+				
Phase Weight, kg	0.1910	0.3421	0.1823	0.1916
Percent Moisture				
Sample 1	22.6	63.2	14.9	38.7
Sample 2	22.2	63.3	15.1	37.7
Average	22.4	63.3	15.0	38.2
Heating Value, kJ/kg				
Sample 1	25,939	13,727	26,999	25,832
Sample 2	25,818	14,212	27,274	25,779
Sample 3	26,080	13,942	—	—
Average	25,946	13,960	27,137	25,806
(Btu/lb)	(11,161)	(6,006)	(11,674)	(11,102)
Bulk Density, Kg/m^3	1,098	1,066	1,099	1,090
(lb/gal)	(9.0)	(8.9)	(9.0)	(8.9)
Aqueous Phase**				
Phase Weight, kg	0.7117	0.5400	0.6666	0.7688
Percent Moisture				
Sample 1	86.9	99.9	89.8	96.0
Sample 2	85.5	99.6	90.2	96.4
Average	86.2	99.8	90.0	96.2
Light Oil***				
Phase Weight, kg	0.0238	0.0238	0.0272	0.0234

*Phases collected in Tube Furnace Off Gas Collection Train. Appendix B.
+Organic and aqueous phases collected in ice cooled traps and demisters
**Water collected in dryer
***Light oil collected in dry ice traps

TABLE 3. CORRECTED CONDENSATE ANALYSIS

Run Number	94-1-1	94-1-2	94-1-3	94-1-4
Catalyst	None	K_2CO_3	Char	Ash
Heating Rate (^oC/minute)	6.5	6.3	7.0	6.1
Separated Oil (water free)				
Yield Weight, kg	0.1482	0.1256	0.1570	0.1184
Higher Heating Value, kJ/kg	33,459	38,040	30,151	41,757
(Btu/lb)	(14,394)	(16,365)	(12,971)	(17,964)
Dissolved/Dispersed Oil (water free)				
Yield Weight, Kg	0.0982	0.0026	0.0667	0.0292
Higher Heating Value, kJ/kg	33,459	38,040	30,151	41,757
(Btu/lb)	(14,394)	(16,365)	(12,971)	(17,964)
Total Heavy Oil (water free)				
Yield Weight, Kg	0.2464	0.1282	0.2237	0.1476
Higher Heating Value kJ/kg	33,459	38,040	30,151	41,757
(Btu/lb)	(14,394)	(16,365)	(12,971)	(17,964)
Water				
Yield Weight, Kg	0.6563	0.5650	0.5082	0.6378
Light Oil				
Yield Weight, Kg	0.0224	0.0238	0.0272	0.0234
Higher Heating Value kJ/kg*	41,841	41,841	41,841	41,841
(Btu/lb)	(18,000)	(18,000)	(18,000)	(18,000)

*Estimate based on previous laboratory of similar condensates.

TABLE 4. GAS CHROMATOGRAPHIC ANALYSIS, RUN 94-1-1

Bag No. Volume (liters)	1 103	2 88	3 82	4 84.6	5 84.4	Final 30.1
Gas	Percent by Volume					
Oxygen	0	0.6	0.9	1.6	0.4	0.1
Nitrogen	43.8	4.1	4.4	7.0	1.9	0.6
Carbon Monoxide	19.9	33.9	31.0	27.8	21.4	14.1
Carbon Dioxide	32.6	36.7	26.9	23.3	21.5	19.5
Hydrogen	0	3.2	7.2	12.9	23.5	36.6
Methane	2.9	13.7	18.7	20.5	26.2	29.7
Ethane	0.3	1.3	1.8	1.3	1.0	0.1
Ethylene	0.2	1.0	1.3	1.3	0.7	0.1
Propane	0.1	0.4	0.5	0.3	0.2	0.1
Propylene	0.1	0.7	1.0	0.9	0.5	0.1
Butanes, Butenes	0.1	0.3	0.4	0.4	0.2	0.1
Total	100.0	95.9	94.1	97.3	97.5	100.6

TABLE 5. GAS CHROMATOGRAPHIC ANALYSIS, RUN 91-1-2

Bag No. Volume (liters)	1 90	2 90	3 90	4 90	5 90	6 90	7 113.7	Final 30.1
Gas	Percent by Volume							
Oxygen	<.1	<<.1	<<.1	<<.1	<<.1	<<.1	<<.1	—
Nitrogen	42.7	3.2	0.9	2.6	<.01	0.2	<.01	—
Carbon Monoxide	12.9	28.1	22.6	18.4	14.7	10.5	13.3	16.0
Carbon Dioxide	47.8	67.8	53.1	42.6	33.1	20.5	8.2	6.1
Hydrogen	<.01	0.6	5.7	15.2	26.9	45.5	59.4	61.3
Methane	0.2	3.1	11.9	14.8	18.2	20.9	17.7	18.1
Ethane	0.22	0.97	3.34	3.82	3.88	3.42	0.74	—
Ethylene	0.01	0.24	0.70	0.81	1.05	0.94	0.21	—
Propane	0.01	0.38	1.18	1.18	1.13	0.88	0.16	—
Propylene	0.01	0.22	0.70	0.72	0.80	0.69	0.14	—
Butanes	<<.01	0.14	0.45	0.46	0.44	0.33	0.05	—
Butenes	<<.01	0.22	0.70	0.72	0.80	0.69	0.14	—
Total	103.9	105.0	101.3	101.3	101.0	104.6	100.0	101.5

TABLE 6. GAS CHROMATOGRAPHIC ANALYSIS, RUN 94-1-3

Bag No.	1	2	3	4	5	6	Final
Volume (liters)	90	90	90	90	90	66.5	30.1
Gas	Percent by Volume						
Oxygen	<.01	<.01	<.01	<.01	<.01	<.01	0
Nitrogen	43.6	2.1	0.1	1.8	0	0	0
Carbon Monoxide	17.3	30.2	29.2	26.7	24.2	17.5	13.9
Carbon Dioxide	34.5	43.5	33.5	28.9	28.2	22.4	15.3
Hydrogen	0.2	5.0	11.8	17.6	21.3	28.8	38.0
Methane	2.0	11.8	18.0	19.7	20.8	28.0	32.4
Ethane	0.30	1.68	2.02	1.78	1.82	1.20	—
Ethylene	0.23	0.94	1.17	1.22	1.07	0.63	—
Propane	0.11	0.49	0.48	0.43	0.28	0.31	—
Propylene	0.09	0.92	1.23	0.97	0.91	0.39	—
Butanes	0.02	0.11	0.09	0.10	0.10	0.03	—
Butenes	0.04	0.21	0.21	0.29	0.32	0.11	—
Total	98.4	98.4	97.8	99.4	99.1	99.4	99.6

TABLE 7. GAS CHROMATOGRAPHIC ANALYSIS, RUN 94-1-4

Bag No.	1	2	3	4	5	6	7	Final
Volume (liters)	90	90	90	90	90	90	69.1	30.1
Gas	Percent by Volume							
Oxygen	1.07	.47	.65	1.77	.66	< .01	1.32	.51
Nitrogen	47.2	4.46	2.51	7.13	2.74	< .01	4.69	1.82
Carbon Monoxide	12.8	23.7	20.3	15.8	13.5	12.2	14.0	16.6
Carbon Dioxide	38.5	58.2	46.4	35.8	32.0	25.5	9.41	7.22
Hydrogen	21	1.55	13.7	19.1	30.6	39.0	49.3	50.5
Methane	.56	6.15	13.4	15.3	16.8	18.8	20.6	21.2
Ethane	.07	1.09	2.61	2.40	2.18	1.98	.42	.15
Ethylene	.10	.82	1.56	1.57	1.52	1.27	.16	.09
Propane	.03	.47	.74	.61	.51	.42	.06	.03
Propylene	.04	.12	.83	.82	.73	.57	.07	.05
Butanes	.01	.45	.19	.17	.13	.10	.02	.02
Butenes	<< .01	<< .01	.28	.35	.28	.19	.03	.02
Total	100.6	97.5	103.2	100.8	101.7	100.0	100.1	98.1

TABLE 8. GRAB SAMPLES OF NONCONDENSIBLE GASES, RUN 94-1-4

Grab No.	1*	2	3	4	5	6	7
Temperature (°C)+	100	118	143	185	376	590	650
Liters Evolved	90	180	270	360	450	540	600
Liters/Minute	8	9	12	16	13	4	0.01
Gas	Percent by Volume						
Carbon Monoxide	—	24.6	19.5	15.7	13.0	12.3	17.0
Carbon Dioxide	—	55.2	43.7	35.8	30.0	15.4	7.40
Hydrogen	—	3.88	15.2	26.5	34.8	46.2	51.7
Methane	—	9.78	16.0	17.6	17.3	24.0	21.7
Ethane	—	2.50	2.73	2.50	2.04	1.36	.15
Ethylene	—	1.44	1.68	1.71	1.48	.52	.09
Propane	—	.83	.72	.62	.45	.21	.03
Propylene	—	.83	.86	.83	.67	.21	.05
Butanes	—	.22	.18	.15	.11	.05	.02
Butenes	—	.47	.39	.47	.39	.13	.02
Total		99.8	101.0	101.9	100.2	100.4	98.1

*Lost sample

+At center of charge

TABLE 9. GASES EVOLVED FROM PYROLYSIS RUN 94-1-1

Gas	Volume (liters)	Moles	Formula Weight	Weight grams	Mass Fraction	HHV kJ/kg (Btu/lb)	HHV kJ/kg mix (Btu/lb mix)
Carbon Monoxide	133.1	5.942	28	166.4	.3088	10,105 (4,347)	3,119 (1,342)
Carbon Dioxide	143.4	6.402	44	281.7	.5227	0 (0)	0 (0)
Hydrogen	55.0	2.455	2	4.9	.0091	142,027 (61,100)	1,292 (556)
Methane	86.0	3.839	16	61.4	.1139	55,507 (22,879)	6,323 (2,720)
Ethane Ethylene	8.9	.397	30	11.9	.0221	51,883 (22,320)	1,146 (493)
Propane Propylene	4.6	.205	44	9.0	.0167	50,351 (21,661)	841 (362)
Butanes Butenes	1.4	.062	58	3.6	.0067	49,530 (21,308)	332 (143)
Total	432.4	19.3		538.9	1.0000		13,054 (5,616)

Average Molecular Weight = 27.9
Density = 1.245 kg/m^3 (0.0776 lb/SCF)
HHV (Volume Basis) = 16,260 kJ/m^3 (407 Btu/SCF)

TABLE 10. GASES EVOLVED FROM PYROLYSIS RUN 94-1-2

Gas	Volume (liters)	Moles	Formula Weight	Weight grams	Mass Fraction	HHV kJ/kg (Btu/lb)	HHV kJ/kg mix (Btu/lb mix)
Carbon Monoxide	116.6	5.205	28	145.7	.2186	10,105 (4,347)	2,204 (948)
Carbon* Dioxide	202.5	9.040	44	397.8	.5951	0 (0)	0 (0)
Hydrogen	171.1	7.638	2	15.3	.0228	142,027 (61,100)	3,238 (1,393)
Methane	87.9	3.924	16	62.8	.0939	55,507 (23,879	5,212 (2,242)
Ethane Ethylene	18.5	.826	30	24.8	.0370	51,883 (22,320)	1,920 (826)
Propane Propylene	7.3	.335	44	14.7	.0220	50,351 (21,661)	1,109 (477)
Butanes Butenes	2.8	.125	58	7.3	.0108	49,530 (21,308)	535 (230)
Total	606.7	27.1		668.4	1.0002		14,218 (6,116)

Average Molecular Weight = 24.7
Density = 1.103 Kg/m^3 (0.0688 Btu/SCF)
HHV (Volume basis) = 15,682 kJ/m^3 (421 Btu/SCF)

*Does not include carbon dioxide from catalyst.

TABLE 11. GASES EVOLVED FROM PYROLYSIS RUN 94-1-3

Gas	Volume (liters)	Moles	Formula Weight	Weight grams	Mass Fraction	HHV kJ/kg (Btu/lb)	HHV kJ/kg mix (Btu/lb mix)
Carbon Monoxide	130.7	5.835	28	163.4	.2695	10,105 (4,347)	2,723 (1,172)
Carbon Dioxide	171.6	7.661	44	337.1	.5559	0 (0)	0 (0)
Hydrogen	81.6	3.643	2	7.3	.0120	142,027 (61,100)	1,704 (733)
Methane	93.7	4.183	16	66.9	.1103	55,507 (23,879	6,122 (2,634)
Ethane Ethylene	12.2	.545	30	16.4	.0270	51,883 (22,320)	1,401 (603)
Propane Propylene	5.9	.263	44	11.6	.0191	50,351 (21,661)	962 (414)
Butanes Butenes	1.4	.063	58	3.7	.0061	49,530 (21,308)	302 (130)
	497.1	22.2		606.4	.9999		13,214 (5,686)

Average Molecular Weight = 27.3
Density = 1.219 kg/m^3 (0.0766 lb/SCF)
HHV (Volume basis) = 16,941 kJ/m^3 (455 Btu/SCF)

TABLE 12. GASES EVOLVED FROM PYROLYSIS RUN 94-1-4

Gas	Volume (liters)	Moles	Formula Weight	Weight grams	Mass Fraction	HHV kJ/kg (Btu/lb)	HHV kJ/kg mix (Btu/lb mix)
Carbon Monoxide	107.7	4.808	28	123.4	.2173	10,105 (4347)	2,197 (945)
Carbon* Dioxide	169.0	7.545	44	332.0	.5847	0 (0)	0 (0)
Hydrogen	148.0	6.607	2	13.2	.0232	142,027 (61,100)	3,296 (1,418)
Methane	85.7	3.826	16	61.2	.1078	55,507 (23,879	5,983 (2,574)
Ethane Ethylene	16.6	.741	30	22.2	.0391	51,883 (22,320)	2,029 (873)
Propane Propylene	5.7	.255	44	11.2	.0197	50,351 (21,661)	993 (427)
Butane Butenes	1.8	.080	58	4.6	.0081	49,530 (21,308)	402 (173)
	534.5	23.9		567.8	.9999		14,900 (6,410)

Average Molecular Weight = 23.8
Density = 1.067 kg/m^3 (0.0666 lb/SCF)
HHV (Volume basis) = 15,898 kJ/m^3 (427 Btu/SCF)

*Does not include 50.1 liters carbon dioxide released by decomposition of the ash catalyst.

TABLE 13. COMPARISON OF GAS YIELD

Run No.	94-1-1	94-1-2	94-1-3	94-1-41	91-1-1	91-1-2	91-1-3	91-1-4
Catalyst	None	K_2CO_3	Char	Ash	None	K_2CO_3	Char	Ash
Gas	Liters/Kg Dry Feed				Percent of Baseline Value			
Carbon Monoxide	66.7	62.4	69.9	57.6	100	93.6	104.8	86.4
Carbon Dioxide	71.9	108.3	91.8	90.4	100	150.6	127.7	125.7
Hydrogen	27.6	91.5	43.7	79.2	100	351.5	158.3	287.0
Methane	43.1	47.0	50.1	45.9	100	109.0	116.2	106.5
Ethane	2.7	8.0	4.1	5.4	100	296.3	151.9	200.0
Ethylene	1.7	1.9	2.5	3.5	100	111.8	147.1	205.9
Propane	0.8	2.4	1.0	1.4	100	300.0	125.0	175.0
Propylene	1.5	1.6	2.1	1.6	100	106.7	140.0	106.7
Butanes	0.7	0.9	0.2	0.4	100	85.7	28.6	57.1
Butenes		0.6	0.5	0.6	—	—	—	—
Total	216.7	324.6	265.9	286.0	100	149.8	122.7	132.0
Density kg/m^3	1.245	1.103	1.219	1.067	100	88.6	97.9	85.7
(Btu/SCF)	.0776	.0688	.0761	.0666				
HHV(Mass Basis)kJ/kg	13,054	14,217	13,214	14,900	100	108.9	101.2	114.1
(Btu/lb)	(5,616)	(6,116)	(5,688)	(6,410)				
HHV (Volume Basis)kJ/m^3	16,252	15,681	16,108	15,898	100	96.5	99.1	97.8
(Btu/SCF)	(436)	(421)	(433)	(427)				

TABLE 14. HEAT AND MASS BALANCE FOR 94-1-1

Component	kg/kg (lb/lb)	kJ/kg (Btu/lb)	Percent of Dry Feed	kJ/kg Dry Feed (Btu/lb Dry Feed)
INPUTS				
Dry Feed	1.000	19,833	100.0	19,833
	(1.000)	(8,532)		(8,532)
Water	0.070	0	7.0	
	(0.070)	(0)		( )
Catalyst	0	0	0	0
	(0)	(0)		(0)
TOTAL	1.070	—	107.0	19,833
	(1.070)	—		(8,532)
OUTPUTS				
Dry Char	0.275	32,980	27.5	9,070
	(0.275)	(14,188)		(3,902)
Heavy Organics	0.132	33,459	13.2	4,417
	(0.132)	(14,394)		(1,900)
Water	0.281	0	28.1	0
	(0.281)	( )		(0)
Light Oil	0.012	41,841	1.2	494
	(0.012)	(18,000)		(216)
Noncondensible Gas	0.288	13,054	28.8	3,760
	(0.288)	(5,616)		(1,617)
Catalyst Solids	0	0	0	0
	(0)	(0)		(0)
Catalyst Off Gas	0	0	0	0
	(0)	(0)		(0)
SUBTOTAL	0.988	—	98.8	17,741
	(0.988)	—		(7,635)
Internal Deposits	0.082	—	8.2	—
	(0.082)	--		—
Heat Losses	—	—	—	2,092
				(897)
TOTAL	1.070		107.0	19,833
	(1.070)	—		(8,532)

TABLE 15. HEAT AND MASS BALANCE FOR 94-1-2

Component	kg/kg (lb/lb)	kJ/kg (Btu/lb)	Percent of Dry Feed	kJ/kg Dry Feed (Btu/lb Dry Feed)
INPUTS				
Dry Feed	1.000	19,833	100.0	19,833
	(1.000)	(8,532)		(8,532)
Water	0.102	0	10.2	0
	(0.102)	(0)		(0)
Catalyst	0.156	0	15.6	(0)
	(0.156)	(0)		(0)
TOTAL	1.258	0	125.8	19,833
	(1.258)	(0)		(8,532)
OUTPUTS				
Dry Char	0.321	29,003	32.1	9,310
	(0.321)	(12,477)		(4,005)
Heavy Organics	0.069	38,040	6.9	2,625
	(0.069)	(16,365)		(1,129)
Water	0.356	0	35.6	0
	(0.356)	(0)		(0)
Light Oil	0.013	41,841	1.3	544
	(0.013)	(18,000)		(234)
Noncondensible Gas	0.358	14,217	35.8	5,090
	(0.358)	(6,116)		(2,190)
Catalyst Solids	0.106	0	10.6	0
	(0.106)	(0)		(0)
Catalyst Gas	0.050	0	5.0	0
	(0.050)	(0)		(0)
SUBTOTAL	1.273	—	127.3	17,569
	(1.273)	—		(7,558)
Internal Deposits	-.015	—	-1.5	—
	(-.015)	—		—
Heat Losses	—	—	—	2,264
				(974)
TOTAL	1.258		125.8	19,833
	(1.258)			(8,532)

TABLE 16. HEAT AND MASS BALANCE FOR 94-1-3

Component	kg/kg (lb/lb)	kJ/kg (Btu/lb)	Percent of Dry Feed	kJ/kg Dry Feed (Btu/lb Dry Feed)
INPUTS				
Dry Feed	1.000	19,832	100.0	19,833
	(1.000)	(8,532)		(8,532)
Water	0.070	0	7.0	0
	(0.070)	(0)		(0)
Catalyst	0.150	33,459	15.0	5,019
	(0.150)	(14,394)		(2,159)
TOTAL	1.220	—	122.0	24,852
	(1.220)	—		(10,691)
OUTPUTS				
Dry Char	0.269	33,633	26.9	9,047
	(0.269)	(14,482)		(3,896)
Heavy Organics	0.120	30,152	12.0	3,618
	(0.120)	(12,971)		(1,557)
Water	0.272	0	27.2	0
	(0.272)	(0)		(0)
Light Oil	0.015	41,841	1.5	618
	(0.015)	(18,000)		(270)
Noncondensible Gas	0.325	13,214	32.5	4,295
	(0.325)	(5,686)		(1,848)
Catalyst Solids	0.150	33,459	15.0	5,019
	(0.150)	(14,394)		(2,159)
Catalyst Off Gas	—	—	0	—
	(—)	(—)		(--)
SUBTOTAL	1.163		115.1	22,597
	(1.163)	( )		(9,730)
Internal Deposits	0.069	—	6.9	—
	(0.069)	(--)		(--)
Heat Losses	—	—	—	2,255
	—	(--)	—	(961)
TOTAL	1.220	—	122.0	24,852
	(1.220)	(--)		(10,691)

TABLE 17. HEAT AND MASS BALANCE FOR 94-1-4

Component	kg/kg (lb/lb)	kJ/kg (Btu/lb)	Percent of Dry Feed	kJ/kg Dry Feed (Btu/lb Dry Feed)
INPUTS				
Dry Feed	1.000	19,833	100.0	19,833
	(1.000)	(8,532)		(8,532)
Water	0.070	0	7.0	0
	(0.070)	(0)		(0)
Catalyst	0.268	0	26.8	0
		(0)		(0)
TOTAL	1.338	—	133.8	19,833
	(1.338)	—		(8,532)
OUTPUTS				
Dry Char	0.279	29,680	27.9	8,281
	(0.279)	(12,768)		(3,562)
Heavy Organic	.079	41,757	7.9	3,299
	(.079)	(17,964)		(1,419)
Water	0.411	0	41.1	0
	(0.411)	(0)		(0)
Light Oil	0.013	41,841	1.3	544
	(0.013)	(18,000)		(234)
Noncondensible Gas	0.304	14,900	30.4	4,530
	(0.304)	(6,410)		(1,949)
Catalyst Solids	0.203	0	20.3	0
	(0.203)	(0)		(0)
Catalyst Off Gas	0.064	0	6.4	0
	(0.064)	(0)		(0)
SUBTOTAL	1.353	—	135.3	16,654
	(1.353)	—		(7,164)
Internal Deposits	-0.015	—	-1.5	—
	(-0.015)	--		—
Heat Losses	—	—	—	3,179
				(1,368)
TOTAL	1.338	—	133.8	19,833
	(1.338)	—		(8,532)

TABLE 18. COMPARISON OF PYROLYSIS YIELDS

Run No.	94-1-1		94-1-2		94-1-3		94-1-4	
Catalyst	None		K_2CO_3		Pine Char		Ash	
Component	Percent*	kJ+ (Btu)**	Percent*	kJ+ (Btu)**	Percent*	kJ+ (Btu)**	Percent*	kJ+ (Btu)**
Char	27.5	9,070 (3,902)	32.1	9,310 (4,005)	26.9	9,047 (3,896)	27.9	8,281 (3,562)
Heavy Organics	13.2	4,417 (1,900)	6.9	2,625 (1,129)	12.0	3,618 (1,555)	7.9	3,299 (1,419)
Water	21.1	0 (0)	25.4	0 (0)	20.2	0 (0)	34.1	0 (0)
Light Oil	1.2	494 (216)	1.3	544 (234)	1.5	618 (270)	1.3	544 (234)
Noncondensible Gas	28.8	3,760 (1,617)	35.8	5,090 (2,190)	32.5	4,295 (1,848)	30.4	4,530 (1,949)
Internal Deposits	8.2		-1.5		6.9		-1.5	
Heat Losses	—	2,092 (897)	—	2,264 (794)	—	2,255 (781)	—	3,179 (1,368)

*Percent of Dry Feed

+kJ/kg Dry Feed

**Btu/lb Dry Feed

BIBLIOGRAPHY

1. Feldman, H. F., Conversion of Forest Residues to a Methane-Rich Gas," Institute of Gas Technology Conference on Biomass and Waste, Washington, D.C., August 14-18, 1978.

2. Cox, J. L.; Willson, W. G.; and Hoffman, E. J., "Conversion of Organic Waste to Fuel Gas," J. Environ. Eng. Div., Am. Soc. Civ. Eng. Series 100, Issue EE3, pp. 717-32 (1974).

3. Appell, H. R.; and Pantages, P. "Decomposition of Carbohydrate Wastes," U.S. Patent No. 3,989,480.

4. Sealock, L. J., Jr.; Robertus, R. J.; Mudge, L. K.; Mitchell, D. H.; and Cox, J. L., "Catalyzed Gasification of Biomass," Conference on Future Sources of Organic Raw Materials, Toronto, Canada, 10 July, 1978.

5. Mudge, L. K.; Sealock, L. J., Jr.; Robertus, R. J.; Mitchell, D. H.; and Baker, E. G., "Investigation of Biomass in the Presence of Catalysts," Biomass Thermochemical Conversion Meeting, Richland, Wa. 19 September, 1978.

6. Feber, R. C.; and Antal, M. J., "Synthetic Full Production from Solid Wastes," Final Report EPA/600/2-77/147, September, 1977.

7. Appell, H. R.; Fu, Y. C.; Illig, G. E.; Steffgen, F. W.; and Miller, R. D., "Conversion of Cellulosic Wastes to Oil," Bu Mines - RI-8013, February, 1975.

8. Kaufman, J. A.; and Weiss, A. H., "Solid Waste Conversion: Cellulose Liquefaction," Final Report, Grant EPA/670/2-75-031, February 1975.

APPENDIX A

15.2 CENTIMETER TUBE FURNACE APPARATUS

1. APPARATUS

The 15.2 cm pyrolysis unit consists of a 152.4 cm length of Schedule 40 six-inch stainless steel pipe heated by a three-zone Lindberg tube furnace. The ends are closed by means of heavy aluminum plates tightly compressed against silicone rubber gaskets. Stainless steel spacers are provided to confine the feed material to the uniformly heated center zone of the apparatus. The temperatures of the three separately controlled furnace zones and of selected locations within the tube are measured by chromel-alumel thermocouples and recorded. A schematic diagram of the tube furnace arrangement is shown in Figure 1, with location of thermocouples numbered 1 through 10. Thermocouples 1, 2 and 3 are furnace zone thermocouples; 5, 6 and 10 are in the charge; 7, 8 and 9 are in the gas outlet stream; and 4 is the stagnant upstream end of furnace.

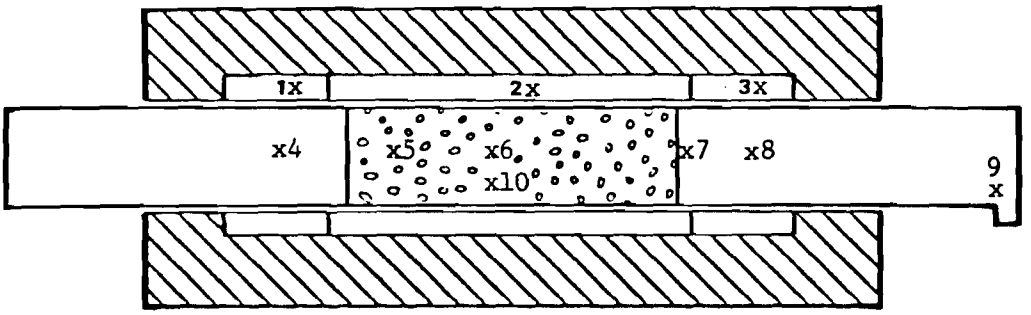

Figure 1. Schematic Diagram of Tube Furnace

The upstream end of the apparatus (left hand end in the diagram) is raised slightly to promote gravity flow of liquid products toward the 2.5 cm stainless steel exit tube located at the bottom of the downstream end of the pyrolysis tube. The spacer on the downstream end of the charge is slotted at the bottom to permit liquid flow. The exit tube ends in a one-inch stainless steel Whitey ball valve. This valve, which is used to exclude air from the pyrolized charge during cooling, is fitted to accept the upstream end of the condensate collection train.

2. OPERATION

The thermocouple leads are connected to a multi-channel recorder located above the furnace control panel outside of the pysolysis laboratory. The furnace and the gas collection train are thoroughly purged with nitrogen before heating is begun.

With the bell valve at the downstream end of the furnace open heating is begun and continued until the rate of gas evolution decreases to less than two liters per hour and the thermocouples inside the charge record a sustained decrease in temperature for at least fifteen minutes. The ball valve is then closed and the furnace power is turned off. The furnace and the sealed tube containing the charge are cooled for 24 hours by a stream of forced air passed between the tubes and the refractory material of the furnace. The cooled furnace is then opened, and the carbonized charge is recovered.

APPENDIX B

TUBE FURNACE OFF-GAS COLLECTION TRAIN

1. APPARATUS

A schematic diagram of the train is shown in Figure 1.

Liquids and gases emerge from the pyrolysis tube through a stainless steel ball valve (1) into a series of water cooled condensers (2) and ice cooled traps (3). The first condenser is a jacketed stainless steel tube, which minimizes the risk of breakage that might occur in a heated metal-to-glass joint. The first trap is a resin kettle rather than a flask so that viscous condensates may easily be recovered. The gas stream then passes through a glass wool demister (4) and a calcium sulfate (Drierite) column (5) into a series of cold condensers (6) and cold "light oil" traps (7). The condensers are chilled by ethanol circulating through a heat exchanger coil immersed in dry ice and ethylene glycol for most experiments or in dry ice and acetone when a large quantity of hydrogen sulfide is anticipated. The traps are immersed in a bath of dry ice and acetone. From the cold traps, the gases pass through a magnesium perchlorate drier (8) and a calibrated dry test meter (9) into a series of 96 liter gas collection bags. The quantity of magnesium perchlorate, which is necessary to prevent subsequent fouling of gas chromatographic columns, is held to a minimum to reduce possible explosion hazards.

2. OPERATION

After assembly and thorough leak testing, the train is connected to the pyrolysis tube and the refrigerants are added. The ball valve is opened at the start of the run and closed when the run is completed. During the run 90 liter quantities of non-condensible gas are collected successively in a series of 96 liter gas collection bags.

After each bag is filled, it is kneaded to mix its contents and then emptied by aspiration through a gas collection tube. When the bag is approximately half-emptied the gas collection tube is closed and labelled for laboratory analysis. If sulfur gases are of interest a measured portion of the gas is drawn through a special sulfur gas absorption train. The remainder of the gas from each bag is then pumped to an exhaust fan.

On completion of the run the ball valve is closed and the weights of the condensates are determined. The condensates are then transferred to tightly closed containers and transported to the wet chemistry laboratory for analysis. The heavy organic and aqueous condensates are stored in a refrigerator. The light oils (from the dry ice traps) are stored in a freezer.

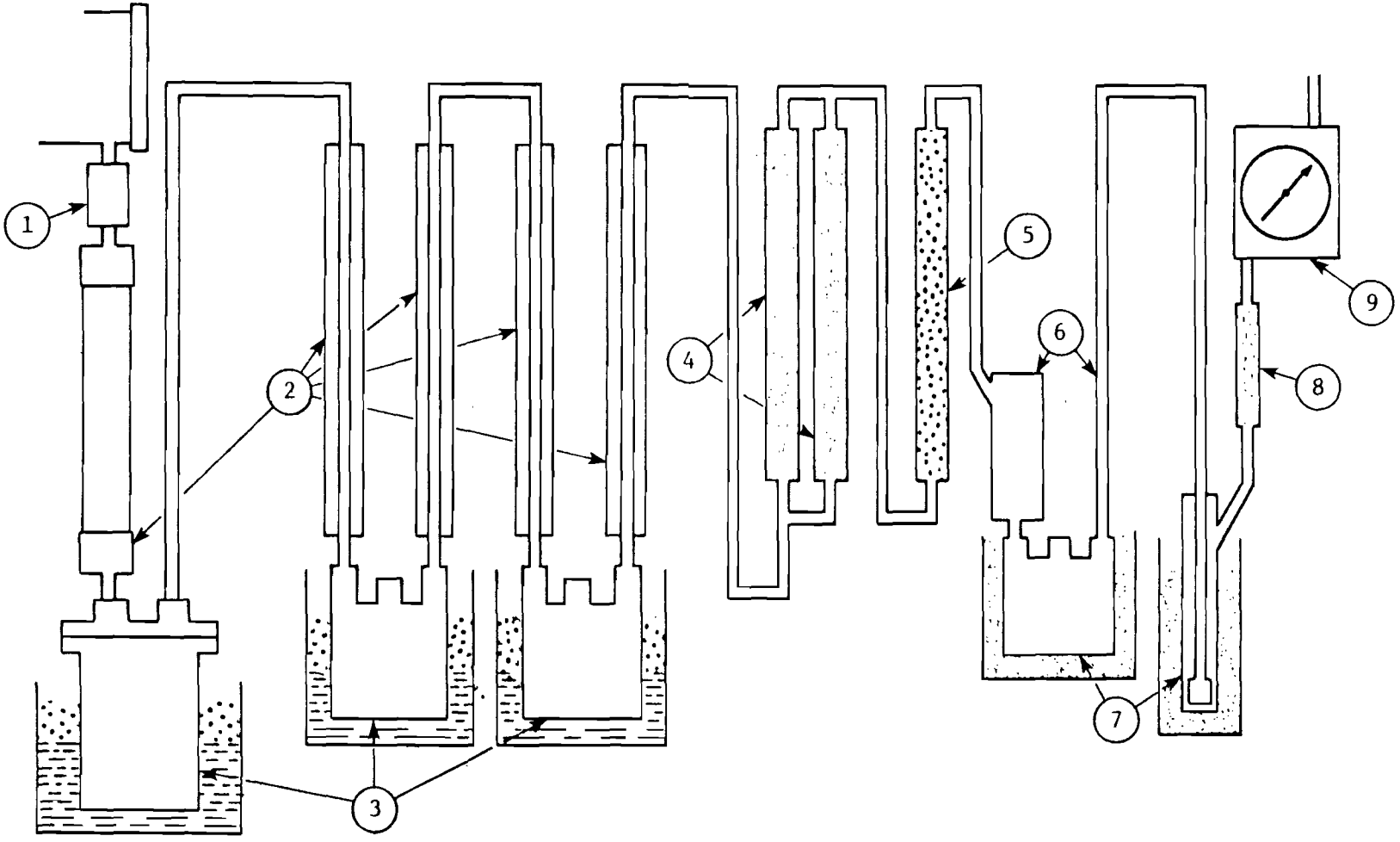

Figure 1. Schematic of Condensation Train.

TASK 2.3.3

MATERIALS AND DESIGNS FOR SOLAR CHEMICAL REACTORS

Steve H. Bomar, Jr.
Henderson C. Ward

Prepared for

Atlanta University
Atlanta, Georgia

by

Georgia Institute of Technology
Engineering Experiment Station
Atlanta, Georgia 30332

FINAL REPORT

December 1980

Georgia Tech Project A-2494-002

TABLE OF CONTENTS

LIST OF ILLUSTRATIONS

LIST OF TABLES

Task 2.3.3 Materials and Designs for Solar Chemical Reactors

INTRODUCTION

The purpose of this task, conducted by the Engineering Experiment Station of the Georgia Institute of Technology, was to develop conceptual designs for chemical reactors using concentrated solar radiation as the energy input source. Reactor type, configuration, materials of construction, and final design are governed in large measure by the physical and chemical properties of the reactants and products of the reactions involved. Therefore, consistent with the time and funds available, solid-gas reaction systems appearing to have the most commercial promise formed the basis for the conceptual designs developed on this task and presented in this report.

BACKGROUND

Only a very few solar chemical reactor concepts have been proposed and studied. They are, of course, governed by the geometry of the available input beam of solar radiation:

(1) CNRS in France operates a batch-type rotary furnace which is used for fusing of refractory oxides. The aperture faces in a horizontal direction. The unit holds several tons of reactant powder and rotates at speeds up to 120 revolutions per minute; the rotation creates a horizontal cavity where the powder fuses to form a hollow egg.

(2) CNRS has operated a small, solar fired fluidized bed for decomposition of calcium carbonate. The unit was operated in a vertical-axis solar furnace with the fluidized bed contained in a cylindrical fused quartz tube. The vertical-axis geometry provided symmetric heating around the wall of the tubular reactor vessel.

(3) Lawrence-Livermore Laboratories has operated a "box reactor" with a horizontally-facing quartz window. The test program decomposed powdered coal and was conducted at the U. S. Army White Sands Solar Furnace in New Mexico.

(4) Princeton University operated a vertical tube reactor for pyrolysis of biomass. The powdered reactant was dropped through the tube. The tests were conducted with a horizontal beam at the CNRS 1000 kW Solar Furnace.

(5) Several organizations have built and operated solar steam boilers, using both once-through and free convection flow schemes. Martin Marietta and Georgia Tech operated a free convection 1 MW boiler at the CNRS Solar Furnace, Georgia Tech operated a 400 kW once-through boiler at the Advanced Components Test Facility in Atlanta, and McDonnell-Douglas operated a once-through 5 MW boiler at the Central Receiver Test Facility in Albuquerque. Francia has operated in Italy several different boilers similar to the Georgia Tech unit.

Since concentrated radiant energy has unique properties, in comparison to conventional chemical process energy generated by burning fuels, it seems desirable to try to exploit these properties for the greatest benefit. One method of exploiting the special properties of concentrated solar radiation would be the direct use of photons to drive a chemical storage reaction, although no candidates with commercial potential have been identified up to now. A less exotic method is the use of solar radiation to heat particulate reactants directly, through a transparent reactor wall or window. This method includes reactions in which gases are heated in the presence of solid particles, as for example: thermal decomposition of biomass, production of syngas using carbon and steam, heating reactant gases in the presence of powdered catalysts, and dehydration of a compound such as calcium hydroxide.

Synthesis Gas

Gas mixtures containing CO, H_2, and N_2 in various ratios are used as feedstocks to produce a number of different chemical commodities including gaseous and liquid fuels. These mixtures, with the ratio of the components suitably adjusted, are called synthesis gases. Table 1 shows the volume ratios of the components required to produce various synthesis gases.

TABLE 1

VOLUME RATIOS IN SYNTHESIS GASES

Commodity or Process	H_2	CO	N_2
Ammonia	3	0	1
Methanol	2	1	0
Fisher-Tropsch (synthol)	2	1	0
Oxo (higher alcohols)	1	1	0
SNG	3	1	0

By reacting steam in a solar reactor with carbon in various forms - coal, biomass, municipal waste, etc. - a basic gas mixture called raw syngas can be produced which can be used to make each of the synthesis gases listed in Table 1, as well as others. In view of the present world situation, the economic production and use of raw syngas is vital to our national economy and security. For these reasons, raw syngas production was chosen as the basis for our preliminary solar reactor designs.

In Table 2 selected results are given of calculations made to determine the concentrations of the various species present at equilibrium and the initial carbon-steam ratio required to provide excess carbon at various operating pressures and temperatures. Also shown in this table are the reactions involved (with carbon in the form of graphite), the percentages of the steam reacted, and the heat requirements per lb atom of carbon reacted at the various pressures and temperatures. The heat input requirement, neglecting heat losses, is approximately 4850 Btu/lb carbon reacted.

Although the carbon-steam reaction has been known and investigated for many years with a large amount of literature available on the reactions involved, it is still not completely characterized or understood. Excellent summaries of the present knowledge and conjectures of the mechanisms involved are given by Smoot and Pratt 1/, Wen and Tone 2/, Wen and Lee 3/, and Von Fredersdroff 4/ with particular interest placed on coal.

TABLE 2

SELECTED RESULTS OF EQUILIBRIUM CALCULATIONS FOR CARBON-STEAM REACTION*

Pressure	Temperature			Required Initial Steam-Carbon Ratio	Equilibrium Gas Composition (%)				Steam Reacted	Heat Required
					H_2O	H_2	CO	CO_2		
(atm abs)	(°C)	(K)	(°F)	(molar)					(%)	(Btu/lb atom C reacted)
0.5	727	1000	1340	$\leq$ 1.16708	3.337	50.518	41.772	4.373	93.80	57,081
0.5	1227	1500	2240	$\leq$ 1.00055	0.0208	49.994	49.980	0.0077	99.96	57,837
1	727	1000	1340	$\leq$ 1.29056	5.881	50.463	36.851	6.806	89.56	56,164
1	827	1100	1520	$\leq$ 1.07836	2.008	49.878	46.352	1.763	96.13	57,946
1	1027	1300	1880	$\leq$ 1.00679	0.2194	49.950	49.712	0.1187	99.56	58,261
1	1227	1500	2240	$\leq$ 1.00114	0.0416	49.987	49.956	0.0154	99.92	57,838
5	727	1000	1340	$\leq$ 1.84413	17.007	47.833	22.488	12.672	73.77	53,101
5	1227	1500	2240	$\leq$ 1.005686	0.2069	49.935	49.782	0.0764	99.59	57,822

*Reactions

		$\Delta H_{25°C}$
1.	$C_{(s)} + H_2O(g) \rightleftarrows CO(g) + H_2(g)$	56,488 Btu/lb atom carbon
2.	$C_{(s)} + 2H_2O(g) \rightleftarrows CO_2(g) + 2H_2(g)$	38,799 Btu/lb atom carbon
3.	$C_{(s)} + CO_2(g) \rightleftarrows 2CO(g)$	74,197 Btu/lb atom carbon
4.	$CO(g) + H_2O(g) \rightleftarrows CO_2(g) + H_2(g)$	-17,709 Btu/lb mole CO.

In summary, here briefly is what is known and conjected about these reactions.

- o equilibrium is seldom attained
- o the percentage conversion of steam is greatly influenced by carbon type and size, time of contact, and temperature
- o temperatures must exceed 1475^{o} F with appreciable reaction occurring around 1800^{o}-1900^{o} F
- o CO and H_2 are the principal reaction products
- o H_2 has a strong retarding effect on the reactions
- o graphitized carbons tend to be the least reactive form of carbon, coconut shell charcoals the most reactive, and coal/chars exhibit immediate reactivity
- o reactivities of coal/chars depend on parent coals and pretreatment conditions
- o the reaction is chemically controlled for smaller carbon/char particles (approximately < 500 μm) and at temperatures up to about 1000^{o}-1200^{o} C with the reaction occurring uniformly throughout the interior of the pore surfaces of the solid particles
- o the reactions are catalyzed by ash in the coke or coal
- o all reactions take place on the carbon surface
- o reaction 4 (Table 2) occurs in space to a negligible extent
- o diffusional effects become important above 2100^{o} F.

Wen and Tone 2/ point out that char-gas reactions are catalyzed by metal salts, particularly alkali, alkali earth and transitional metals and that some of the metal salts are present in coal ash. They list catalysts for various purposes as given in Table 3.

These authors also discussed recent experiments in coal gasification by Exxon and Battelle using catalysts. In the Exxon experiments, it was found that Illinois coal treated with Na_2CO_3 and/or K_2CO_3 (up to 15 percent K in C) had significantly less agglomerating tendency than when untreated and further

TABLE 3

CATALYST (STRONG → WEAK)

For production of CH_4	Li_2CO_3, Pb_3O_4, Fe_3O_4, MgO
For production of H_2	K_2CO_3, Li_2CO_3, Pb_3O_4, CuO
For production of CO	K_2CO_3, Li_2CO_3, Fe_3O_4, Cr_2O_3
For gasification of C	K_2CO_3, Li_2CO_3, Pb_3O_4, Cr_2O_3

that the gasification rate was proportioned to the catalyst concentration. Battelle found that impregnation of CaO into coal before gasification prevented agglomeration and greatly influenced the reactivity and hydrocarbon yields even with large coal particles.

From a study of kinetic data 1-12/ obtained mainly on systems using conventional heat sources it has been concluded that there is no rate equation or equations that are universally applicable -- each system must be individually investigated and characterized. This is particularly true for solar reactors where the direct interactions of reactants with fluxes of radiant energy may produce results not enumerated in most of the investigations in the past.

Recent investigations 12-15/ have demonstrated the feasibility of producing syngas, as well as other products, from coal and biomass using concentrated solar radiation as the energy input source. Economic analyses have been reported 16,17/ and the unique high fluxes possible using solar radiation have been stressed 18-21/. Basic kinetic data for such systems is lacking.

Production of CO from CO_2

Very large quantities of carbon dioxide are produced by the combustion of fossil fuels for production of thermal energy. In some facilities, such as electric power plants, this gas is available in quantities of many tons per day and in concentrations of 10 to 18 percent mixed with other flue gases. Furthermore, there is concern among environmental scientists that accumulation

of carbon dioxide in the atmosphere may lead to permanent changes in the earth's climate over an extended period of time.

The Electric Power Research Institute considers the problem serious enough that coal-burning electric generating plants might someday be required to remove carbon dioxide from flue gas. EPRI is presently conducting a research program to explore methods for removing CO_2 from flue gas in the event such technology is needed in the future. In the meantime, there is considerable debate in the scientific community concerning whether CO_2 accumulation in the atmosphere is a real or imagined problem. Although the concentration of CO_2 appears to have risen over the past 50 years, many persons believe that the oceans constitute a very large "sink" for the gas and that its rate of release by man is trivial in comparison to the oceans' ability to absorb it.

This situation suggests that conversion of stack-gas CO_2 to carbon monoxide, and subsequently to liquid fuels, might be a useful endeavor at some time in the future if solar energy could be used to provide the required process energy and temperature levels. It is also clear, however, that the direct production of electricity by solar thermal or other solar technology might make more sense than burning coal to produce electricity and using solar energy to dispose of the resulting CO_2. Investigation of these system design issues is clearly beyond the scope of this task, but within its scope is consideration of the restricted question of whether it is feasible to convert CO_2 into CO using solar thermal energy.

CO_2 decomposes into CO and O_2 according to the reaction

$$CO_2 \rightleftarrows CO + \frac{1}{2} O_2 \qquad \Delta H_{25^oC} = 121{,}745 \text{ Btu/lb mole } CO_2$$

Calculated equilibrium mole fractions of CO in the equilibrium mixture resulting from 1 mole of CO_2 are shown in Figure 1 as functions of temperature from 1500 K to 4500 K and pressure from 0.25 atm to 1 atm abs. The entire equilibrium mixture composition is given in Table 4 for selected temperatures and pressures. As can be noted, the amount of CO increases

rapidly with temperature and decreases with pressure until about 3600 K. At 2000 K (3140^{o} F), the CO mole fraction varies from 0.0235 at 0.25 atm to 0.0149 at 1 atm. At 2500 K (4040^{o} F), the corresponding CO mole fractions are 0.180 at 0.25 atm and 0.122 at 1 atm while at 3000 K (4940^{o} F) these increase to 0.525 at 0.25 atm and 0.514 at 1 atm. Above 3600 K (6020^{o} F), the mole fractions of CO become roughly constant at about 0.5 and the pressure effect becomes negligible. Since temperatures presently attainable in solar facilities are in the 3000^{o}-4000^{o} F range, direct cracking of CO_2 appears promising. Possible processes have been briefly discussed 22/ and some of the separation problems pointed out 23/. To circumvent the high temperature required, a number of closed cycle CO_2 processes have been proposed 24,25/.

It has been noted that hydrogen is needed in the feed gas mixtures used for synthesis of liquid fuels. To explore the possibility of increasing yields as well as simultaneously providing H_2, calculations have been made of the equilibrium compositions resulting from combined CO_2 and H_2O cracking. The results are summarized in Figures 2 through 5 where it can be observed that certain CO_2/H_2O feed ratios improve the decompositions of both CO_2 and H_2O. The continuation of these studies form part of a proposal under consideration.

CONCEPTUAL DESIGNS FOR SOLAR CHEMICAL REACTORS FOR GAS-SOLID SYSTEMS

Conceptual designs for four types of solar chemical reactors for gas-solid systems were developed and several optical analyses made. The four types are: (1) fluidized bed, (2) vortex flow, (3) plug-flow, and (4) entrained flow. These designs are presented and discussed in the following sections.

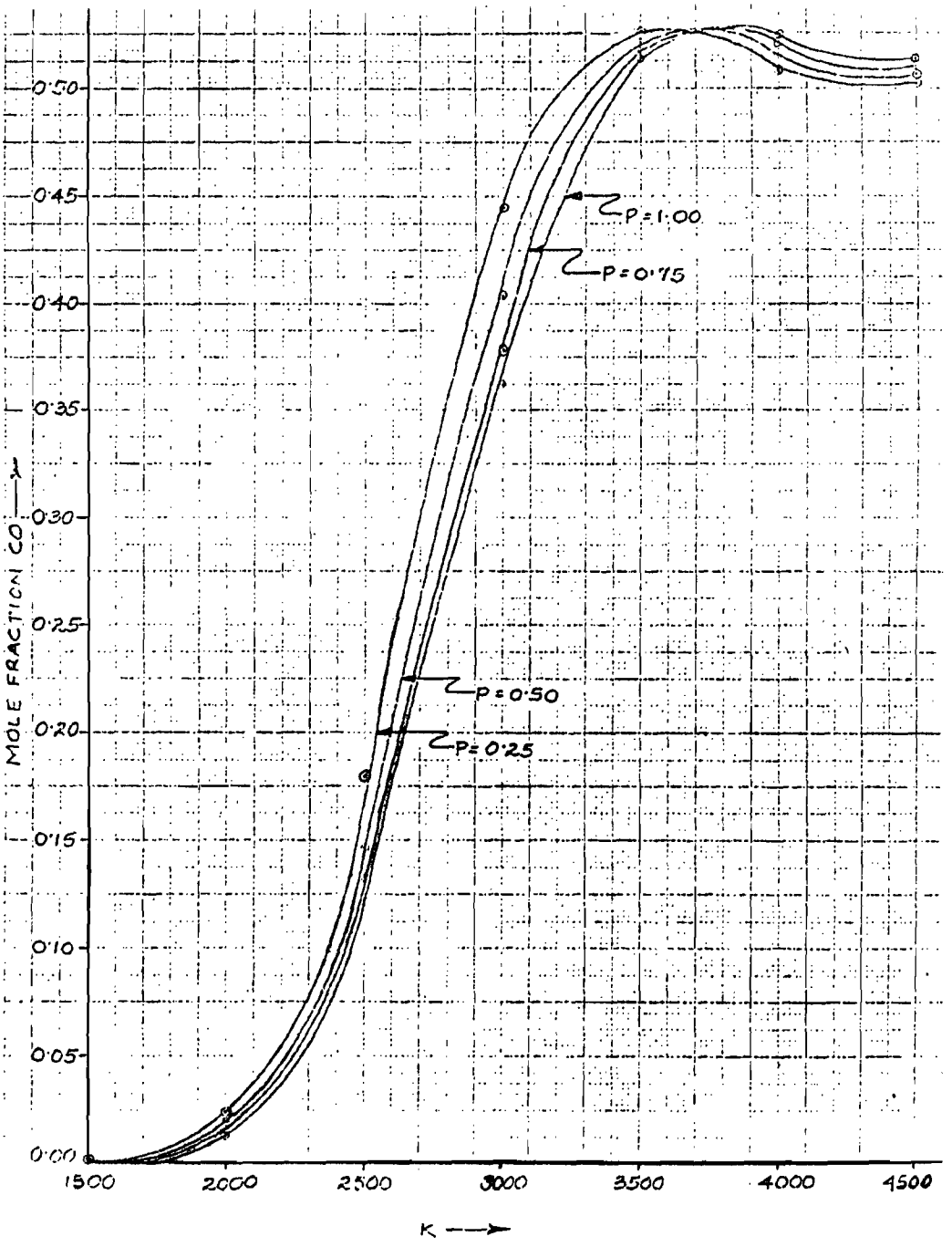

Figure 1. Equilibrium Concentration of CO as a Function of Temperature and Pressure for CO_2 Cracking.

TABLE 4. EQUILIBRIUM COMPOSITIONS FOR THERMAL CRACKING OF CO_2

Pressure = .25 atmosphere

Mole Fraction

Species	Temperature (k)						
	1500	2000	2500	3000	3500	4000	4500
C	0.12173×10^{-10}	0.49498×10^{-18}	0.31828×10^{-13}	0.45613×10^{-10}	0.84219×10^{-8}	0.50399×10^{-6}	0.22990×10^{-4}
C_2	0.61238×10^{-16}	0.88592×10^{-28}	0.26753×10^{-21}	0.30524×10^{-17}	0.47585×10^{-14}	0.19783×10^{-11}	0.35123×10^{-9}
C_3	0.29570×10^{-20}	0.66448×10^{-35}	0.18310×10^{-27}	0.94167×10^{-23}	0.24142×10^{-19}	0.27390×10^{-16}	0.13403×10^{-13}
C_4	0.12205×10^{-37}	0.14907×10^{-47}	0.40018×10^{-38}	0.38582×10^{-32}	0.86406×10^{-28}	0.75263×10^{-24}	0.23257×10^{-20}
C_5	0.15237×10^{-49}	0.16840×10^{-56}	0.31727×10^{-45}	0.17034×10^{-38}	0.12685×10^{-33}	0.40439×10^{-29}	0.43943×10^{-25}
CO	0.28994×10^{-3}	0.23453×10^{-1}	0.18002	0.44535	0.52488	0.50815	0.50178
CO_2	0.99971	0.96489	0.72621	0.28488	0.54680×10^{-1}	0.80223×10^{-2}	0.14707×10^{-2}
O	0.25323×10^{-7}	0.14245×10^{-3}	0.77820×10^{-2}	0.94407×10^{-1}	0.31618	0.45966	0.49178
O_2	0.56213×10^{-11}	0.11512×10^{-1}	0.85989×10^{-1}	0.17536	0.10426	0.24171×10^{-1}	0.49506×10^{-2}
O_3	0.10247×10^{-25}	0.31934×10^{-10}	0.28284×10^{-8}	0.33544×10^{-7}	0.37614×10^{-7}	0.78361×10^{-8}	0.74818×10^{-9}
C_3O_2	0.68907×10^{-8}	0.17204×10^{-21}	0.69353×10^{-18}	0.66700×10^{-16}	0.35825×10^{-15}	0.35348×10^{-14}	0.27962×10^{-13}

(Continued)

TABLE 4. EQUILIBRIUM COMPOSITIONS FOR THERMAL CRACKING OF CO_2 (Continued)

Pressure = .50 atmosphere

Mole Fraction

Species	Temperature (k)						
	1500	2000	2500	3000	3500	4000	4500
C	0.74517×10^{-11}	0.31232×10^{-18}	0.20357×10^{-13}	0.29826×10^{-10}	0.51246×10^{-8}	0.30891×10^{-6}	0.11715×10^{-4}
C_2	0.45883×10^{-16}	0.33965×10^{-28}	0.21889×10^{-21}	0.34546×10^{-17}	0.36662×10^{-14}	0.11591×10^{-11}	0.17940×10^{-9}
C_3	0.21523×10^{-20}	0.29071×10^{-36}	0.19163×10^{-27}	0.10528×10^{-22}	0.23089×10^{-19}	0.17403×10^{-16}	0.70944×10^{-14}
C_4	0.16405×10^{-37}	0.65733×10^{-51}	0.53570×10^{-38}	0.56405×10^{-32}	0.10258×10^{-27}	0.51680×10^{-24}	0.12546×10^{-20}
C_5	0.40751×10^{-49}	0.43168×10^{-63}	0.50013×10^{-45}	0.32563×10^{-38}	0.18694×10^{-33}	0.30018×10^{-29}	0.24196×10^{-25}
CO	0.28993×10^{-3}	0.18718×10^{-1}	0.14869	0.40483	0.52359	0.51358	0.50340
CO_2	0.99971	0.97202	0.77458	0.36005	0.87666×10^{-1}	0.15140×10^{-1}	0.29047×10^{-2}
O	0.19847×10^{-7}	0.89905×10^{-4}	0.50247×10^{-2}	0.65629×10^{-1}	0.25409	0.42915	0.48409
O_2	0.50958×10^{-11}	0.91704×10^{-2}	0.71699×10^{-1}	0.16949	0.13466	0.42137×10^{-1}	0.95940×10^{-2}
O_3	0.12818×10^{-25}	0.32109×10^{-10}	0.30186×10^{-8}	0.47626×10^{-7}	0.77675×10^{-7}	0.25237×10^{-7}	0.15625×10^{-8}
C_3O_2	0.78519×10^{-8}	0.81178×10^{-22}	0.12082×10^{-17}	0.14414×10^{-15}	0.32498×10^{-15}	0.10575×10^{-13}	0.32702×10^{-13}

(Continued)

TABLE 4. EQUILIBRIUM COMPOSITIONS FOR THERMAL CRACKING OF CO_2 (Continued)

Pressure = .75 atmosphere

Mole Fraction

Species	Temperature (k)						
	1500	2000	2500	3000	3500	4000	4500
C	0.57641×10^{-11}	0.19469×10^{-18}	0.15654×10^{-13}	0.23237×10^{-10}	0.39604×10^{-8}	0.24021×10^{-6}	0.79526×10^{-5}
C_2	0.42243×10^{-16}	0.15736×10^{-28}	0.19415×10^{-21}	0.19204×10^{-17}	0.32346×10^{-14}	0.88159×10^{-12}	0.12520×10^{-9}
C_3	0.25477×10^{-20}	0.27080×10^{-36}	0.19606×10^{-27}	0.11204×10^{-22}	0.23435×10^{-19}	0.14137×10^{-16}	0.49929×10^{-14}
C_4	0.26800×10^{-37}	0.22901×10^{-50}	0.63206×10^{-38}	0.70221×10^{-32}	0.11978×10^{-27}	0.44841×10^{-24}	0.89904×10^{-21}
C_5	0.10490×10^{-48}	0.40286×10^{-61}	0.64128×10^{-45}	0.47202×10^{-38}	0.25110×10^{-33}	0.27859×10^{-29}	0.17654×10^{-25}
CO	0.28993×10^{-3}	0.16399×10^{-1}	0.13247	0.37911	0.51891	0.51740	0.50489
CO_2	0.99971	0.97551	0.79949	0.40516	0.11228	0.21580×10^{-1}	0.43045×10^{-2}
O	0.17151×10^{-7}	0.68651×10^{-4}	0.38809×10^{-2}	0.52574×10^{-1}	0.21890	0.40478	0.47683
O_2	0.47635×10^{-11}	0.80216×10^{-2}	0.64159×10^{-1}	0.16315	0.14992	0.56233×10^{-1}	0.13963×10^{-1}
O_3	0.14121×10^{-25}	0.32173×10^{-10}	0.31229×10^{-8}	0.52721×10^{-7}	0.11107×10^{-6}	0.48162×10^{-7}	0.28289×10^{-8}
C_3O_2	0.90323×10^{-8}	0.22451×10^{-23}	0.16564×10^{-17}	0.22166×10^{-15}	0.30149×10^{-14}	0.10571×10^{-13}	0.48481×10^{-13}

(Continued)

TABLE 4. EQUILIBRIUM COMPOSITIONS FOR THERMAL CRACKING OF CO_2 (Concluded)

Pressure = 1.00 atmosphere

Mole Fraction

Species	Temperature (k)						
	1500	2000	2500	3000	3500	4000	4500
C	0.47108×10^{-11}	0.19794×10^{-18}	0.12985×10^{-13}	0.19463×10^{-10}	0.33015×10^{-8}	0.19155×10^{-6}	0.60681×10^{-5}
C_2	0.38273×10^{-16}	0.56451×10^{-28}	0.17813×10^{-21}	0.29473×10^{-17}	0.29861×10^{-14}	0.74018×10^{-12}	0.97899×10^{-10}
C_3	0.25101×10^{-20}	0.61937×10^{-35}	0.19896×10^{-27}	0.11701×10^{-22}	0.24003×10^{-19}	0.12558×10^{-16}	0.39434×10^{-14}
C_4	0.38009×10^{-37}	0.25889×10^{-49}	0.70924×10^{-38}	0.81831×10^{-32}	0.13611×10^{-27}	0.42146×10^{-24}	0.72243×10^{-21}
C_5	0.20045×10^{-48}	0.29835×10^{-57}	0.75961×10^{-45}	0.61648×10^{-38}	0.31657×10^{-33}	0.27705×10^{-29}	0.14435×10^{-25}
CO	0.28992×10^{-3}	0.14929×10^{-1}	0.12187	0.36036	0.51354	0.52018	0.50627
CO_2	0.99971	0.97772	0.81572	0.43179	0.13215	0.27487×10^{-1}	0.56721×10^{-2}
O	0.15452×10^{-7}	0.56679×10^{-4}	0.32281×10^{-2}	0.44761×10^{-1}	0.19526	0.38463	0.46997
O_2	0.45574×10^{-11}	0.72924×10^{-2}	0.59185×10^{-1}	0.15769	0.15905	0.67697×10^{-1}	0.18085×10^{-1}
O_3	0.15099×10^{-25}	0.32201×10^{-10}	0.31948×10^{-8}	0.59442×10^{-7}	0.13918×10^{-6}	0.73460×10^{-7}	0.15487×10^{-7}
C_3O_2	0.97161×10^{-8}	0.44605×10^{-21}	0.20643×10^{-17}	0.29814×10^{-15}	0.43680×10^{-14}	0.14265×10^{-13}	0.12021×10^{-12}

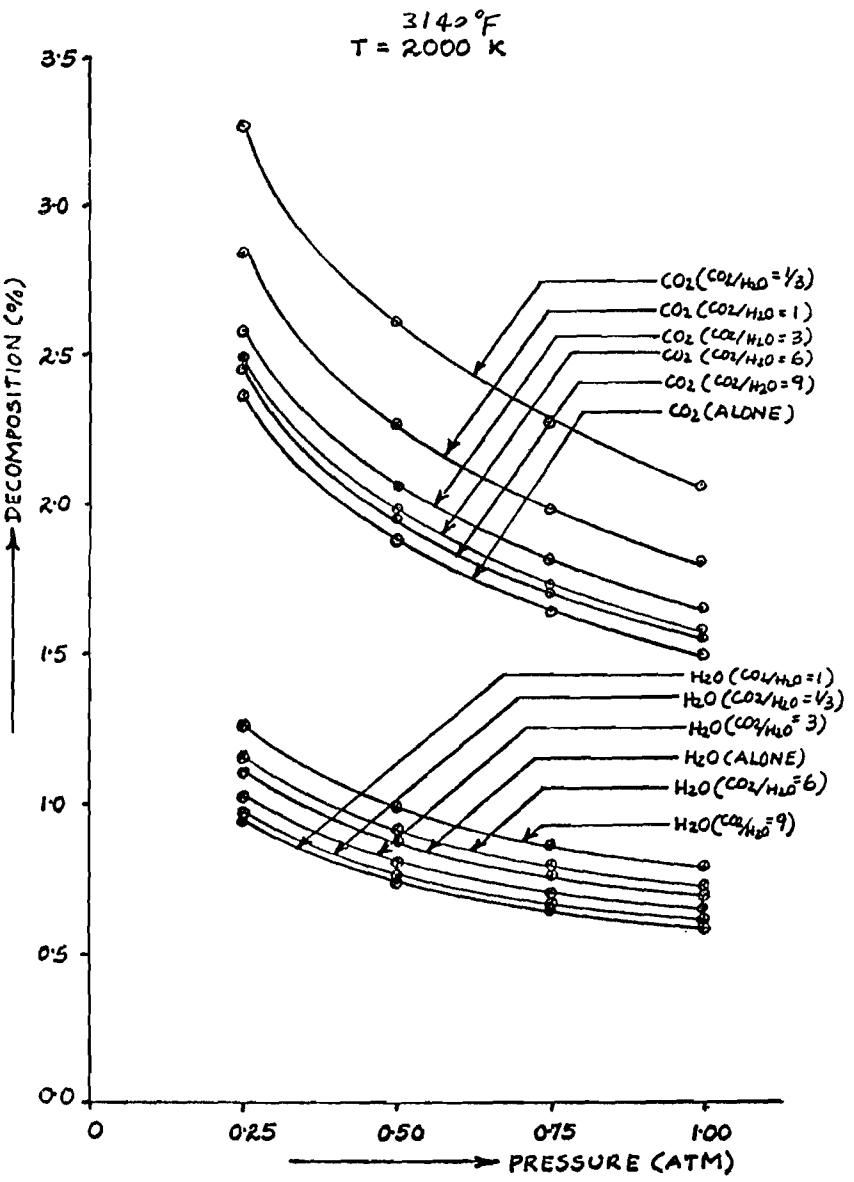

Figure 2. Fraction of CO_2 and H_2O Decomposed at Equilibrium During Thermal Cracking of Gas Mixtures.

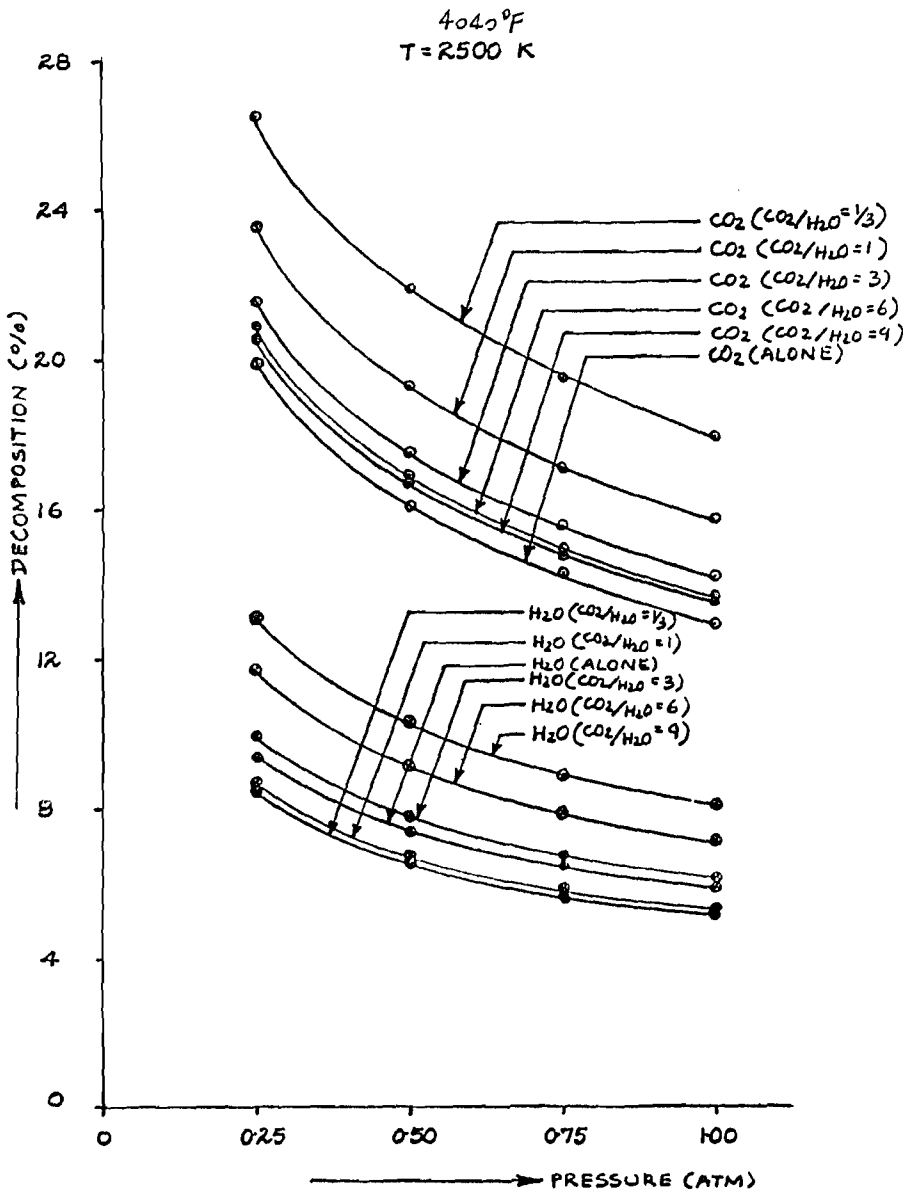

Figure 3. Fraction of CO_2 and H_2O Decomposed at Equilibrium During Thermal Cracking of Gas Mixtures.

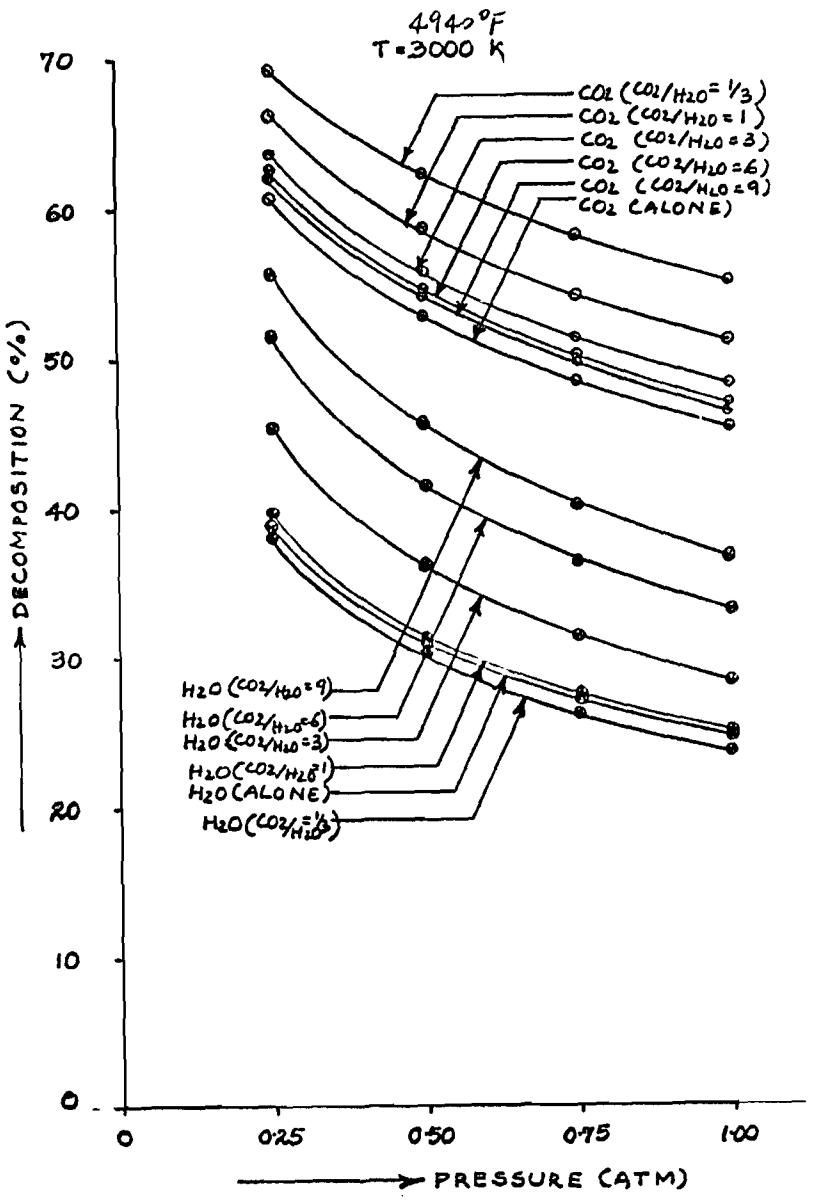

Figure 4. Fraction of CO_2 and H_2O Decomposed at Equilibrium During Thermal Cracking of Gas Mixtures.

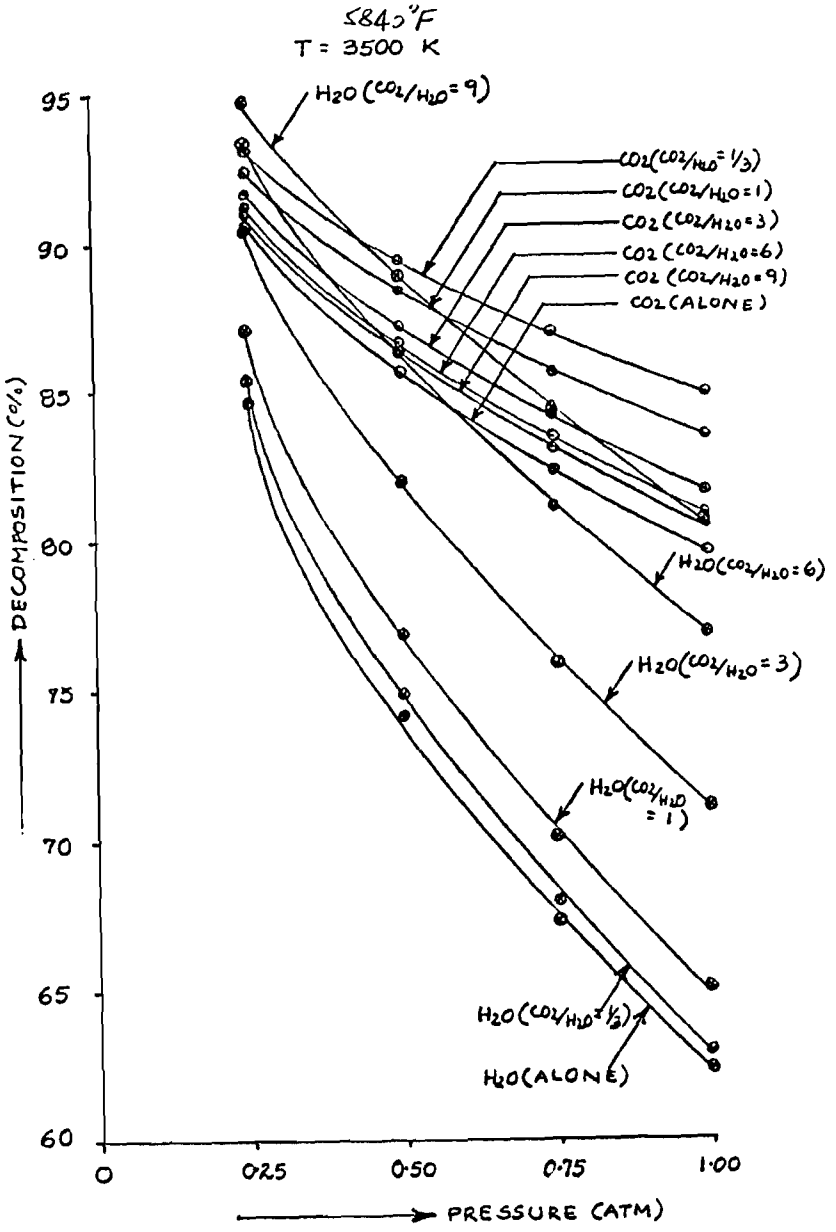

Figure 5. Fraction of CO_2 and H_2O Decomposed at Equilibrium During Thermal Cracking of Gas Mixtures.

1. Fluidized Bed Solar Chemical Reactor

Configuration: Reactor is a vertical, fused quartz tube placed on the optical axis of the concentrator. Solid reactant particles are fluidized by an upward flowing gas stream.

Advantages:

1. The design is simple.
2. Radiation is uniform.
3. Considerable design data available in the literature.

Disadvantages:

1. Maximum operating temperature limited by material of construction.
2. Gas flow rates limited to fluidization range.
3. Reflection losses high if bed not surrounded by a thermal cavity.

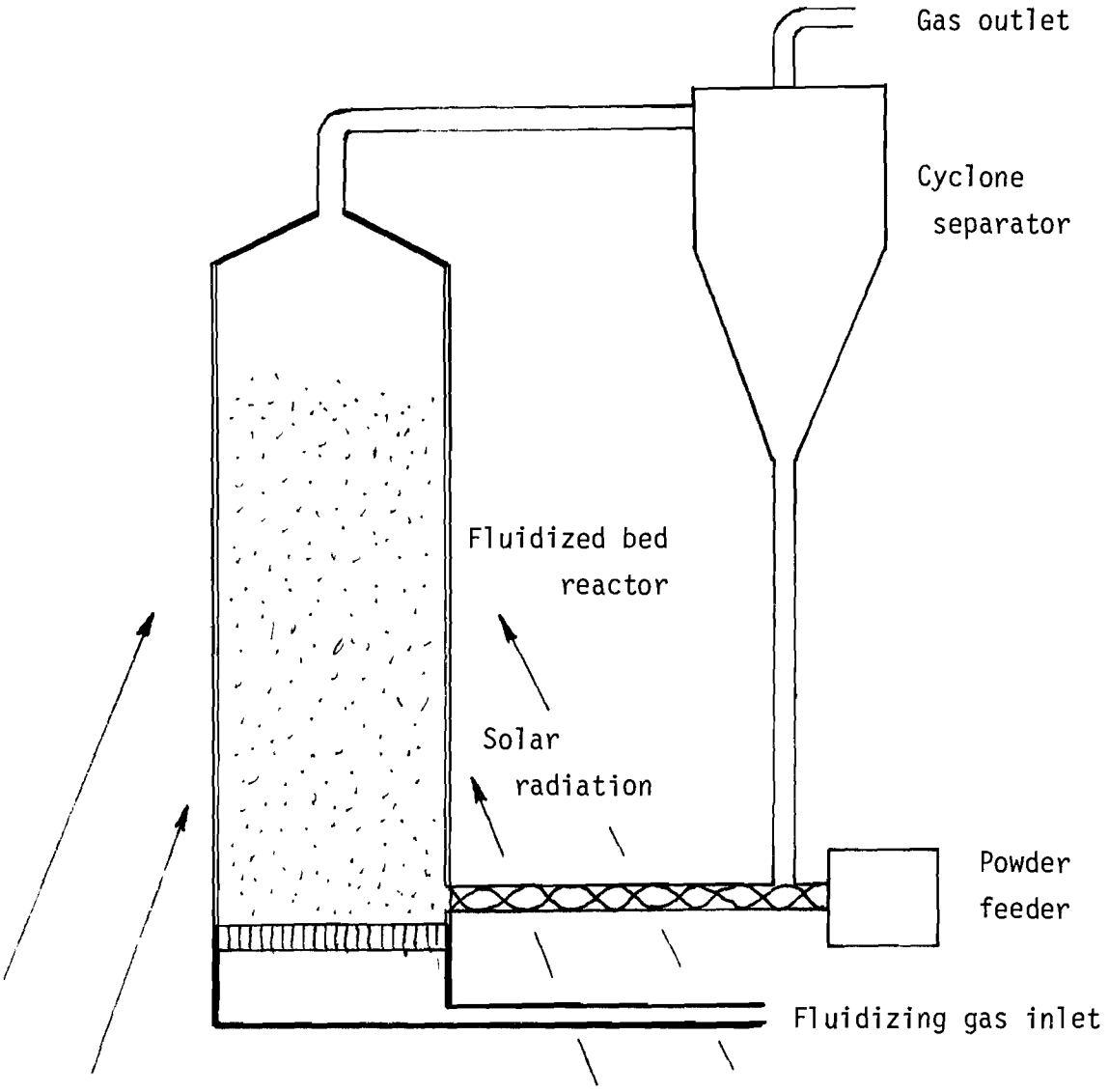

Figure 6. Fluidized Bed Solar Chemical Reactor.

2. Vortex-Flow Solar Chemical Reactor

Configuration: Reactor is a vertical, cylindrical cavity in which solid reactant particles are suspended in a vortex of gases.

Radiation enters through a flat window at the bottom of the reator.

The vortex flow of the gas stream is kept in motion by an externally mounted fan.

Gas products are withdrawn through a tube in the center of the reactor; unconsumed particles fall back into the vortex.

Advantages:

1. The particles can readily interact with solar radiation.
2. Product withdrawal rates and reactant inlet rates can be independently controlled.
3. Residence time in reaction zone can be made relatively long.
4. Design is unique.
5. No secondary reflector is needed since the radiation enters from the bottom.

Disadvantages:

1. An external fan operating at the reactor temperature is needed, with shaft seals, etc.
2. The reactor and fan assembly must be kept at a fairly uniform temperature to avoid cooling the steam.
3. The reactor might be difficult to construct.

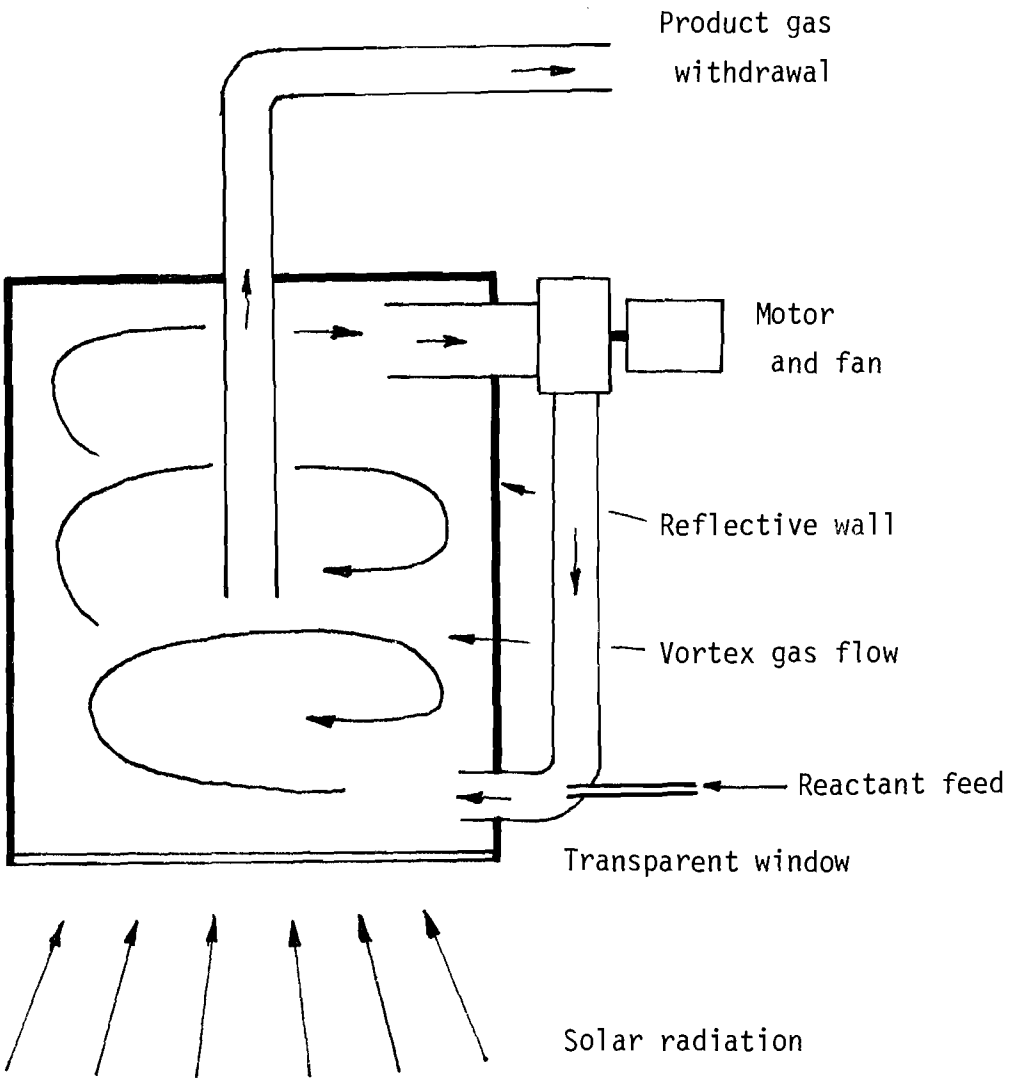

Figure 7. Vortex-Flow Solar Chemical Reactor.

3. Plug-Flow Solar Chemical Reactor

Configuration: Vertical, cylindrical carbon bed, fed by screw feeder from below.

Solar radiation arrives on upper surface of carbon bed through upward-facing, horizontal window.

Water preheated in shielding and injected directly on bed surface.

Advantages:

1. Carbon will not come into contact with window; no danger of abrasion or deposits on window surface.
2. The carbon and water injection rates can be varied independently in response to radiant power input levels.
3. Reactant residence times can be long (several seconds) in order to approach chemical equilibrium.

Disadvantages:

1. A secondary reflector is required to turn the solar beam downward in any high-power test facility currently available.
2. The reaction may be stalled by accumulation of ash on top surface of carbon bed.

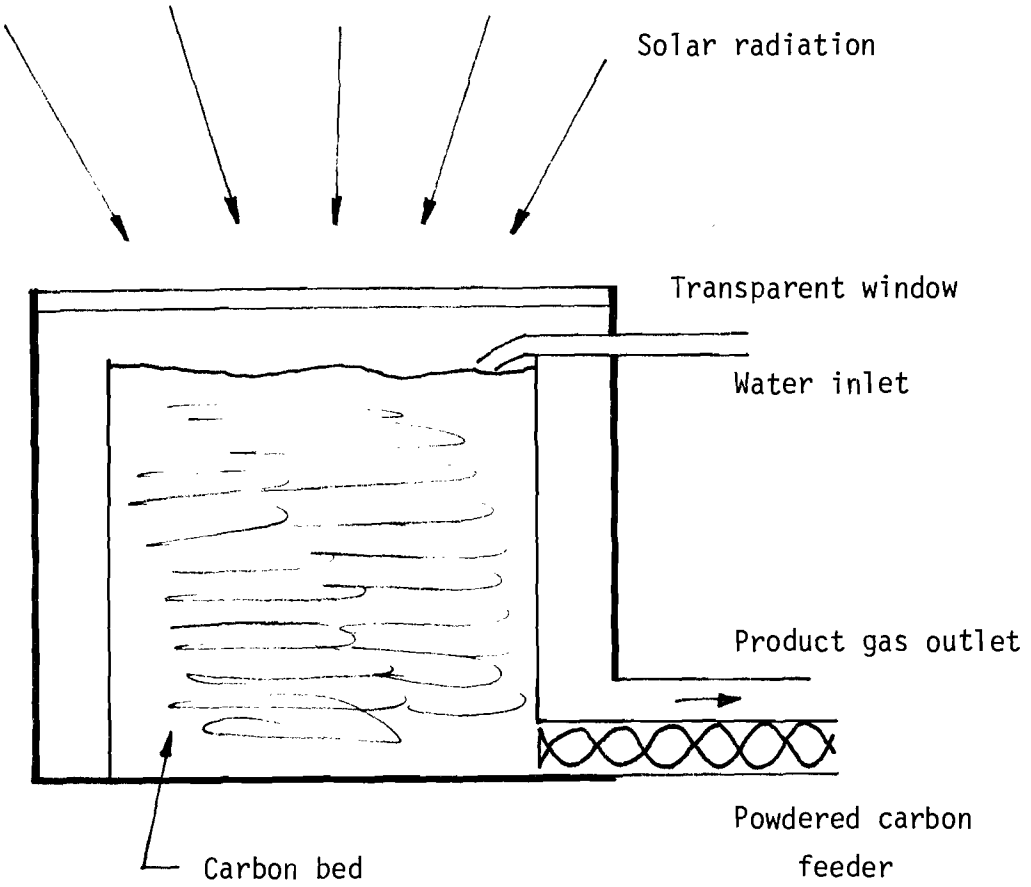

Figure 8. Plug-Flow Solar Chemical Reactor.

4. Entrained-Flow Solar Chemical Reactor

Configuration: Solar radiation arrives through a flat window at the top of the reactor.

Solid carbon particles are entrained in a cylindrical, vertical reactor volume in a flowing gas stream.

Gas stream is kept in motion by a fan within the reactor.

Advantages:

1. The particles can be readily heated by direct interaction with radiation.
2. Carbon and water injection rates can be controlled as required to respond to radiant power input levels.

Disadvantages:

1. Non-caking carbon powders must be used.
2. The entire reactor must be kept at a fairly uniform temperature to avoid the cooling of steam.
3. An internal fan and high-temperature shaft seal are required.
4. Control of particle residence time in reaction zone may be difficult.
5. A secondary reflector is required to turn the solar beam downward in any high-power solar facility available now.

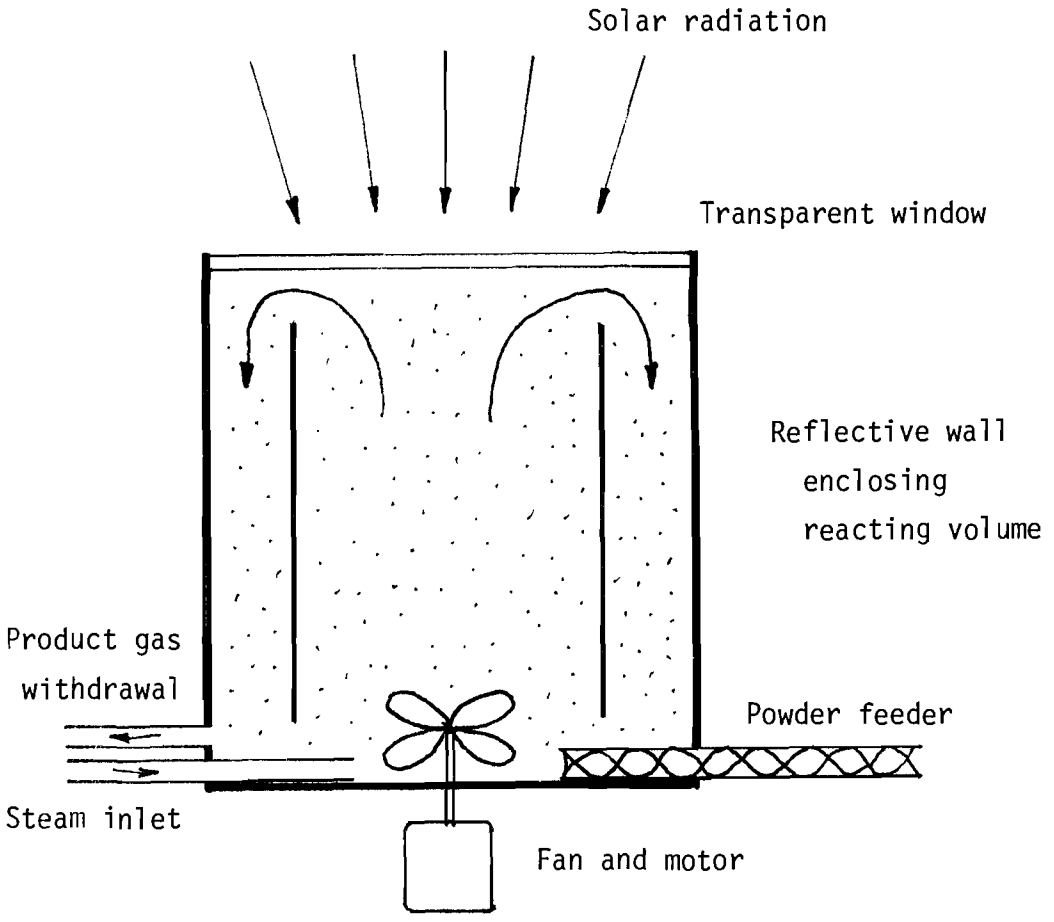

Figure 9. Entrained-Flow Solar Chemical Reactor.

Optical Analyses

Fluidized Bed Solar Chemical Reactor

The basic configuration of the fluidized bed reactor, as discussed previously, was a cylinder placed on the optical axis of the concentrator.

A transparent fused quartz tube wall was assumed, and the first issue inspected was the fraction of arriving energy which would be transmitted by the tube wall into the bed. The mirror field angles associated with the Advanced Components Test Facility were assumed, with flux symmetric about the concentrator axis, as would be observed in a tracking dish. For an alternate case, an absorbing wall such as silicon carbide was taken in place of the transparent quartz wall.

The reflection coefficient for light rays arriving at a glass surface is a function of the angle of incidence measured from the normal to the surface. Since the outer edge of the concentrator represents most of the concentrator area, most of the energy striking the tubular reactor will have angles of incidence less than 60 degrees and reflection coefficients less than 10 percent. Rays which arrive from the inner portions of the concentrator, however, will have higher angles of incidence and higher reflection coefficients. The fraction of the energy passing through the wall into the bed is obtained by summing the components arriving from various angles with appropriate concentrator areas and reflectivities.

The optical analysis computer program with which Georgia Tech models solar receivers accounts for the finite diameter of the sun and appropriate heliostat aiming errors. This program was modified to model the cylindrical receiving surface of the fluidized bed reactor. For the particular cases run, the flux was assumed to come from an 11-meter faceted paraboloidal concentrator, masked to provide 67 kW of thermal power at the focal plane; facets at the center were removed.

The results of this analysis for absorbing and transmitting vessel walls were:

(1) Peak fluxes on the walls are dependent on wall diameter.

(2) The flux patterns are sharply peaked along the length of the vessel wall.

(3) The peak flux passing through a transparent wall is about 10 percent lower than that passing through an absorbing wall, because of reflection losses in the transparent wall.

(4) The integrated flux passing through a transparent wall is about 13 percent lower than that passing through an absorbing wall.

These conclusions represent only one fluidized bed vessel geometry and do not account for other losses such as convection, thermal emission from hot surfaces, etc. They do show, however, that reflective losses are less serious than expected and that a fluidized bed with transparent walls is tentatively feasible.

Solar Furnaces

Optical modeling studies were conducted on several solar furnace configurations which would focus concentrated solar radiation onto upward facing, horizontal focal planes. These system configurations were: a true vertical-axis solar furnace having a symmetric paraboloid dish concentrator and a system having a horizontal optical axis with an asymmetric concentrator which turns the radiation onto a horizontal receiving plane.

The modeling was carried out using a ray-tracing computer program written at Georgia Tech. The program tracks a large number of solar rays and sums the number of rays arriving at various positions on the focal plane. Each ray is traced from a point on the solar disk to a point on the paraboloid surface to a position on the receiving surface. The solar disk is represented by 13 points placed at four radii and at randomly selected angular positons; the power emitted by each point is weighted by the area it represents on the solar disk. The reflecting points on the parabola have a slope error whose direction varies randomly and whose magnitude varies to give a specified standard deviation (for example, if the specified standard deviation is 2 milliradians, the slope error magnitudes will have different values but collectively will have a standard deviation of 2). The receiving surface can be planar or conical, but in the present study was always taken as a horizontal plane through the origin of the coordinate system (focus).

The number of ray positions sampled on the paraboloid surface ranges from a few hundred to several thousand, depending on the precision desired in the output data (each ray position is hit by 13 sun rays). In the present study, calculations using 10,800 and 21,600 ray positions were performed; the 21,600 ray cases gave somewhat smoother plots, but otherwise were identical to the 10,800 ray cases. For the present application, the ray-tracing program was incremented in steps of radius and angle about the x-axis of the coordinate system, with the condition that the flux contribution from a reflecting point was not summed if that point was outside the boundaries of the paraboloid mirror. (The assumption of perfect heliostat alignment is implied by the fact that rays are traced from the solar disk to the paraboloid surface to the receiving plane, without an intermediate reflection at a heliostat.)

Flux patterns at the focal plane are shown for four cases in Figures 10 through 13. It is recognized that the assumptions used in the analyses limit the ability of these plots to show the true incident fluxes which might be obtained in real solar furnaces. They are, however, valid for comparing the various design alternatives.

Figures 10 and 11 are plots for what we presently believe to be an optimum asymmetric paraboloid reflector; they differ only in the number of ray positions sampled on the concentrator. As mentioned earlier, the 21,600 ray case is somewhat smoother than the 10,800 ray case, but otherwise they are essentially the same.

Figures 12 and 13 are for two symmetric paraboloid concentrators in true vertical-axis facilities. Comparison of Figures 11, 12, and 14 gives support to the proposition that good performance could be obtained from a solar furnace having a horizontal optical axis and an asymmetric paraboloid concentrator.

CONCEPTUAL DESIGNS AND ANALYSES OF INTEGRATED FUELS AND CHEMICALS SYSTEMS USING SOLAR-PRODUCED FEEDSTOCKS

A major problem that must be addressed when considering the use of solar-produced feedstocks is that solar reactors can only be operated when the sun is available. Therefore, if these feedstocks are to be used in an integrated

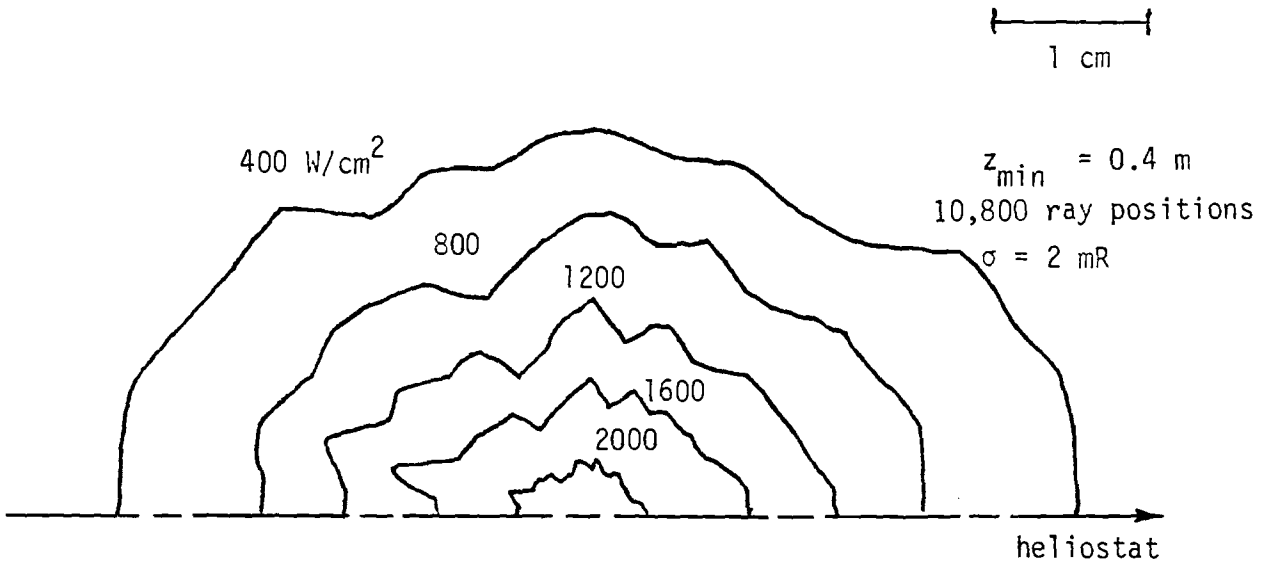

Figure 10. Flux Plot for Asymmetric Paraboloid Concentrator.

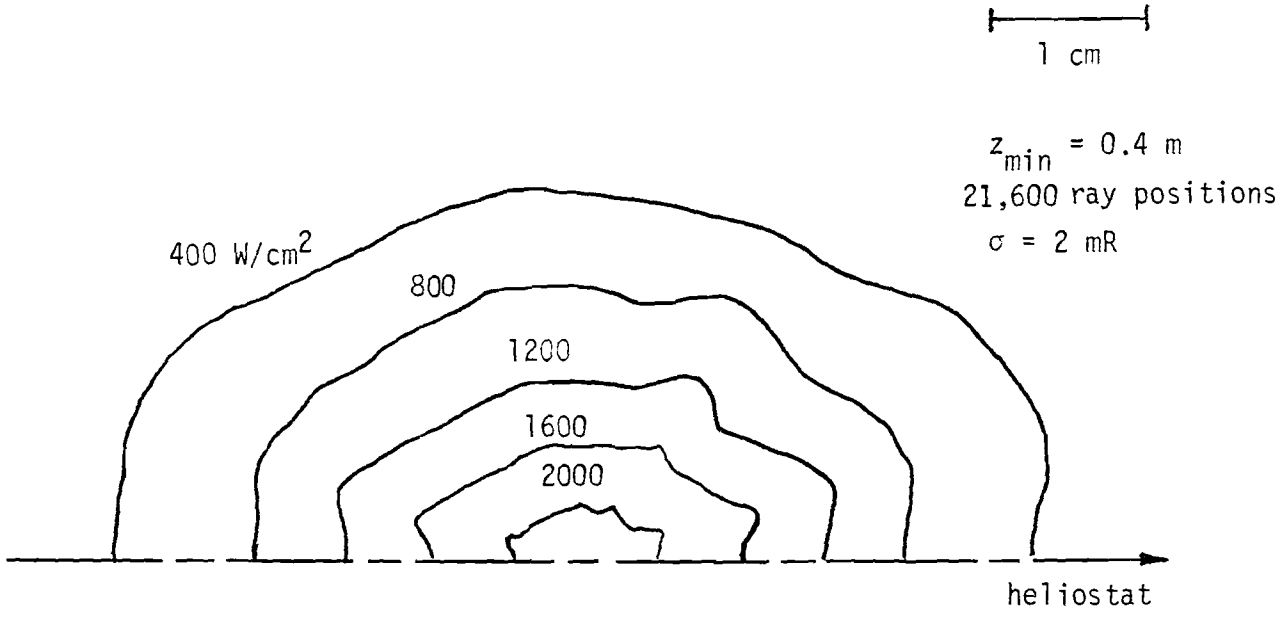

Figure 11. Flux Plot for Asymmetric Paraboloid Concentrator.

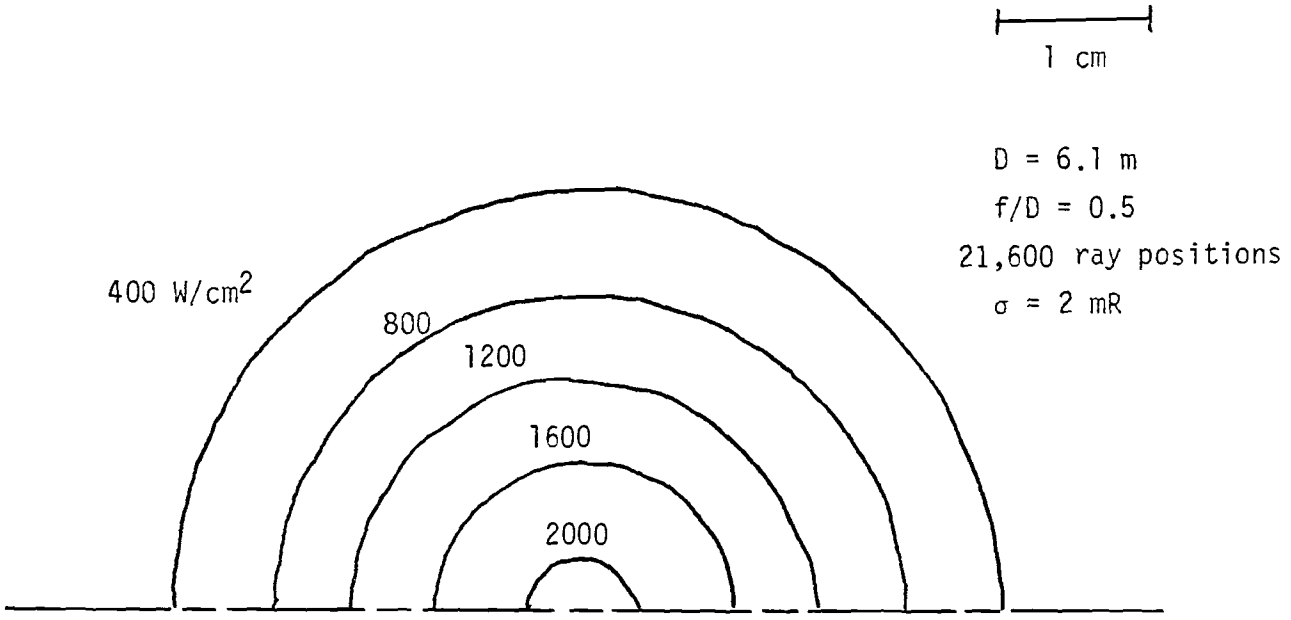

Figure 12. Flux Plot for Symmetric Paraboloid Concentrator.

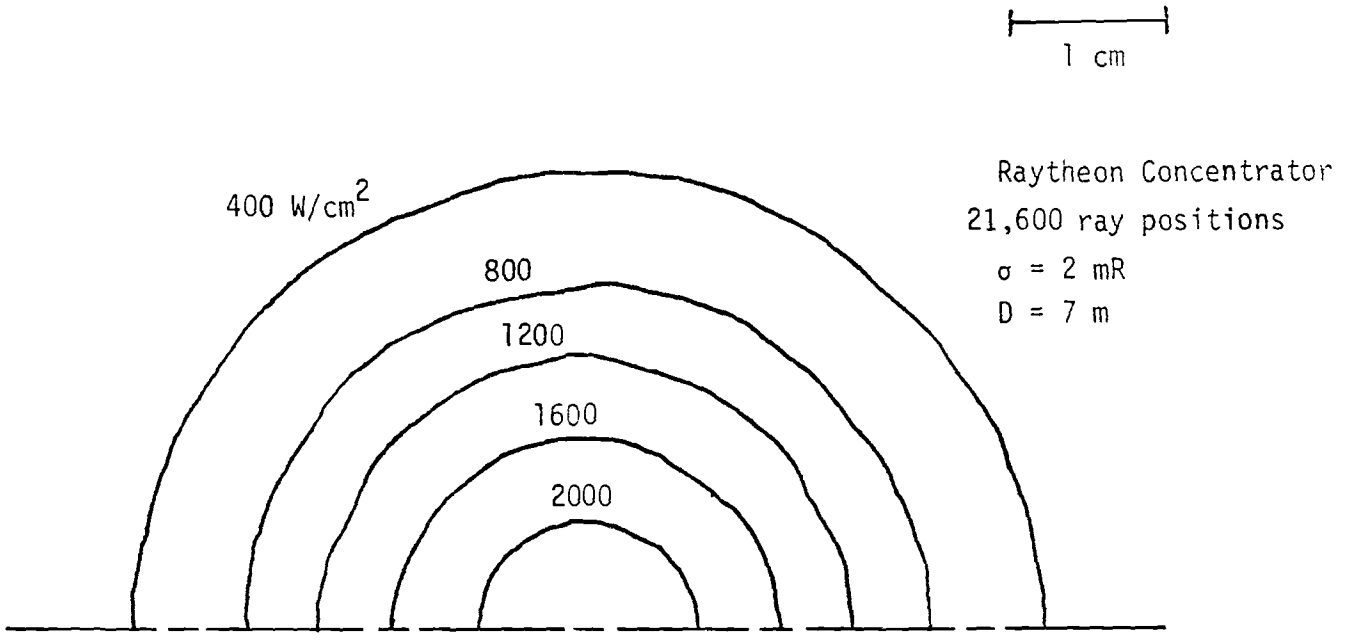

Figure 13. Flux Plot for Symmetric Paraboloid Concentrator.

liquid fuel or other subsequent processing facility, they must either be stored for the facility to run in a continuous manner or the facility must be operated in a batchwise mode. Since both feedstock storage and batch operations are undesirable, economically viable methods must be established for continuous operation of the facility. These methods could well have important bearings not only on the facility design but on the solar reactor design as well. This is illustrated below where several very preliminary alternative systems and operational modes are compared to the base case of an all solar system.

Base Case: All solar system for feedstock production

Advantages	Disadvantages
(1) all solar	(1) products must be readily storable; preferably liquids
(2) no combustible materials used for process energy	(2) storage expensive

Alternative 1

Hybrid solar system using two reactors -- a conventional reactor using auxiliary fuel and a solar reactor using concentrated solar energy. Downstream processes designed to run at approximately 75 percent capacity with no sun and at full capacity when sun is available.

Advantages	Disadvantages
(1) conventional plant plus all solar add on	(1) different feedstocks produced by conventional plant and solar plant
(2) storage not required for solar produced feedstocks	(2) requires additional processing steps over each plant separately to produce common feedstock
	(3) requires complex process controls

Alternative 2

Hybrid solar system using two reactors -- one heated externally by auxiliary fuel and the other a solar reactor using concentrated solar energy.

Downstream processes designed to run at approximately 75 percent capacity with no sun and at full capacity when sun is available.

Advantages	Disadvantages
(1) storage not required for solar-produced feedstocks	(1) requires design of reactor heated externally by auxiliary fuel
(2) uniform quality feedstocks produced	(2) requires complex controls
(3) solar reactor is add on	

Alternative 3

Hybrid solar system using a single hybrid reactor heated internally by auxiliary fuel or externally by concentrated solar energy.

Advantages	Disadvantages
(1) storage not required for solar-produced feedstocks	(1) different feedstocks produced by each heating mode
(2) downstream process design simplified	(2) additional processing steps required to produce common feedstock
	(3) requires complex reactor controls
	(4) requires complex reactor design

Alternative 4

Hybrid solar system using a single hybrid reactor designed to operate using externally supplied energy -- either solar or auxiliary.

Advantages	Disadvantages
(1) storage not required for solar-produced feedstocks	(1) requires complex reactor design
(2) uniform quality feedstocks produced	(2) requires complex reactor controls
(3) downstream plant design facility conventional	

In comparing these preliminary alternatives, it can be seen that a number of tradeoff factors are involved and before a decision could be made as to which alternative is best, more detailed analyses are required. In addition, each alternative involves a different type of reactor system and thus the final alternative selection affects the design of this system. The design of the reactor system in turn is dependent on the operating conditions which in themselves establish or severely limit the design of the downstream facilities.

Other alternative systems and operating modes in addition to those outlined above need to be identified and factors, such as reactor location in the solar field (tower top, ground level, etc.), reactor size, facility location, etc., considered. The more promising systems should then be investigated in depth including economic analyses for various size facilities producing selected final products compatible with the initial feed material and for each economically viable system identified, criteria established for the solar reactor system required.

REFERENCES

1. Smoot, L. D. and D. T. Pratt, Pulverized-Coal Combustion and Gasification, Plenum Press, New York, 1979.

2. Wen, C. Y. and S. Tone, "Coal Conversion Reaction Engineering," Chemical Reaction Engineering Reviews - Houston, American Chemical Society Symposium Series 72, 57-109 (1978).

3. Wen, C. Y. and E. S. Lee, Coal Conversion Technology, Addison-Wesley, Reading, Mass., 1979.

4. Von Fredersdroff, C. G., "Reactions of Carbon with Carbide Dioxide and with Steam," Chicago Institute of Gas Technology Research Bulletin 19, 1955.

5. Von Fredersdroff, C. G. and M. A. Elliott, "Coal Gasification," in Lowry, Chemistry of Coal Utilization, Suppl. Vol., Wiley, New York, 1963.

6. Riede, B. E. and D. Hanesian, "Kinetic Study of the Carbon-Steam Reaction," IEC, Process Design and Development, 14, No. 1, 70-74, 1975.

7. Klei, H. E., J. Sahagian and D. W. Sundstrom, "Kinetics of the Activated Carbon-Steam Reaction," IEC, 14, No. 4, 470-473, 1975.

8. Scott, G. S., "Mechanism of the Steam-Carbon Reaction," IEC, 33, No. 10, 1279-1285, 1941.

9. Foster, J. F., "Production of Water Gas From Pulverized Coal - A Continous Process," IEC, 40, No. 4, 586-592, 1948.

10. Mitchell, D. H., L. K. Mudge, R. J. Robertus, S. L. Weber, and L. J. Sealock, Jr., "Methane/Methanol by Catalytic Gasification of Biomass," Chemical Engineering Progress, 76, No. 9, 53-57, September 1980.

11. Cubicciotti, D., "Proposed Experiment to Utilize A Solar Facility to Provide Process Heat for Carbon Gasification," Proceedings of Annual Meeting Technical Sessions, Solar Thermal Test Facilities Users Association, Golden, Colorado, April 11-12, 1978, pages 326-342.

12. Gregg, D. W., "Solar Coal Gasification," Proceedings of Solar Fuels Workshop held by Solar Thermal Test Facilities Users Association at Albuquerque, N. M., November 28-29, pages 33-41.

13. Aiman, W. R. and D. W. Gregg, "Gasification of Coal with Solar Energy," Preprint of paper to be presented at the 88th National Meeting of AIChE, Philadelphia, Pa., June 8-12, 1980.

14. Taylor, R. W., R. Berjoan and J. P. Coutures, "Solar Gasification of Charcoal, Wood and Paper," Preprint of paper to be presented at the Users Association Annual Meeting, Las Cruces, N. M., April 15-17, 1980.

15. Antal, M. J., Jr., "Synthesis Gas Production from Organic Wastes by Pyrolysis/Steam Reforming," Paper presented at ICT's Conference on Energy from Biomass and Wastes, Washington, D. C., August 1978.

16. Gregg, D. W., W. R. Aiman, H. H. Otuski and C. B. Thorsness, "Solar Coal Gasification," Proceedings of Solar High Temperature Industrial Processes Workshop held at Atlanta, Ga., Sept. 28-30, 1978, pages 352-359.

17. Lakashmanan, S. M., F. K. Manasse and V. K. Mathur, "Economics and Technology of Solar Gasification," Proceedings of Solar Fuels Workshop held by Solar Thermal Test Facilities Users Association at Albuquerque, N. M., November 28-29, 1979, pages 53-59.

18. Antal, M. J., Jr., "Radiant Flash Pyrolysis of Biomass," Proceedings of Solar Fuels Workshop held at Albuquerque, N. M., November 28-29, 1979, pages 71-75.

19. Antal, M. J., Jr., M. Rodot, C. Royere and A. Vialaron, "Solar Flash Pyrolysis of Biomass," Proceedings of Facility Operators and Experimenters Workshop held at Albuquerque, N. M., May 3-4, 1979.

20. Antal, M. J., Jr., "Results of Research on the Use of Pyrolysis/Gasification Reactions of Biomass to Consume Solar Heat and Produce a Useable Gaseous Fuel," Proceedings of Annual Meeting Technical Sessions, Solar Thermal Test Facilities Users Association, Golden, Colorado, April 11-12, 1978, pages 318-325.

21. Antal, M. J., Jr., "Solar Flash Pyrolysis: Syngas from Biomass," Proceedings of Solar High Temperature Industrial Processes Workshop held at Atlanta, Ga., Sept. 28-30, 1978, pages 345-351.

22. Beall, S. E., Jr. and H. E. Goeller, "A Central Receiver for the Production of Monoxides of Carbon and Nitrogen," Proceedings of Solar High Temperature Industrials Processes Workshop held at Atlanta, Ga., Sept. 28-30, 1978, pages 327-343.

23. Bowman, M. G., "High Temperature Thermochemical Hydrogen Cycles for Solar Heat Sources," Proceedings of Solar Fuels Workshop held by Solar Thermal Test Facilities Users Association at Albuquerque, N. M., November 28-29, 1979, pages 125-140.

24. Childress, T. E., "Closed Cycle CO_2 Processes," Ph.D. Thesis, Georgia Institute of Technology, August 1977.

25. Webb, H. M., "Solar Possibilities for 500^{o}-2500^{o} F," Proceedings of Solar-High Temperature Industrial Processes Workshop held at Atlanta, Ga., Sept. 28-30, 1978, pages 149-165.

GEORGIA INSTITUTE OF TECHNOLOGY

Engineering Experiment Station

Atlanta, Georgia

Final Technical Report

October 1, 1979 - December 31, 1980

Project A-2494-003

COAL DESULFURIZATION

by

J. A. Knight, D. R. Hurst, and L. W. Elston

December 31, 1980

CONTENTS

FIGURES

TABLES

SECTION 1

INTRODUCTION

The purpose of this study was to explore the feasibility of partially desulfurizing pulverized coal by exposure to a heated stream of inert gas.

The literature shows that some desulfurization of coal occurs when heated under a variety of conditions and the amount of devolatization varies considerably. The removal of sulfur from coal prior to combustion for large scale users, such as utilities, could possibly eliminate the need for removal of sulfur dioxide from the stack gases or reduce drastically the necessary clean-up of the stack gases in order to comply with environmental regulations. The overall concept on which this study was based for the desulfurization of coal is as follows. The pulverized coal would be treated in a hot inert gas environment in a dilute phase reactor with recovery of the coke and volatiles. The sulfur containing components in the volatile phase would be removed by current industrial processes. The coke and volatile phase without the sulfur components would then be used as fuels, and the sulfur emissions would be reduced accordingly. The rationale for using hot inert gas in a dilute phase reactor is to prevent oxidation of any of the fuels and of the sulfur to sulfur dioxide.

It was necessary to approach the experimental phase with the idea of using a simplified laboratory reactor and minimum chemical analytical work because of the limited resources. The approach, therefore, led to a reactor in which the coal particles were allowed to free-fall through a heated zone of nitrogen gas. The solid products were recovered for chemical analysis whereas the volatiles were not. Experiments were conducted with two high volatile bituminous coals - a low sulfur Kentucky coal and a high sulfur Illinois coal.

SECTION 2

LITERATURE

The literature describing reactions of pulverized coal at elevated temperatures in fixed bed, fluidized bed, entrained flow, and free fall conditions in the presence of active or inert gases is voluminous. Only a few examples of literature directly related to the partial thermal desulfurization of pulverized coal with minimal losses of mass and energy are cited here.

Van Krevelen and Schuyer (1), Lowry (2) and Anthony and Howard (3) have presented excellent reviews, which include the thermal treatment of pulverized coal. Huang (4) used thermobalance methods to examine the devolatilization and desulfurization of Iowa Coals in several gases over a wide range of temperatures. Wen and Tone (5) compared the characteristics of fixed bed, fluidized bed, entrained flow, and free fall coal gasifiers. Koch, et al (6) have indicated that in entrained or free fall gasifiers the reactions shift from chemical control to heat transfer control with increasing particle size, increasing heating rate, or when the equipment design prevents the rapid removal of volatile matter. Badzioch and Hawksley (7) used an entrained flow device to demonstrate that rapid heating of pulverized coal increases the yield of volatiles. Attar, et al (8) described the transformation of sulfur functional groups during the pyrolysis of coal. Haldipur (9) examined the removal of organic and pyritic sulfur from coal in a fluidized bed in the temperature range of 220 to 410^{o}C using hydrogen and oxygen. Maa, et al (10) investigated pyrolysis and treatment with mixtures of hydrogen and hydrogen sulfide for the desulfurization of western Kentucky coal. Black, et al (11) explored the desulfurization of pulverized high volatiles bituminous coals with air, steam, and hydrogen at temperatures up to 900^{o}C. Oxidative pretreatment increased the subsequent rate of desulfurization. Sinha and Walker (12-13) compared the effectiveness of several gases and found that the order of desulfurizing ability was air>steam-CO mixture>CO>N_2. Cernic-

Simic (14) listed factors that influenced the behavior of coal sulfur during carbonization. McKinley and Henke (15) claimed the partial desulfurization by means of heating under a hydrogen pressure of 300-350 atmospheres.

SECTION 3

EXPERIMENTAL PROCEDURES

SAMPLE PREPARATION

Coal samples from Kentucky and from Illinois were used in these experiments.

KENTUCKY COAL SAMPLE FROM GEORGIA POWER COMPANY

The coal sample used in the first series of experiments was collected from the Unit 1 "C" pulverizer at the Georgia Power Company Plant McDonough-Atkinson on Saturday, February 9, 1980. It is described as bituminous coal from the Jellico and River Gem Seam, Knox County, Kentucky Coal District NO. 8.

CLASSIFICATION

The pulverized coal was well mixed, and a 100g sample was withdrawn for screen size analysis on a Ro-tap sieve shaker. The particle size distribution is shown in Table 1.

TABLE 1. PARTICLE SIZE DISTRIBUTION IN PULVERIZED KENTUCKY COAL

U.S. Standard Screen Sizes		
Passes	Retained On	Percent
50 x	100	6.8
100 x	200	14.7
200 x	325	23.3
325 x	400	4.6
400	---	52.0

Approximately 10 kg of the pulverized coal was separated into the particle size ranges shown in Table 1, and the separated cuts were stored in tightly closed containers.

PRETREATMENT

The Kentucky coal is a strongly agglomerating coal. For experiments with pretreated coal, portions of the 50 X 100 mesh cut were partially oxidized in a heated air stream. A schematic diagram of the coal pretreatment apparatus is shown in Figure 1.

The preoxidation apparatus consisted of a modified stainless steel beaker and cover inserted into a crucible furnace. The granular coal was evenly spread over the air disperser. This disperser consisted of a 1 cm layer of "Pyrex" glass wool retained between two layers of "Nichrome" wire gauze approximately 2 cm above the bottom of the beaker. A pulsating stream of air from a stainless steel bellows pump passed through a flow regulating valve to stir and oxidize the granular coal. The pretreatment temperature was observed by means of a thermocouple immediately above the sample. The furnace temperature was regulated by means of a controller and a thermocouple (not shown) located between the beaker and the furnace wall.

In the first pretreatment a 69.8g charge of 50 x 100 Mesh granular coal was added at an initial pot temperature of 209^{o}C. The temperature dropped to 50^{o}C, then rose rapidly to 193^{o}C during the twenty minute heating period. The air flow rate was 18 liters per minute. A strong odor of coal volatiles was observed. At the end of the heating period the pot was tightly closed and rapidly cooled outside the furnace. The treated coal yield was 66.7g (95.6 per cent of the charge weight).

A second charge of 50 x 100 mesh coal was heated for 30 minutes at 232^{o}C using an air flow rate of 1.5 liters per minute. The charge weight was 97.6g, and the treated coal yield was 90.0g (92.2 per cent).

ILLINOIS COAL SAMPLE

A 25 pound sample of fresh Illinois NO. 6 coal from Randolph County, Illinois was supplied by the State Geological Survey Division of the Illinois Institute of Natural Resources. The coal was received May 1, 1980.

CLASSIFICATION

This coal sample was in lumps ranging in size from 1/4 inch to 3/4 inch in diameter and was free from fines. Approximately 3 kg of the lump coal was

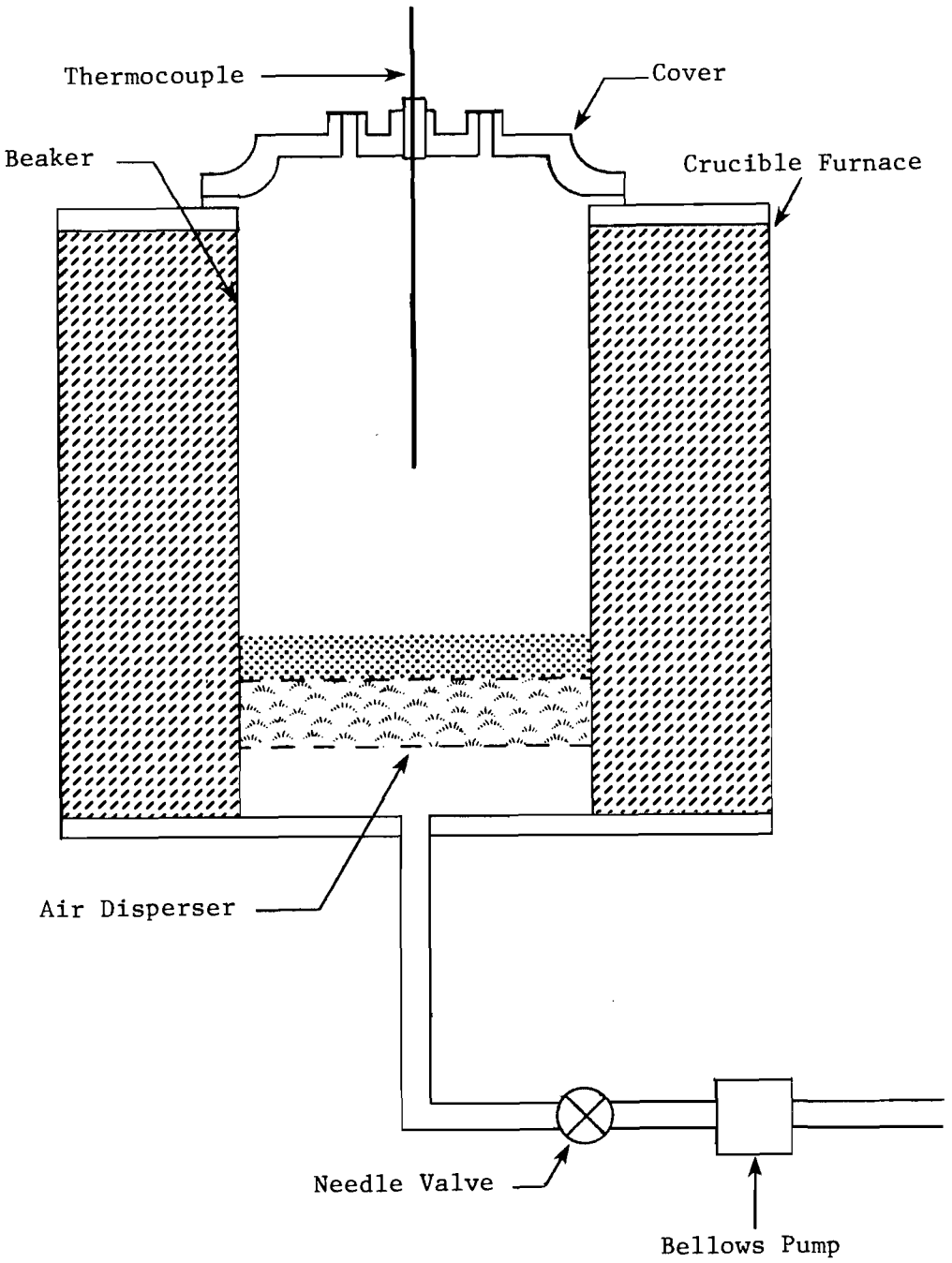

Figure 1. Coal Pretreater

passed through a Model 4 Wiley Mill using a 6 mm screen. The coarsely ground material was again passed through the mill using a 2 mm screen. The twice ground coal was separated on a Ro-tap sieve shaker. Material passing a 50 mesh screen and retained on a 100 mesh screen (50 x 100) was stored in a tightly closed container. Material passing the 100 mesh screen (about 2 per cent by weight) was stored separately. Material retained on the 50 mesh screen (+50) was reground and rescreened until no more of the coarse granules remained. The 50 x 100 cuts were combined, well mixed, and stored in tightly closed containers for subsequent use in experimental work.

PRETREATMENT

For experiments with pretreated coal, a 153.2g sample of 50 x 100 Illinois coal was preoxidized for 30 minutes at 232°C in a 1.5 liter per minute stream of air. A strong odor of volatiles and visible fumes were observed. The weight of the recovered preoxidized coal was 121.3g (79.2 per cent of the charge weight).

REACTOR EXPERIMENTS

The reactor experiments were of three types - - cold suspended entrainment, heated suspended entrainment, and heated free-fall at several temperatures.

COLD SUSPENDED ENTRAINMENT

A 2.5 cm ID x 93 cm "Pyrex" cylinder fitted with a glass side tubular adapter and a flask at its lower end was used to simulate a suspended coal reactor. A 1.2 cm steel ball above a constriction in the lower adapter diverted the gas stream toward the side of the tube. A schematic diagram of the apparatus is shown in Figure 2. A stream of air from a stainless steel bellows pump entered the apparatus through the side tubulation and caused the steel ball to oscillate vertically above the constriction. Several gas flow rates and particle size ranges were examined in attempts to obtain a suspended entrainment of coal particles 10 to 18 cm in length at a fixed position in the tube. This suspension was achieved with a 50 x 100 particle size cut using a nitrogen flow rate of 14 liters per minute; i.e., a mean linear flow rate of 46 cm per second. Smaller particle size ranges led to partial sample loss as fines were blown from the tube at the gas flow rates

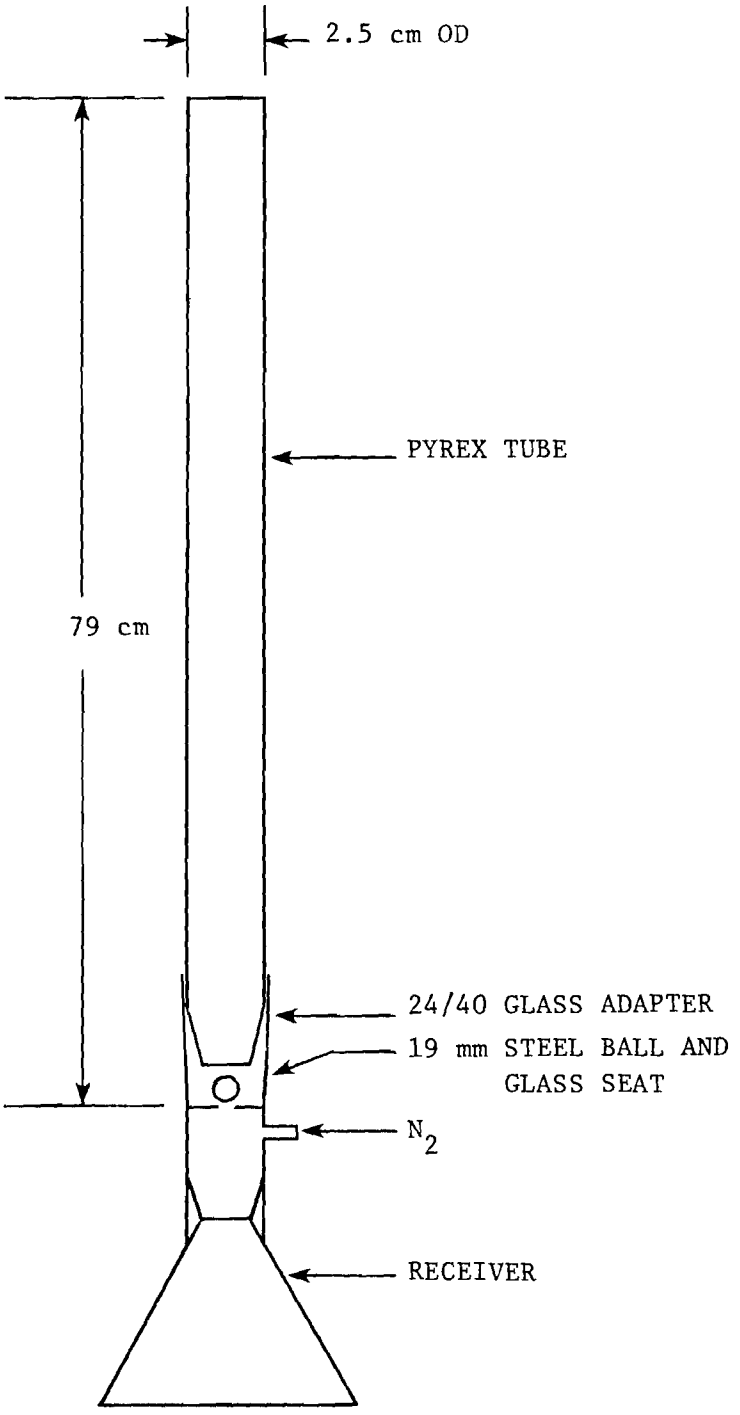

Figure 2. Glass Simulated Reactor

necessary to suspend the bulk of the charge and from caking of the material in the tube. Reducing the gas flow rate and raising the steel ball by means of an external magnet allowed the sample to flow into the receiver.

HEATED SUSPENDED ENTRAINMENT

A schematic diagram of the apparatus for the heated suspended entrainment experiments is shown in Figure 3. A heated entrainment reaction tube was fabricated from a thin wall type 304 stainless steel tube 2.54 ID x 98 cm long. An inverted truncated conical stainless steel restrictor was silver soldered 8 cm above the lower end of the tube to serve as a seat for the oscillating 1.2 cm steel ball. A 1 mm OD stainless steel sheathed thermocouple was attached to the outer wall of the reaction tube 30 cm above its lower end, and the tube and thermocouple were wrapped with asbestos paper extending 16 cm above and below the tip of the thermocouple. Heat was supplied by a split type "Thermolyne" nominal 1 inch ID tube furnace surrounding the asbestos sheathed tube zone and potentiometrically controlled by the thermocouple attached to the reaction tube. A 2 liter resin kettle attached to the lower end of the tube served as the receiver. Nitrogen admitted through the resin kettle cover passed upward through the tube to suspend the sample. As the tube assembly and insert were fabricated from non-magnetic stainless steel, the external magnet technique was adequate to raise the steel ball at the end of a run.

Each experiment was initiated by establishing a constant nitrogen flow rate, typically 8 liters per minute, and heating the reaction tube to the selected temperature, typically 650^{o}C. A 3g sample of 50 x 100 mesh coal was added to the top of the heated tube. After 5 seconds the gas flow was cut off and the ball was raised to allow the coal to flow into the receiver. Only a small fraction of the heated coal flowed into the receiver. The tube was removed from the furnace and cooled quickly. Most of the charge adhered to the walls of the tube just above its hottest zone. The materials in the receiver and those recovered from the tube wall were weighed separately to determine yields. Several nitrogen flow rates, furnace temperature, and coal particle size ranges were employed, but the strong adhesive and agglomerating properties of the Kentucky coal defeated all efforts to recover pulverized coal from the apparatus. No detailed analytical work was attempted on the

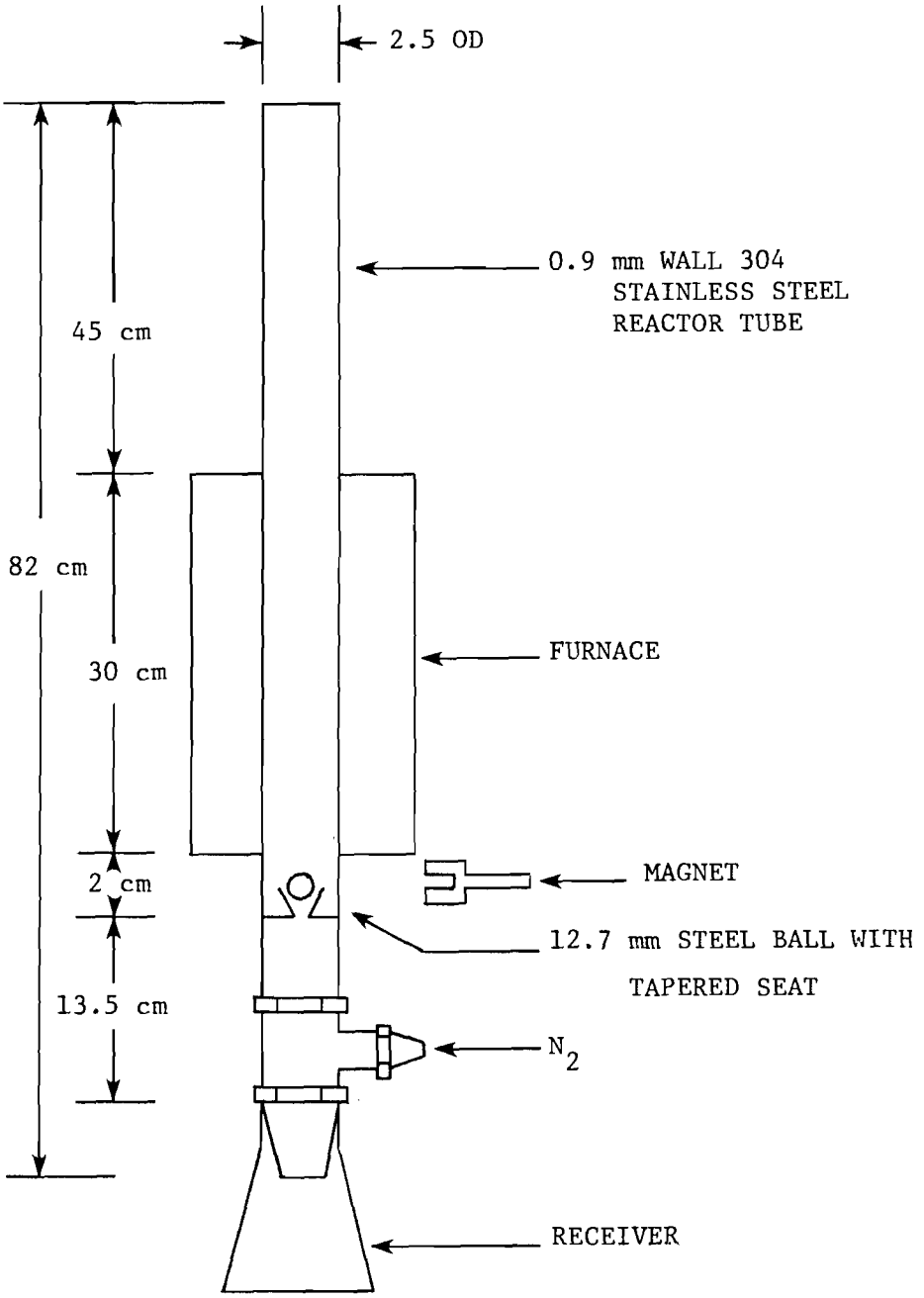

Figure 3. Pulsed Counterflow Reactor

products from these experiments.

FREE-FALL ENTRAINMENT

The vertical reactor tube was modified by removing the steel ball and the constriction. A vibratory feeder was constructed to supply 50 x 100 mesh coal at a controlled rate, which could be adjusted from 0.1 to 10g per minute. The upward nitrogen gas flow was reduced to 1.5 liters per minute; i.e., a linear velocity of 5 cm per second. A schematic diagram of this apparatus is shown in Figure 4.

In these experiments the input from the vibratory feeder was adjusted to the desired feed rate by adjusting the slope of the feed delivery chute, the gap width between the reservoir and the feed chute and the voltage supplied to the vibrator. Feed rates were determined by weighing the granular coal delivered into a tared cup over a known time.

Temperature measurements were taken at 10 cm intervals along the reaction tube. A temperature profile of the free-fall reactor equilibrated at 650^{o}C with a 1.5 liter per minute gas flow is shown in Figure 5.

With the furnace temperature and gas flow rate established at the desired values the feeder was turned on, and a steady stream of granular coal was dropped into the top of the heated reaction tube. At the end of the experiment, usually one hour, the feeder was turned off, and the reaction tube was rapidly cooled outside the furnace. The granular material collected in the receiver (resin kettle) and the coked material scraped from the reaction tube were weighed separately and stored in separately tightly closed containers.

ANALYTICAL METHODS

Proximate Analysis

Percent Moisture - -

The per cent moisture in the coal and coal products was determined by ASTM Method D 3173-73.

Percent Volatiles - -

The per cent volatiles in the coal and coal products was determined by

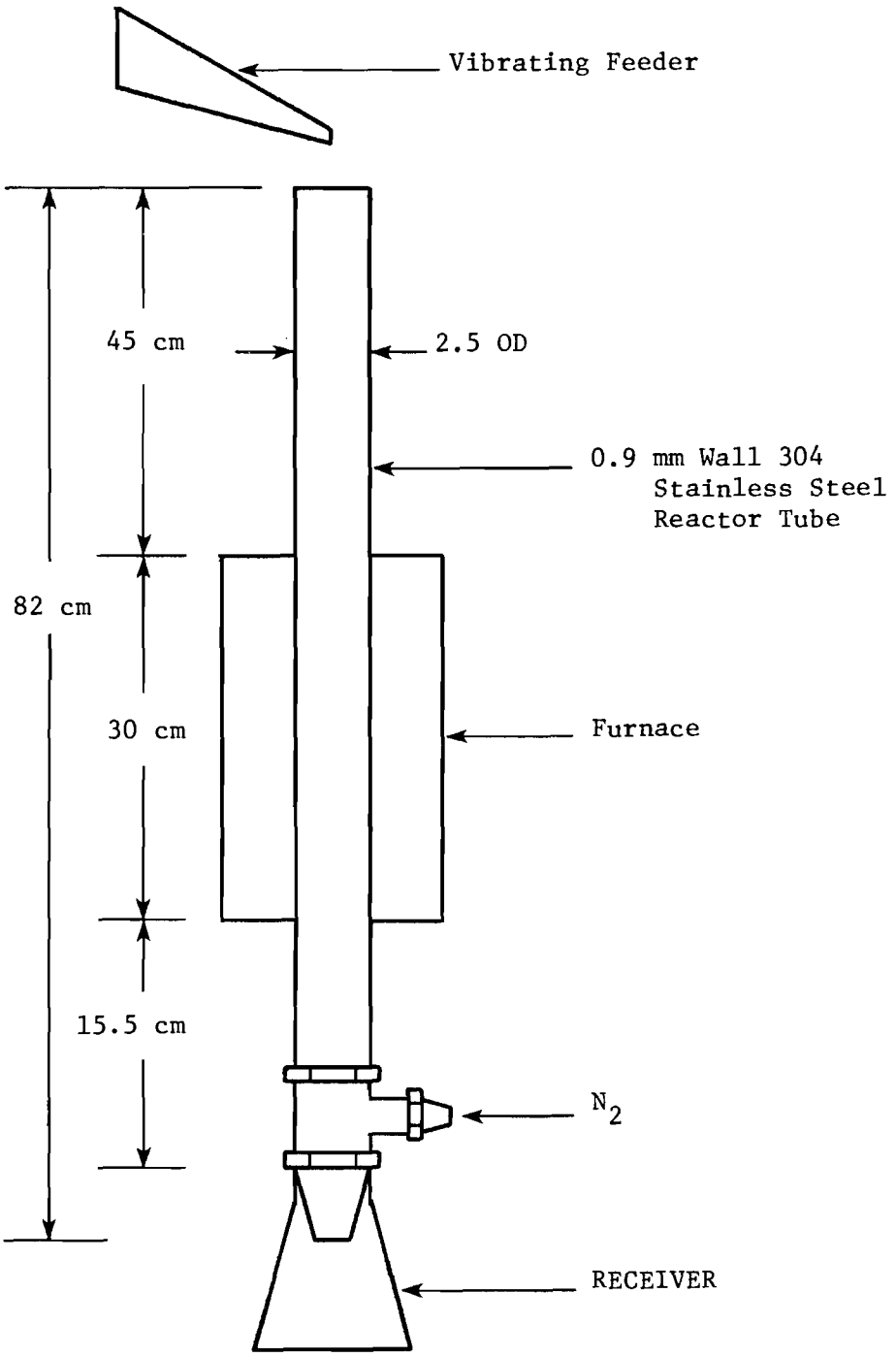

Figure 4. Free-Fall Reactor

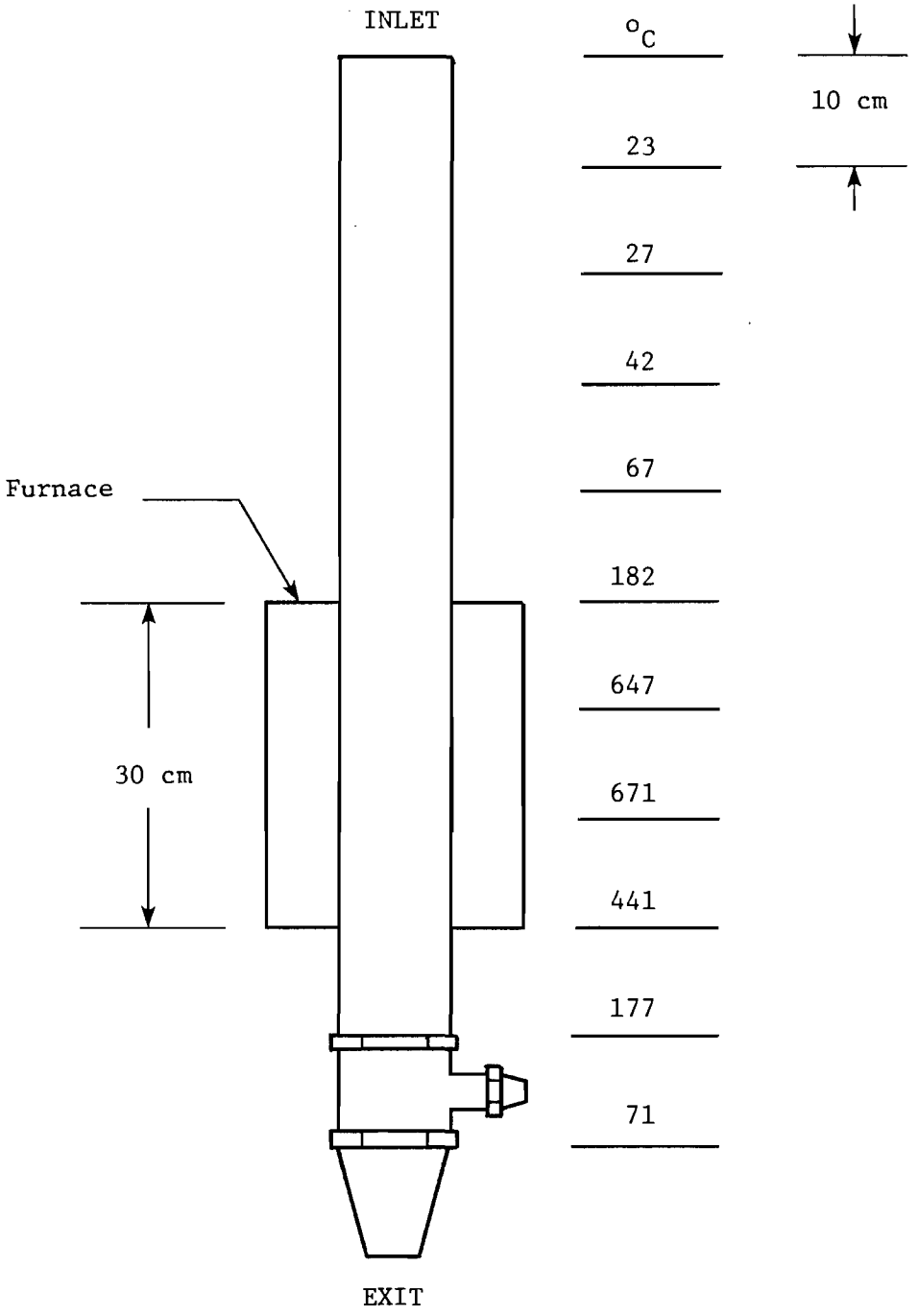

Figure 5. Temperature Profile of "Free-Fall" Reactor at 650°C

the "Modified Procedure for All Sparking Fuels" described in ASTM Method D 3175-73.

Percent Ash - -

The per cent ash was determined by ASTM Method D 3174-73.

Percent Acid Insoluble Ash - -

The per cent acid Insoluble Ash was determined by treating the ash by the Association of Florida Phosphate Chemists acid digestion method for sand and insoluble silicates.

Higher Heating Value

The higher heating values were determined by ASTM Method D 3286-73.

Percent Sulfur

The per cent sulfur in the coal and recovered products was determined by the "Bomb Washing Method" described in ASTM Method D 3177-75. The per cent sulfur in the volatile products was estimated by difference.

Calcium Analysis

Duplicate 0.1000g samples of coal or coal reaction products were fused with potassium carbonate in platinum crucibles. When clear, the melts were cooled and dissolved in 20 ml 10 per cent hydrochloric acid. The solution was filtered through a Whatman NO. 40 filter paper into a 100 ml volumetric flask. The filter paper and insoluble residue were washed with 5 successive 10 ml portions of 5 per cent hydrochloric acid, and the combined filtrate and washings were diluted to 100.0 ml with deionized water. The solution were shaken well, and 50 ml aliquot portions were transferred to 100 ml volumetric flasks containing 25 ml of 10 per cent lanthanum oxide solution. The mixtures were diluted to 100 ml with deionized water and shaken well. The calcium concentrations in these lanthanum ion buffered solutions were determined by standard atomic absorption spectrophotometry.

SECTION 4

RESULTS AND DISCUSSION

SAMPLE COMPOSITION

Both of the coal samples used, Kentucky and Illinois, were strongly agglomerating bituminous coals. The agglomerating properties of these samples were considerably reduced by partial oxidation in a stream of heated air. Weight losses during the pretreatment are shown in Table 1.

TABLE 2. WEIGHT LOSSES FROM OXIDIZED COAL FEEDS

Coal Type	Oxidizing Temperature* °C	Volatiles** Wt%	Yield Wt%
Kentucky	193	4.4	95.6
Kentucky	232	7.8	92.2
Illinois	232	20.8	79.2

* A constant 30 minute treatment was used throughout.

** By difference.

The effect of oxidative pretreatment on the proximate analysis of the coal feedstocks is shown in Table 2.

TABLE 3. PROPERTIES OF COAL FEEDS USED IN FREE-FALL REACTOR EXPERIMENTS

Type of Coal	Kentucky		Illinois	
	Nonoxidized	Oxidized	Nonoxidized	Oxidized
Moisture Wt%	1.68	0.0	7.0	1.5
Volatiles Wt%	33.5	32.7	34.0	29.2
Sulfur Wt%	1.47	1.91	4.43	5.58
Ash Wt%	5.23	7.45	13.0	13.2
Calcium Wt%	----	0.57	1.77	2.18
kJ/kg	28,617	29,549	29,761	27,815*
(Btu/lb.)	(12,311)	(12,712)	(12,803)	(11,966)

*Hydrocarbon volatiles losses were noted during pretreatment step.

Examination of the experimental data indicates that the loss of volatiles from the Illinois coal was nearly three times greater than that from Kentucky coal during 30 minutes at 232°C (Table 1) although the original volatiles content of the two coals is similar (Table 2). The per cent sulfur and the per cent ash in the Illinois coal were appreciably higher than the corresponding components in the Kentucky coal. The per cent sulfur in the oxidized coals increased by more than 25 per cent, relative to the per cent sulfur in the corresponding unoxidized coals. The heating value of the pretreated Kentucky coal was slightly increased over that of the raw coal, while that of the Illinois oxidized coal showed a 5.9 per cent decrease.

REACTOR EXPERIMENTS

In order to study the desulfurization of pulverized coal in contact with a hot inert gas stream, it was necessary to develop a relatively simple reactor. Initially, the approach was to design a reactor in which the coal particles would be exposed to the hot inert gas in a suspended or entrained mode. The solid product would be recovered for chemical analysis, whereas the volatile phase would not be recovered. The major analytical data needed were sulfur content and heating value of the solid products. The final experimental technique used in this study was developed as follows. A cold entrained suspension model produced data for the design of heated en-

trained suspension apparatus which was tested with both raw and preoxidized coal samples. Agglomeration of the samples in the heated suspension reactor led to the free-fall technique, which was employed in the major portion of the experimental program.

Cold Suspended Entrainment Experiments

The full scale glass model of the suspended entrainment reactor was fabricated to permit visual observation of the charge distributions and flow patterns that could be anticipated in the heated metal apparatus. This glass model permitted rapid demonstration of the need for narrow particle size ranges and carefully controlled gas flow rates to keep the coal suspended in the zone which would be heated in the test reactor. The value of a pulsed gas flow in breaking up caked masses of coal dust was also shown. The observations obtained from the glass model were used in the design of the heated reactor tube.

Heated Suspended Entrainment Experiments

Repeated experiments in the heated suspended entrainment apparatus, Figure 3, at several temperatures and gas flow rates and with raw and preoxidized coals produced only annular deposits of fused coal on the tube walls slightly above the hottest point in the tube. At 650^{o}C the deposition zone was relatively narrow (1.5-2 cm) and glossy in appearance. At 450^{o}C the deposition zone was somewhat broader (4-5 cm), and some residue of sintered particulates was visible. Only a small fraction, 5 per cent or less, of the coal input was collected in the receiver. The agglomeration of the coal particles in this experimental mode was such that no useful experimental data could be obtained, and therefore, the remaining experimental effort was with the free-fall technique.

Free-Fall Reactor Experiments

A schematic diagram of the apparatus for these experiments is shown in Figure 4. Removal of the restrictor from the reactor tube as shown in Figure 3, and reduction of the nitrogen flow rate decreased the turbulence within the tube and permitted the treated granular coal to reach the receiver with decreased or no losses to fusion on the tube wall.

Kentucky Coal - -

Results of the first series of experiments with unoxidized and oxidized 50 x 100 mesh Kentucky coal are shown in Table 3.

TABLE 4. FREE-FALL REACTOR EXPERIMENTAL DATA USING KENTUCKY COAL

Exp. No.*	Coal Pretreatment	Feedrate gm/min	Runtime Minutes	Percent Yields Receiver Wt%	Reactor Wt%	Volatiles** Wt%
1	Nonoxidized	2	6	0	55	45
2	Nonoxidized	0.5	6	26.7	64.3	9
3	Oxidized 193°C	1.5	6	10.0	27.2	62.8
4	Oxidized 232°C	1.12	5	32.1	23.2	44.7
5	Oxidized 232°C	5.2	5	2.9	41.1	56.0
6	Oxidized 232°C	0.12	60	29.2	24.3	46.5

* Reactor temperature at constant 650°C

** By difference

These data indicate that the fraction of the coal adhering to the tube wall increases with increasing feed rate and that preoxidation reduces the tendency of the coal granules to adhere to the reactor walls.

The distribution of the sulfur among the reaction products, expressed as per cent of the 1.91 per cent by weight sulfur in the feedstock, is given in Table 4.

TABLE 5. DISTRIBUTION OF SULFUR IN KENTUCKY COAL EXPERIMENTS

Exp. No.	Per cent Sulfur Relative Distribution* Receiver Wt%	Reactor Wt%	Volatiles** Wt%
3	8.8	13.6	77.6
4	30.6	19.9	49.4
5	4.0	36.6	59.4
6	37.7	16.0	46.2

* Sulfur content of feedstock, oxidized, 1.91% Wt.

** By difference.

The recovered yields from the first two experiments were insufficient to permit a precise sulfur analysis. The sulfur fraction in the volatiles appears to have been enriched by sulfur distilled from the feed fraction which adhered to and was coked on the wall of the reactor.

The heating values of the recovered products from the experiments with oxidized Kentucky coal are shown in Table 5.

TABLE 6. DISTRIBUTION OF HEATING VALUE IN OXIDIZED KENTUCKY COAL EXPERIMENTS

Exp. No.	Receiver kJ/kg (Btu/lb)	%	Reactor kJ/kg (Btu/lb)	%	Volatiles* kJ/kg (Btu/lb)	%
3	31,950	10.8	30,660	28.1	28,675	61.0
	(13,745)		(13,190)		(12,335)	
4	30,293	32.9	29,986	23.5	28,787	43.5
	(13,032)		(12,900)		(12,384)	
5	28,171	2.8	31,555	43.9	28,147	53.3
	(12,119)		(13,575)		(12,109)	
6	30,888	30.5	30,934	25.4	27,985	44.1
	(13,288)		(13,308)		(12,039)	

* By difference.

At best, less than one third of the original heating value of the coal samples remained in the treated granular material which reached the receiver. At the highest feedrate (Experiment 5) the energy per unit mass of the receiver coal was less than that of the feedstock. The lower energy fraction recoveries in the receiver resulted from the higher throughput rates (Run 3 and Run 5).

The calcium analyses were undertaken as a tracer experiment. Since calcium is present in the coal feedstock but not in the materials from which the reactor is constructed, it was believed that the per cent calcium in the reaction products would be a better indication of yield distribution than apparent per cent ash, which is influenced by oxidation states and included

erosion products from the reactor wall. Results of the calcium analysis are shown in Table 6.

TABLE 7. CALCIUM DETERMINATIONS IN KENTUCKY COAL EXPERIMENTS

Exp. No.	Per cent Calcium	
	Receiver Wt%	Reactor Wt%
3	0.39	1.02
4	1.67	0.56
5	1.66	0.53
6	1.68	0.67

The low total per cent calcium in Experiment 3 indicates an experimental error in the heat treatment or in the analysis. However, the sums of the per cent calcium in the receiver and in the material adhering to the reactor tube for 4, 5 and 6 are in good agreement (2.27 ± 0.08 per cent) and the calcium concentration in the receiver coal is roughly three times that found in the reactor coke. This observation indicates that much of the reactor coke is a cracked residue from the volatiles rather than fused feedstock particles.

Illinois Coal - -

Free-fall experiments were performed with unoxidized 50 x 100 mesh Illinois coal at three temperatures. The yield distributions for these experiments are shown in Table 7.

TABLE 8. FREE-FALL REACTOR EXPERIMENTAL DATA USING NONOXIDIZED ILLINOIS COAL

Exp. No.*	Reactor Temperature °C	Coal Feedrate gm/min	Runtime Minutes	Yields		
				Receiver Wt%	Reactor Wt%	Volatilea** Wt%
7	650	1.0	20	11	64	24
8	650	0.2	60	53	22	25
9	650	0.14	60	56	2	42
10	550	0.14	60	75	0	25
11	540	0.14	60	76	0	24

* All feeds were nonoxidized.

** By difference.

At a constant temperature of 650°C (Experiments 7, 8 and 9) the fraction of the input feed reaching the receiver increased while the yield of reactor coke decreased with decreasing feed input rate. At a constant feed input rate, decreasing the reactor temperature from 650°C to 550°C (Experiments 9 and 10) led to a sharp increase in the receiver yield and a corresponding decrease in volatiles. Further decreasing the temperature (Experiment 11) had little or no effect on yield distribution.

The relative sulfur distributions (based on the 4.43 per cent sulfur in the original sample) are shown in Table 8.

TABLE 9. DISTRIBUTION OF SULFUR IN NONOXIDIZED ILLINOIS COAL

	Per cent Sulfur Relative Distribution		
Exp. No.*	Receiver Wt%	Reactor Wt%	Volatiles** Wt%
7	11	85.8	3.1
8	63.6	21.7	14.6
9	77.2	1.7	21.1
10	68.6	0	31.6
11	100.0	0	0

* Nonoxidized feedstock.

** By difference.

The distributions of the heating values resulting from the Illinois nonoxidized coal experiments are shown in Table 9.

TABLE 10. DISTRIBUTION OF HEATING VALUE IN NONOXIDIZED ILLINOIS COAL EXPERIMENTS

Exp. No.	Receiver kJ/kg (Btu/lb)	%	Reactor kJ/kg (Btu/lb)	%	Volatiles** kJ/kg (Btu/lb)	%
7	29,826	11	31,309	68.4	25,537	20.6
	(12,831)*		(13,469)		(10,986)	
8	29,826	53.1	29,033	21.5	30,270	25.4
	(12,831)		(12,490)		(13,022)	
9	30,072	56.6	29,056	2.0	29,377	41.4
	(12,937)		(12,500)**		(12,638)	
10	27,624	69.6	- - - - -	0.0	36,169	30.4
	(11,884)		- - - - -		(15,560)	
11	28,928	73.0	- - - - -	0.0	32,394	27.0
	(12,445)		- - - - -		(13,936)	

* Assumed average value due to small sample size.

** By difference.

Less energy was lost in heating Illinois coal than was the case with Kentucky coal. The higher weight yields of receiver coal from the Illinois feed more than offset its lower energy per unit mas.

Results from the calcium analyses performed on the reaction products from nonoxidized Illinois coal are shown in Table 10.

TABLE 11. CALCIUM DETERMINATIONS IN NONOXIDIZED ILLINOIS COAL EXPERIMENTS

	Calcium*	
Exp. No.	Receiver Wt%	Reactor Wt%
7	2.78	1.17**
8	2.79	1.13**
9	2.54	1.42**
10	2.21	1.19**
11	1.77	N.S.

* Feedstock calcium level 1.77%.

** Low levels of calcium below feed levels indicate dilution with sublimed solids.

The per cent calcium in the reactor coke is lower than that of the feedstock. The observation supports the belief that the reactor coke is a mixture of trapped and partially decomposed feed particles and cracked residues from the volatiles.

Oxidized Illinois Coal - -

Free-fall experiments were conducted with 50 x 100 mesh oxidized Illinois coal at several temperatures. The yield distributions from these experiments are shown in Table 11.

TABLE 12. FREE-FALL REACTOR EXPERIMENTAL DATA USING OXIDIZED ILLINOIS COAL

Exp. No.	Reactor Temperature °C	Conl. Feedrate gm/min	Runtime Minutes	Yields Receiver Wt%	Reactor Wt%	Volatiles* Wt%
12	500	0.14	60	93.3	0.0	6.7
13	550	0.14	60	54.7	0.0	45.3
14	600	0.14	60	49.2	1.5	49.3
15	650	0.14	60	62.7	0.0	37.3

* By difference.

The receiver coal yields decreased with increasing temperature while the degree of volatilization rose during the first three runs (Experiments 12, 13 and 14). The anomalous high receiver coal yield at 650°C (Experiment 15) can only be attributed to an undetected surge in the feeder rate.

The sulfur distribution (expressed as relative per cent of the sulfur in the feedstock) are shown in Table 12.

TABLE 13. DISTRIBUTION OF SULFUR IN OXIDIZED ILLINOIS COAL

Exp. No.	Sulfur Content Relative Distribution Receiver Wt%	Reactor Wt%	Volatiles* Wt%
12	68.5	0.0	31.5
13	44.1	0.0	55.9
14	31.7	1.0	67.3
15	41.6	0.0	58.4

*By difference

Comparing Tables 11 and 12 indicates that the per cent of the sulfur (Table 12) in the volatiles is greater than the weight per cent of the feed volatilized (Table 11). A comparison of the relative per cent of the sulfur carried away as volatiles with the weight per cent of the oxidized Illinois coal feedstock volatilizes is shown in Table 13.

TABLE 14. RELATIVE PER CENT VOLATILE SULFUR AND VOLATILE FEED-ILLINOIS OXIDIZED COAL

Exp. No.	Temperature (^{o}C)	Relative Per cent Sulfur(s)	Relative Per cent (wt) Volatiles(v)	Ratio (s/v)
12	500	31.5	6.7	4.7
13	550	55.9	45.3	1.2
14	600	67.3	49.3	1.4
15	650	58.4	37.3	1.6

These data indicate that the most favorable ratio of sulfur removal to loss of volatiles occured at 500^{o}C (Experiment 12).

The energy yield distribution resulting from the free-fall treatment of oxidized Illinois coal are shown in Table 14.

TABLE 15. DISTRIBUTION OF HEATING VALUE IN OXIDIZED ILLINOIS COAL EXPERIMENTS

Exp. No.	Receiver kJ/kg (Btu/lb)	%	Reactor kJ/kg (Btu/lb)	%	Volatiles* kJ/kg (Btu/lb)	%
12	29,307 (12,608)	98.3	-	-	27,739 (11,933)	1.7
13	25,442 (10,945)	49.3	-	-	26,276 (11,304)	50.7
14	26,174 (11,260)	46.3	26,174 (11,260)	1.4	18,289 (7,868)	52.3
15	29,986 (12,900)	67.6	-	-	18,819 (8,096)	32.4

* By difference.

The anomalous high energy value of the receiver coal in Experiment 15 is attributed to the apparent experimental error in the mass yield reported in Table 11.

Combining the relative per cent volatile sulfur and the per cent of the feedstock energy which appears in the volatile phase shows the fraction of the input energy required to remove sulfur from the feedstock coal at several temperatures. These data are presented in Table 15.

TABLE 16. RELATIVE PER CENT VOLATILE SULFUR AND ENERGY VOLATILES ILLINOIS OXIDIZED COAL

Exp. No.	Temperature (°C)	Relative Percent Sulfur(s)	Relative Percent Volatiles Energy(H)	Ratio (S/H)
12	500	31.5	1.7	18.5
13	550	55.9	50.7	1.1
14	600	67.3	52.3	1.3
15	650	58.4	32.4	1.8

The highest ratio of sulfur volatilized to energy transferred into the volatiles phase occurs at the lowest temperature.

No analysis of the distribution of calcium among the products from oxidized Illinois coal was attempted as the quantity of coke in the reactor tube was not sufficient.

SECTION 5

SUMMARY

The preliminary data from the free-fall experiments indicate that the technique is one that can yield useful and meaningful results on the desulfurization and volatilization of coal samples in a dilute phase mode. For example with the Kentucky coal using the free-fall apparatus, Figure 4, the results showed that the agglomerating characteristics of this particular coal had to be minimized to reduce the amount of material that would collect on the walls of the reactor. Samples of Kentucky coal were pretreated, as described in the Experimental Section, in the apparatus shown in Figure 1. This treatment reduced the amount of material adhering the reactor walls by approximately 50%.

The data from preliminary experiment 6 with the Kentucky coal are indicative of the potential reductions in sulfur that can be obtained. If it is assumed that the sulfur components in the volatiles can be removed and that both the coke and the sulfur-free volatiles are used as a combined fuel, then the sulfur content of the original coal has been reduced by approximately 46 per cent. The data from the preliminary experiments with both the nontreated and treated Illinois coal indicated that the sulfur content, based on the assumptions above for the combined fuels, could be reduced significantly. The reduction with the nontreated coal was approximately 31 per cent, experiment 10, and with the treated coal was approximately 57 per cent, experiments 14 and 15. These data are sufficiently encouraging that this technical approach has promise as a method for the desulfurization of coal to acceptable levels.

SECTION 6

FUTURE WORK

Additional work on the free-fall technique would require an improved design of the experimental reactor so that the adherence of material on the walls of the reactor would be minimized or eliminated. Also, provision would have to be made so that the volatile products could be collected for chemical analysis. The variables that need to be considered in the desulfurization step are the nature of the coal, coal rank, particle size, temperature, residence time, ratio of coal-to-inert gas, and pretreatment of the coal. The chemical nature of the sulfur in the coal should also be known. With the necessary data, energy and mass balances could be calculated and an overall flow diagram developed for the process. An economic evaluation of the process could then be made for comparison with other desulfurization processes.

REFERENCES

1. Van Krevelen, D. W. and J. Schuyer, Coal Science, Elsevier, Amsterdam (1957).

2. Lowry, H. H. ed, Chemistry of Coal Utilization, Suppl. Vol., Wiley, New York, N.Y. (1963).

3. Anthony, D. B., and J. B. Howard, "Coal Devolatilization and Hydrogasification", AICHE(Am. Inst. Chem. Engrs.) J. 22, 625-656 (1976).

4. Huang, E. T. K. "Devolatilization and Desulfurization of Iowa Coal" Ph.D. thesis. Iowa State University, Ames. IA. (1977).

5. Wen, C. Y., and S. Tone, "Coal Conversion Reaction Engineering", Chemical Reaction Engineering Reviews, Houston, ACS Symposium Series 72, 57-109 (1978).

6. Koch, V., H. Juntgen, and W. Peters "Non-Isothermal Reactions of Coal Pyrolysis", Brennstoff-Chem. 50, 369-373 (1969).

7. Badzioch, S., and P. G. Hawksley, "Kinetics of Thermal Decomposition of Pulverized Coal Particles", Ind. Eng. Chem. Process Des. Develop. Vol. 9 NO. 4, 521-530 (1970).

8. Attar, A., W. H. Coreoran, and G. S. Gibson, "Transformation of Sulfur Functional Groups During Pyrolysis of Coal", Division of Fuel Chem. Vol. 21 NO. 7 p. 106. 172nd National Meeting Am. Chem. Soc., San Francisco, CA, 1976.

9. Haldipur, G. B., Iowa State University of Science and Technology, Ames. Energy Research and Development Administration "Desulfurization of Coal in a Fluidized Bed Reactor at Elevated Temperatures". M.S. Thesis, Iowa State University, Ames, IA. Oct., 1976.

10. Maa, P. S., C. R. Lewis, and C. E. Hambin, Jr., "Sulfur Transformation and Removal for Western Kentucky Coal", Fuel 54; 62-69 (1975).

11. Block, J. B., S. S. Sharp, and L. J. Darlage, "Effectiveness of Gases in Desulfurization of Coal", Fuel 54, 113-119 (1975).

12. Sinha, R. K. and P. L. Walker, Jr., "Desulfurization of Coals and Chars by Treatment in Various Atmospheres Between 400 and 600^{o}C", Fuel 51, 329-331 (1972).

13. Sinha, R. K. and P. L. Walker, Jr., "Removal of Sulfur from Coal by Air

Oxidation at 350°-450°C", Fuel 51, 125-129 (1972).

14. Cernic-Simic, S. "A Study of Factors That Influence the Behavior of Coal Sulfur During Carbonization", Fuel 41, 141-151 (1952).

15. McKinley, J. B., and A. M. Henke, "Production of Low Sulfur Carbonaceous Fuels", U.S. Patent NO. 2, 726, 148, December 6, 1955.